(NASA-CR-168107) STABILITY ANALYSIS OF FLEXIBLE WIND TURBINE BLADES USING FINITE ELEMENT METHOD Final Report (Massachusetts Inst. of Tech.) 156 p HC A08/MF A01 CSCL 10A G3/44

N83-21508

Unclas
03175

DOE/NASA/3303-2
NASA CR-168107
M.I.T. ASRL TR 197-3

Stability Analysis of Flexible Wind Turbine Blades Using Finite Element Method

Anargiros Kamoulakos
Massachusetts Institute of Technology

August 1982

Prepared for
NATIONAL AERONAUTICS AND SPACE ADMINISTRATION
Lewis Research Center
Under Grant NSG-3303

for
U.S. DEPARTMENT OF ENERGY
Conservation and Renewable Energy
Division of Photovoltaic Energy Technology

DOE/NASA/3303-2
NASA CR-168107
M.I.T. ASRL TR 197-3

Stability Analysis of Flexible Wind Turbine Blades Using Finite Element Method

Anargiros Kamoulakcs
Aeroelastic and Structures Research Laboratory
Massachusetts Institute of Technology
Cambridge, Massachusetts 02139

August 1982

Prepared for
National Aeronautics and Space Administration
Lewis Research Center
Cleveland, Ohio 44135
Under Grant NSG-3303

for
U.S. DEPARTMENT OF ENERGY
Conservation and Renewable Energy
Division of Photovoltaic Energy Technology
Washington, D.C. 20545
Under Interagency Agreement DE-AI01-76ET20320

FOREWORD

This work was carried out in the Aeroelastic and Structures Research Laboratory, M.I.T., and was supported by NASA Lewis Research Center under Grant No. NSG-3303, "Development of a Methodology for Horizontal Axis Wind Turbine Dynamic Analysis". The NASA Technical Officer for this work was David C. Janetzke. The principal investigator for the grant was Professor John Dugundji.

The present document constitutes an M.S. thesis by the author. The author wishes to acknowledge helpful discussions with Professor John Dugundji who served as his thesis advisor.

Table of Contents

List of Symbols

$\alpha_x\ \alpha_y\ \alpha_z$ = blade accelerations along the xyz axes respectively

α = lift curve slope

α_i = coefficients in the $\underset{\sim}{M}_s, \underset{\sim}{C}_G$ and $\underset{\sim}{K}_M$ matrices

A_i = coefficients of the p_x loading in Appendix B

A = cross-sectional area of the blade

b_i = coefficients of the $\underset{\sim}{K}_s, \underset{\sim}{K}_G$ matrices

B_i = coefficients of the p_y loading in Appendix B

$\bar{b}_i$ = coefficients of the $\underset{\sim}{K}_s$ and $\underset{\sim}{K}_G$ matrices

c = chord length

C_{d_0} = drag coefficient

C_T = thrust coefficient

$\underset{\sim}{C}_A$ = aerodynamic damping matrix (see equation (52))

$\underset{\sim}{C}_G$ = gyroscopic matrix (see equation (52))

$\bar{\underset{\sim}{C}}$ = reduced damping matrix (see Flutter Analysis)

D = drag force on the aerofoil (see figure 7)

e = distance between the mass centre and the shear centre of a cross-section

e_A = distance between the centroid and the shear centre of a cross-section

e_0 = offset of the blade from the Z axis

EI_1, EI_2 = flexural stiffnesses of the blade about the major and minor neutral axes respectively (both passing through the centroid)

EB_1, EB_2 = cross-sectional constants defined in appendix M

$\overline{EI}_2$ = modified EI_2 for non-straight elastic axis

$\overline{EB}_1, \overline{EB}_2$ = modified EB_1, EB_2 for non-straight elastic axis

E_i = coefficients of the p_x loading in appendix J

$\underset{\sim}{F}$ = transformation matrix given in equation (2a), (6a)

F_η = aerodynamic force in the η direction (see equation (46b))

F_ζ = aerodynamic force in the ζ direction (see equation (46a))

GJ = torsional rigidity of the blade

$\overset{\circ}{h}$ = vertical velocity of a vibrating blade

$H'_{01}\ H'_{11}\ H'_{02}\ H'_{12}\ H^{\circ}_{01}\ H^{\circ}_{02}$ = Hermitian Interpolation polynomials (see equations (50))

$\underset{\sim}{H}_1\ \underset{\sim}{H}_0$ = Hermitian Interpolation matrices (see equations (50))

H_i = coefficients of the p_z loading in appendix J

$\vec{i}_x\ \vec{i}_y\ \vec{i}_z$ = unit vectors along the xyz system of axes

$\vec{i}_\xi\ \vec{i}_\eta\ \vec{i}_\zeta$ = unit vectors along the $\xi\ \eta\ \zeta$ system of axes

$\vec{I}\ \vec{J}\ \vec{K}$ = unit vectors along the XYZ system of axes

$\vec{i}_{x_L}\ \vec{i}_{y_L}\ \vec{i}_{z_L}$ = unit vectors along the $x_L\ y_L\ z_L$ system of axes

I_i = coefficients of the q_y loading in appendix J

K_A = polar radius of gyration of cross-sectional area about elastic axis

K_m = polar radius of gyration at cross-sectional mass about elastic axis

K_{m_1}, K_{m_2} = mass radii of gyration about the major neutral axis and about an axis perpendicular to the chord through the elastic axis, respectively

K_s = assembled structural stiffness matrix

$\underset{\sim}{K}_G$ = assembled geometric stiffness matrix (see equation (52))

$\underset{\sim}{K}_A$ = assembled aerodynamic stiffness matrix (see equation (52))

$\underset{\sim}{K}_M$ = assembled mass stiffness matrix (see equation (52))

$\underset{\sim}{\bar{K}}$ = reduced total assembled stiffness matrix for flutter analysis (see Flutter Analysis)

$\underset{\sim}{k}_s$ = local element structural stiffness matrix for non-straight elastic axis analysis (see equation (82))

$\underset{\sim}{k}_G$ = local element geometric stiffness matrix for non-straight elastic axis analysis (see equation (82))

$\underset{\sim}{k}_M$ = local element "mass" stiffness matrix for non-straight elastic axis analysis (see equation (83))

K_i = coefficients of the q_z loading in appendix J

$\underset{\sim}{K}$ = total assembled stiffness matrix for non-straight elastic axis (see equation (87))

L = total lift force on the aerofoil

L_c = circulatory lift component (see figure 7)

L_{NC} = non-circulatory lift component (see figure 7)

$\underset{\sim}{L}_i$ = secondary (constituent) matrices displayed in appendix C

ℓ_i = length of each finite element

M = pitching moment on the blade (see figure 7)

M_c = circulatory pitching moment component

M_{NC} = non-circulatory pitching moment component

$\underset{\sim}{M}_A$ = assembled aerodynamic mass matrix (see equation (52))

$\underset{\sim}{M}_s$ = assembled structural mass matrix (see equation (52))

M_y = bending moment component along the y-axis (see equation (57a))

M_z = bending moment component along the z-axis (see equation (57b))

$\bar{\underset{\sim}{M}}$ = reduced total assembled mass matrix for flutter analysis (see Flutter Analysis)

$\underset{\sim}{m}_L$ = local element mass matrix (see equation (83))

$\underset{\sim}{M}$ = total assembled mass matrix in the non-straight elastic (see equation (87))

$p_x\ p_y\ p_z$ = distributed loadings along the xyz axes

$\underset{\sim}{P}_L$ = load vector in the non-straight elastic axis analysis (see equation (82))

$q_\xi\ q_y\ q_z$ = distributed moments along the ξ , y and z axes.

$\underset{\sim}{q}_v\ \underset{\sim}{q}_w\ \underset{\sim}{q}_\phi$ = generalised coordinate vector for v, w, ϕ deflections,respectively (see equation (49))

$\underset{\sim}{q}$ = total assembled generalised coordinate vector (see equation (51))

$\underset{\sim}{Q}$ = load vector in the straight elastic axis analysis

$\underset{\sim}{Q}_{steady}$ = steady load vector in the straight elastic axis analysis (see equation (52))

$\bar{\underset{\sim}{q}}$ = normal generalised coordinate vector (see Vibration Analysis)

$\bar{\underset{\sim}{q}}_p$ = reduced normal generalised coordinate vector for flutter analysis (see Vibration Analysis)

$\underset{\sim}{q}_{u_L}\ \underset{\sim}{q}_{v_L}\ \underset{\sim}{q}_{w_L}\ \underset{\sim}{q}_{\phi_L}$ = generalised coordinate vector for u_L v_L w_L ϕ_L deflections, respectively in the non-straight elastic axis analysis (see equation (80))

$\underset{\sim}{q}_L$ = total generalised coordinate vector for the non-straight elastic axis analysis (see equation (81))

r = distance from the Ξ-axis (radius)

$$r = e_o \cos\beta + x\cos(\beta+\delta)$$

R = tip radius of the cantilever blade

$\underset{\sim}{S}$ = transformation matrix given in equations (4), (6b)

T = centrifugal tension in the straight elastic axis analysis ($= \int_x^R p_x\, dx$)

T_i = nodal values of T (see equation (60))

T_{av_i} = average value of T along the i^{th} element

$\underset{\sim}{T}$ = transformation matrix given in equations (66), (71b)

T_c = centrifugal tension in the non-straight elastic axis analysis given in equation (75b)

$\underset{\sim}{T}_M$ = transformation matrix given in appendix L defined in equation (85)

$\underset{\sim}{T}_A$ = transformation matrix defined in equation (86)

$\underset{\sim}{T}_B$ = transformation matrix defined and given in appendix L

u = elastic axis displacement along the x-axis

u_L = elastic axis displacement along the x_L-axis in the non-straight elastic axis analysis

U_w = wind velocity along the X-axis

$U_\xi\ U_\eta\ U_\zeta$ = wind velocities along the $\xi\,\eta\,\zeta$ axes, respectively

U = total wind velocity felt by the blade

v = elastic axis displacement along the y-axis

V_w = wind velocity along the Y -axis

v_i = induced velocity (along the Z -axis)

V = air free stream velocity in Greenberg theory

V_h = equivalent air velocity due to the blade vibration $\dot{h}$

V_{y_i} V_{z_i} = nodal values of the shear forces along the y and z axes, respectively

v_L = elastic axis displacement along the y_L -axis in the non-straight elastic axis analysis

w = elastic axis displacement along the z-axis

W = work done by all loadings on the blade

W_w = wind velocity along the Z -axis

w_L = elastic axis displacement along the -axis in the non-straight elastic axis analysis

$X\,Y\,Z$ = orthogonal cartesian system of axes fixed in space, defined in figure 1

$x\,y\,z$ = orthogonal cartesian system of axes, describing the undeformed blade only in the straight elastic axis analysis (see figure 1), also defined in figure 24 for the non-straight elastic axis analysis

$x_L\,y_L\,z_L$ = orthogonal cartesian system of axes describing the undeformed blade element in the non-straight elastic axis analysis (see figure 25)

$\overline{Z}_i$ = coefficients of the p_y loading in appendix J

α = angle of incidence of the blade defined in Figure 5

$\hat{\alpha}$ = "in-plane" inclination angle of a given element in the non-straight elastic axis analysis, defined in figure 25

β = blade precone angle shown in figure 1

$\hat{\beta}$ = "out-of-plane" inclination angle of a given element in the non-straight elastic axis analysis, defined in figure 25

β_i = secondary coefficients defined in appendix B

γ_i = secondary coefficients defined in appendix B

$\gamma_{\xi\eta}\ \gamma_{\xi\zeta}$ = shear strains of the blade cross-section

Γ_i = coefficients of the p_ζ loading in appendix B

δ = blade droop angle shown in figure 1

Δ_i = coefficients of the q_ξ loading in appendix B

$\epsilon_{\xi\xi}$ = longitudinal strain of the blade cross-section

ϵ = blade pitch angle defined in figure 6

$\xi\ \eta\ \zeta$ = curvilinear system of axes, following the blade throughout its deformation (see figures 2 and 26)

θ_M = direction of motion of the blade defined as $\tan^{-1}\frac{w}{v}$

Θ_i = coefficients of the q_ξ loading in appendix J

$\underset{\sim}{\Lambda}$ = eigenvalue matrix in vibration analysis

$\underset{\sim}{\Lambda}_c$ = complex eigenvalue matrix in flutter analysis

μ = real part of a complex eigenvalue

μ_i = secondary coefficients defined in appendices I and J

$\underset{\sim}{\Xi}$ = matrix defined in equation (62)

π = total potential energy functional

ρ = air density

ρ_b = blade density

σ = solidity ratio = $\frac{(\text{no. of blades})\cdot c}{2\pi R}$

ϕ_0 = blade pretwist

$\underset{\sim}{\Phi}$ = eigenvector matrix in vibration analysis

$\underset{\sim}{\Phi}_i$ = eigenvector of a particular mode in vibration analysis

$\underset{\sim}{\Phi}_c$ = complex eigenvector matrix in flutter analysis

$\underset{\sim}{\Phi}_{c}$ = complex eigenvector of a particular mode in flutter analysis

ϕ = elastic twist of the blade about the ξ-axis

ϕ_L = elastic twist of the blade element about the ξ-axis in the non-straight elastic axis analysis

$\underset{\sim}{\Psi}$ = reduced generalised coordinate vector for flutter analysis (see Flutter Analysis)

$\underset{\sim}{\bar{\Psi}}$ = normal reduced generalised coordinate vector (see Flutter Analysis)

$\underset{\sim}{\bar{\Psi}}_{\bullet}$ = constant coefficient matrix for (see Flutter Analysis)

$\omega_\xi\ \omega_\eta\ \omega_\zeta$ = angular velocity components of a point on the blade cross-section, along the $\xi\ \eta\ \zeta$ system of axes, respectively

ω = vibration frequency of the blade, or imaginary part of the complex eigenvalues

Ω = angular velocity of the "rigid" blade defined in figure 1

$\overset{\circ}{(\ )}$ = $\dfrac{\partial}{\partial t}(\ )$

$(\ )'$ = $\dfrac{\partial}{\partial x}(\ )$

$\delta(\ )$ = first variation of ( )

$\forall$ = volume of the blade

$\forall_i$ = volume of the i^{th} element

1. INTRODUCTION

In an effort to convert wind power to electricity in the most efficient way, large, slender, high aspect ratio blades are being used. Aeroelasticians for the last twenty years increasingly have developed more accurate and complex ways to model the aeroelastic response of such wind turbine blades.

The overall structural behavior of such turbine blades was generally accepted to be sufficiently represented by an Euler-Bernoulli beam. Since good design often requires nonuniform properties and complex, twisted geometry, the overall equations of motion of a wind turbine blade cannot be obtained easily from first principles. A systematic way that this has been done in the past is by variational methods; i.e., Hamilton's Principle and the Principle of Minimum Total Potential Energy. It has to be noted that research done for wind turbine blades parallels greatly research done for helicopter blades, since the real difference between the two structures is only the structural stiffness. (Wind turbine blades are stiffer than helicopter blades.)

Houbolt and Brooks in 1956 (Ref. 1) presented for the first time the full linear differential equations of motion for rotating nonuniform helicopter rotor blades. They also presented a total potential energy functional whose variation would provide the same differential equations of motion. Finally, they proposed a solution based on modal methods (Galerkin and Lord Rayleigh's method).

Hodges and Ormiston in 1976 (Ref. 2) presented the stability analysis of uniform untwisted cantilever rotor blades for hovering flight. The general nonlinear equations of motion were linearized about the equilibrium operating position using Galerkin's method.

Kottapolli and Friedmann in 1979 (Ref. 3) showed the nonlinear differential equations of motion with periodic coefficients for a horizontal axis wind turbine. Later Friedmann (Ref. 4) and Straub and Friedmann (Ref. 5) solved these nonlinear differential equations of motion by a local Galerkin method resulting in a finite element formulation. This was done for a helicopter in hover.

The stability of a rotor blade in hover was also examined by Stephens and Hodges (Ref. 6) in the same year, 1980. They used a mixed deflection and force, formulation and they solved the nonlinear static equilibrium equations by a collocation method.

Kata (Ref. 7) presented the nonlinear equations of motion for nonuniform, twisted, horizontal axis, wind turbine blades using Hamilton's Principle.

Finally, Sivaneri and Chopra (Ref. 8) in 1981 presented the aeroelastic stability of a helicopter rotor blade in hover by finite element method based on Hamilton's Principle. The flutter analysis was done with normal rotating modes obtained from the finite element method.

In the present analysis, the linear differential equations of motion of a horizontal axis wind turbine blade are solved using the finite element method coupled with the total potential energy formulation of the structure.

According to the finite element method, the structure is discretized into a number of finite elements. The field variables within each element are interpolated with respect to the nodal values of some generalized coordinates, using piecewise continuous functions. The assembly of all the elements will then represent the complete structure (Ref. 9).

With the finite element method, complex geometries and nonuniform properties can be easily represented by averaging them inside each element and then decreasing the size of the element.

The matrices involved in the global equations of motion of the assembled structure will have smaller bandwidth as simpler finite elements are used (e.g., the 2 node beam element used in this analysis).

For a cantilever blade, a small amount of finite elements is sufficient for a good displacement solution, while a larger number of elements is required for a good stress solution.

In Chapter 2, the static and the vibration analysis of a straight elastic axis (rotating) cantilever blade was done using finite element method. The flutter analysis was done using a modal method, the modes having been the normal rotating modes of the blade obtained by the finite element method.

In Chapter 3 the vibration analysis of a nonstraight elastic axis beam was performed. The blade was discretized into a number of straight elastic axis finite elements sufficient to describe the curved shape of the beam. The stiffness and mass matrices were first obtained along the local axes of each individual element and then they were transformed along a set of axes common to all the elements. The problem was then solved in a similar manner with the straight elastic axis case.

2. STRAIGHT ELASTIC AXIS ANALYSIS

2.1 Mathematical Model

A global orthogonal system of axes, fixed in space, X,Y,Z is defined as shown in Figure 1, with the blade rotating at a constant angular velocity Ω about the Z axis.

The blade is set at an offset e_o from the Z axis, as shown in Figure 1. A new orthogonal system of axes x,y,z is now defined, with the x-axis being the elastic axis of the undeformed blade. The blade is also inclined to the XY plane by a precone angle β and a droop angle δ. The cross-section of the blade is symmetrical about the major principal axis and pretwisted at an angle ϕ_o . The shear center E.A., the center of gravity C.G., and the centroid of the cross-section are not necessarily coincident.

All blade properties are in general nonuniform. The blade is allowed to deform under the action of rotary, vibratory and aerodynamic loadings, according to linear small deflection engineering beam theory. Since the blade is of moderate to high aspect ratio, plate bending effects are not significant and the deformation due to shear is neglected. Also torsional warping has been neglected.

The deformation mode of the structure consists of three translations u, v and w and one cross-section rotation ϕ as shown in Figure 2, under the assumption that the cross-section shape does not change throughout the deformation of the structure. The three translations u, v and w describe the behavior

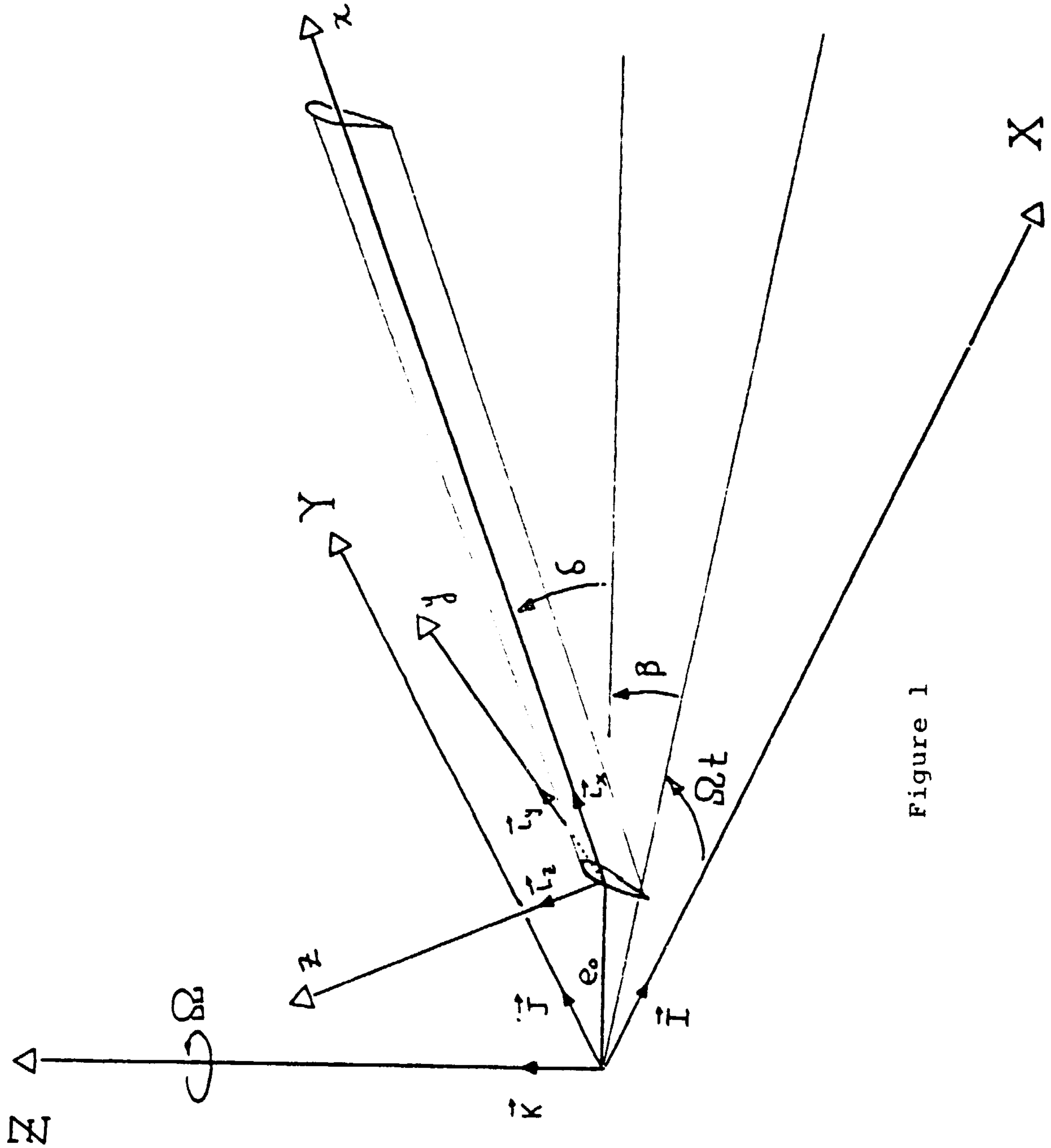

Figure 1

of the elastic axis only.

The equations of equilibrium of the blade are written with respect to the undeformed blade axes x,y,z.

The aerodynamic forces are calculated according to strip theory based on quasi-steady, two dimensional, incompressible unsteady aerodynamics. The position of a point A in the blade can be defined by blade coordinates ξ, η and ζ which follow the blade (see Figure 2). The position of the same point with respect to the xyz system of axes will be

$$\begin{Bmatrix} x \\ y \\ z \end{Bmatrix} = \begin{Bmatrix} \xi + u \\ v \\ w \end{Bmatrix} + \underset{\sim}{F} \begin{Bmatrix} 0 \\ \eta \\ \zeta \end{Bmatrix} \tag{1}$$

where ξ is equal to the x-axis coordinate of point A in the undeformed blade.

$$\underset{\sim}{F} = \begin{bmatrix} 1 & -v'\cos(\phi_0+\phi) - w'\sin(\phi_0+\phi) & v'\sin(\phi_0+\phi) - w'\cos(\phi_0+\phi) \\ v' & \cos(\phi_0+\phi) & -\sin(\phi_0+\phi) \\ w' & \sin(\phi_0+\phi) & \cos(\phi_0+\phi) \end{bmatrix} \tag{2a}$$

for small ϕ

$$\cos(\phi_0+\phi) = \cos\phi_0 - \phi\sin\phi_0$$
$$\sin(\phi_0+\phi) = \sin\phi_0 + \phi\cos\phi_0$$

then to first order terms

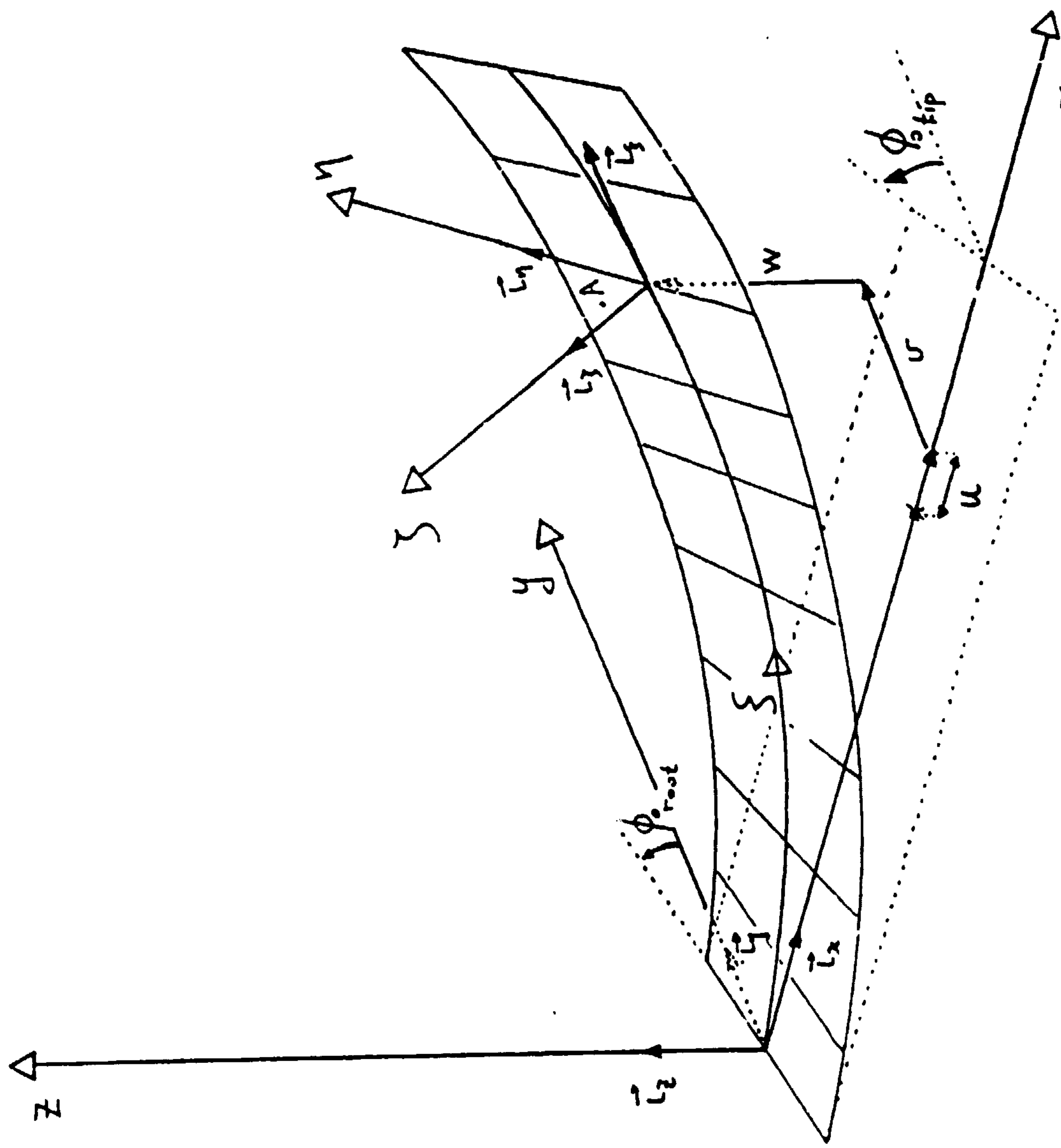

Figure 2

$$\underset{\sim}{F} = \begin{bmatrix} 1 & -v'\cos\phi_o - w'\sin\phi_o & v'\sin\phi_o - w'\cos\phi_o \\ v' & \cos\phi_o - \phi\sin\phi_o & -\sin\phi_o - \phi\cos\phi_o \\ w' & \sin\phi_o + \phi\cos\phi_o & \cos\phi_o - \phi\sin\phi_o \end{bmatrix} \qquad (2b)$$

The position of the previous point A, with respect to the fixed system of axes X,Y,Z will be

$$\begin{Bmatrix} X \\ Y \\ Z \end{Bmatrix} = \underset{\sim}{S} \begin{Bmatrix} x \\ y \\ z \end{Bmatrix} + e_o \begin{Bmatrix} \cos\Omega t \cos\phi_o \\ \sin\Omega t \sin\phi_o \\ \sin\phi_o \end{Bmatrix} \qquad (3)$$

where

$$\underset{\sim}{S} = \begin{bmatrix} \cos\Omega t \cos(\beta+\delta) & -\sin\Omega t & -\cos\Omega t \sin(\beta+\delta) \\ \sin\Omega t \cos(\beta+\delta) & \cos\Omega t & -\sin\Omega t \sin(\beta+\delta) \\ \sin(\beta+\delta) & 0 & \cos(\beta+\delta) \end{bmatrix} \qquad (4)$$

It should be also noted that

$$\underset{\sim}{F}^{-1} = \underset{\sim}{F}^{T}$$
$$\underset{\sim}{S}^{-1} = \underset{\sim}{S}^{T} \qquad (5)$$

and

$$\begin{Bmatrix} \vec{i}_x \\ \vec{i}_y \\ \vec{i}_z \end{Bmatrix} = \underset{\sim}{F} \begin{Bmatrix} \vec{i}_\xi \\ \vec{i}_\eta \\ \vec{i}_\zeta \end{Bmatrix} \tag{6a}$$

$$\begin{Bmatrix} \vec{I} \\ \vec{J} \\ \vec{K} \end{Bmatrix} = \underset{\sim}{S} \begin{Bmatrix} \vec{i}_x \\ \vec{i}_y \\ \vec{i}_z \end{Bmatrix} \tag{6b}$$

2.2 Minimum Total Potential Energy Formulation

We can define the functional π where

$$\pi = (\text{Strain Energy}) - (\text{Work of External Loads}) \tag{7}$$

and

$$\text{Strain Energy} = \frac{1}{2} \iiint_{V} \left(E\epsilon_{\xi\xi}^2 + G\gamma_{\xi\eta}^2 + G\gamma_{\xi\zeta}^2 \right) d\xi \, d\eta \, d\zeta \tag{8}$$

$$\begin{aligned} \text{Work of External Loads} = & \int_0^R \frac{1}{A} \left(\int_x^R p_x \, dx \right) \cdot \left(\iint_A \epsilon_{\xi\xi} \, d\eta \, d\zeta \right) d\xi \\ & + \int_0^R p_y v \, dx + \int_0^R p_z w \, dx + \int_0 q_\xi \phi \, d\xi \\ & + \int_0^R q_y w' \, dx + \int_0^R q_z v' \, dx \end{aligned} \tag{9}$$

Then, among all the possible displacements u,v,w and ϕ that satisfy compatibility inside and on the boundary of the blade, the one that satisfies equilibrium everywhere in the structure will also minimize the functional π of equation (7).

Hence, the condition

$$\delta \pi = 0 \tag{10}$$

will provide the solution for the displacements u,v,w and ϕ .

We can express the strains in equation (8), with respect to displacements u,v,w and ϕ as follows.

Let ds and ds_1 be the lengths of an infinitesimal element along the blade before and after deformation respectively.

Let AB, AC and AD be three mutually perpendicular line elements before deformation (see Figure 3), with

$$(ds)^2 = (AB)^2 + (AC)^2 + (AD)^2$$

and AB', AC' and AD' be the same elements after deformation, hence

$$(ds_1)^2 = (AB')^2 + (AC')^2 + (AD')^2$$

Then, for small deflections

$$AB = \frac{ds}{d\xi} d\xi$$

$$AB' = \frac{ds_1}{d\xi} d\xi$$

and

$$\epsilon_{\xi\xi} = \frac{AB' - AB}{AB} = \frac{\frac{ds_1}{d\xi} - \frac{ds}{d\xi}}{\frac{ds}{d\xi}} \tag{11}$$

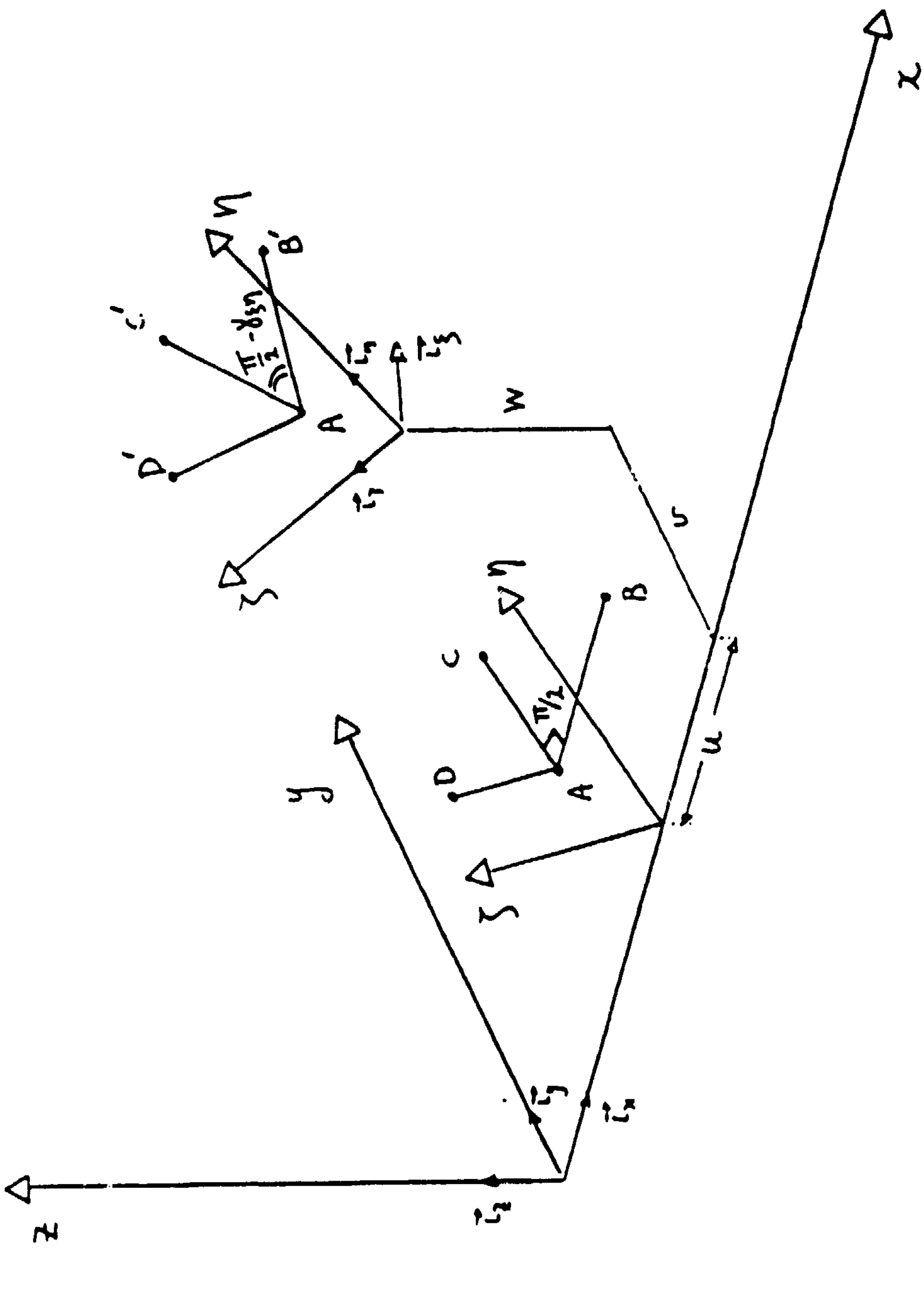

Figure 3

Let the coordinates of point A, with respect to the x,y,z axes to be given by equation (1). Then differentiating it with respect to ξ and substituting into the following

$$\frac{ds_1}{d\xi} = \sqrt{\left(\frac{dx}{d\xi}\right)^2 + \left(\frac{dy}{d\xi}\right)^2 + \left(\frac{dz}{d\xi}\right)^2}$$

$\frac{ds_1}{d\xi}$ could be obtained.

To find $\frac{ds}{d\xi}$, we simply substitute

$$u = v = w = \phi = 0$$

into the $\frac{ds_1}{d\xi}$ equation above. Then by substituting the expressions fc $\frac{ds_1}{d\xi}$ and $\frac{ds}{d\xi}$ into equation (11), dropping nonlinear and higher order terms, we get

$$\begin{aligned} \epsilon_{\xi\xi} = u' - \eta\left(v''\cos\phi_0 + w''\sin\phi_0\right) - \zeta\left(-v''\sin\phi_0\right. \\ \left. + w''\cos\phi_0\right) + \left(\eta^2 + \zeta^2\right)\phi_0'\phi \end{aligned} \qquad (12)$$

Substituting equation (12) into the tension equation

$$T = E \iint_A \epsilon_{\xi\xi}\, d\zeta\, d\eta$$

we get

$$u' = \frac{T}{EA} + e_A\left(v''\cos\phi_0 + w''\sin\phi_0\right) - K_A^2\phi_0'\phi' \qquad (13)$$

Substituting equation (13) into equation (12) we can eliminate u in favor of v, w and ϕ and hence obtain

$$\epsilon_{\xi\xi} = \frac{T}{EA} + (e_A - \eta)(v''\cos\phi_0 + w''\sin\phi_0) + \zeta(v''\sin\phi_0$$
$$- w''\cos\phi_0) + (\eta^2 + \zeta^2 - K_A^2)\phi_0'\phi' \tag{14}$$

Similarly from Figure 3

$$AB' = \frac{ds_1}{d\xi} d\xi$$

$$AC' = \frac{ds_1}{d\eta} d\eta$$

$$B'C' = \sqrt{\left(\frac{dx}{d\xi} d\xi - \frac{dx}{d\eta} d\eta\right)^2 + \left(\frac{dy}{d\xi} d\xi - \frac{dy}{d\eta} d\eta\right)^2 + \left(\frac{dz}{d\xi} d\xi - \frac{dz}{d\eta} d\eta\right)^2}$$

Since

$$\cos\left(\frac{\pi}{2} - \gamma_{\xi\eta}\right) = \sin\gamma_{\xi\eta} \approx \gamma_{\xi\eta}$$

then

$$\cos\left(\frac{\pi}{2} - \gamma_{\xi\eta}\right) = \frac{(AB')^2 + (AC')^2 - (B'C')^2}{2(AB')(AC')} = \gamma_{\xi\eta} \tag{15}$$

Or, substituting the expressions for AB', AC' and B'C' into equation (15) we get

$$\gamma_{\xi\eta} = \frac{(ds_1/d\xi)^2 d\xi^2 + (ds_1/d\eta)^2 d\eta^2 - \Big[\left[(dx/d\xi)d\xi - (dx/d\eta)d\eta\right]^2}{2(ds_1/d\xi)(ds_1/d\eta)\, d\xi\, d\eta}$$
$$\frac{+\left[(dy/d\xi)d\xi - (dy/d\eta)d\eta\right]^2 + \left[(dz/d\xi)d\xi - (dz/d\eta)d\eta\right]^2\Big]}{2(ds_1/d\xi)(ds_1/d\eta)\, d\xi\, d\eta} \quad (1$$

Differentiating equation (1) with respect to η and substituting into equation (16) together with the following equation

$$\frac{ds_1}{d\eta} = \sqrt{\left(\frac{dx}{d\eta}\right)^2 + \left(\frac{dy}{d\eta}\right)^2 + \left(\frac{dz}{d\eta}\right)^2} \tag{17}$$

we get, after deleting higher order and nonlinear terms

$$\gamma_{\xi\eta} = -\zeta\phi' \tag{18}$$

Similarly, substituting η by ζ into equations (16) and (17) and repeating the former analysis we get

$$\gamma_{\xi\zeta} = \eta\phi' \tag{19}$$

Substituting equations (14), (18) and (19) into equation (8) for the strain energy, we get

$$\begin{aligned}\text{Strain Energy} = \frac{1}{2}\int_0^R\!\!\int \Big\{ & \frac{T^2}{EA} + \left[EI_1\sin^2\phi_0 + EI_2\cos^2\phi_0\right](v'')^2 \\ & + \left[EI_1\cos^2\phi_0 + EI_2\sin^2\phi_0\right](w'')^2 + 2\cos\phi_0\sin\phi_0\left[EI_2 - EI_1\right]\cdot \\ & \cdot v''w'' + \left[GJ + EB_1(\phi_0')^2\right](\phi')^2 - 2EB_2\cos\phi_0(\phi_0')v''\phi' \\ & - 2EB_2\sin\phi_0(\phi_0')w''\phi' \Big\}\, d\xi \end{aligned} \tag{20}$$

where EB_1 and EB_2 are given in Appendix M. Since the above equation is up to second order of magnitude when we come to form work done by the centrifugal tension, i.e.,

$$\int_0^R \frac{1}{A}\left(\int_x^R p_x\, dx\right)\left(\iint_A \epsilon_{\xi\xi}\, d\eta\, d\zeta\right) d\xi$$

or

$$\int_0^R \left(-\frac{T}{A}\right) \iint_A \epsilon_{\xi\xi}\, d\eta\, d\zeta\, d\xi \tag{21}$$

we need to consider $\epsilon_{\xi\xi}$ up to second order of magnitude, too. Hence, if we kept second order terms into equation (14) we would get

$$\begin{aligned}\epsilon_{\xi\xi} = {} & u' + \frac{1}{2}\left[(v')^2 + (w')^2\right] + (\eta^2+\zeta^2)\left[\frac{1}{2}(\phi')^2 + \phi_0'\phi'\right] \\ & - \eta\left[v''\cos\phi_0 + w''\sin\phi_0 + \phi\left(-v''\sin\phi_0 + w''\cos\phi_0\right)\right] \\ & + \zeta\left[v''\sin\phi_0 - w''\cos\phi_0 + \phi\left(v''\cos\phi_0 + w''\sin\phi_0\right)\right]\end{aligned} \tag{22}$$

Then, substituting equation (22) into equation (21) and ignoring the u' term since it is one order of magnitude higher than the other displacements, we get

$$\begin{aligned}\text{Work of Centrifugal Tension} = \int_0^R T\Big\{ & -\frac{1}{2}\left[(v')^2 + (w')^2\right] \\ & + e_A\left(v''\cos\phi_0 + w''\sin\phi_0\right) - e_A\,\phi\left(v''\sin\phi_0 - w''\cos\phi_0\right) \\ & - K_A^2\left[\frac{1}{2}(\phi')^2 + \phi_0'\phi'\right]\Big\}\, d\xi\end{aligned} \tag{23}$$

Substituting equations (23) and (20) into equations (9) and (7) respectively, and ignoring the term $\frac{T^2}{EA}$ which does not contribute in the variation of π, we get

$$\begin{aligned}
\pi = \frac{1}{2}\int_0^R \Big\{ & \left[EI_1 \sin^2\phi_0 + EI_2 \cos^2\phi_0\right](v'')^2 + \left[EI_1 \cos^2\phi_0 \right. \\
& \left. + EI_2 \sin^2\phi_0\right](w'')^2 + 2\cos\phi_0 \sin\phi_0\left[EI_2 - EI_1\right]v''w'' \\
& + \left[GJ + EB_1(\phi_0')^2\right](\phi')^2 - 2EB_2 \cos\phi_0\, \phi_0' v'' \phi' \\
& - 2EB_2 \sin\phi_0\, \phi_0' w'' \phi \Big\} d\xi \\
- \int_0^R \Big(\int_x^R p_x\, dx\Big) \Big\{ & -\frac{1}{2}\left[(v')^2 + (w')^2\right] + e_A\left[v''\cos\phi_0 \right. \\
& \left. + w''\sin\phi_0\right] - e_A\phi\left[v''\sin\phi_0 - w''\cos\phi_0\right] \\
& - K_A^2\left[\frac{1}{2}(\phi')^2 + \phi_0'\phi'\right]\Big\} d\xi \\
- \int_0^R p_y v\, dx & - \int_0^R p_z w\, dx - \int_0^R q_\xi \phi\, d\xi \\
- \int_0^R q_y w'\, dx & - \int_0^R q_z v'\, dx \qquad (24)
\end{aligned}$$

Note that rotation ϕ is about the deformed ξ axis and hence the work done would involve q_ξ rather than q_x.

The above functional π is equivalent to the one given in Ref. 1.

2.3 Forces and Moments Applied on the Blade

(a) Blade Absolute Acceleration Vector

It is essential to know the magnitudes of the absolute acceleration components along the x,y,z system of axes (undeformed blade axes) to be able to formulate the inertial (D'Alambert) loadings exerted on the structure.

A systematic way this can be done without losing Coriolis and Centrifugal effects is the following:

Assume a point on the undeformed elastic axis to be displaced by u,v,w and then the cross-section to be rotated by ϕ (Figure 2).

The global coordinates of any point A of the above cross-section will be, according to equation (3),

$$\begin{Bmatrix} X \\ Y \\ Z \end{Bmatrix} = \underset{\sim}{S} \begin{Bmatrix} x \\ y \\ z \end{Bmatrix} + e_o \begin{Bmatrix} \cos\Omega t \cos\phi_o \\ \sin\Omega t \cos\phi_o \\ \sin\phi_o \end{Bmatrix}$$

where, according to equation (1),

$$\begin{Bmatrix} x \\ y \\ z \end{Bmatrix} = \begin{Bmatrix} \xi + u \\ v \\ w \end{Bmatrix} + \underset{\sim}{F} \begin{Bmatrix} 0 \\ \eta \\ \zeta \end{Bmatrix}$$

Matrices S and F are given in equations (4) and (2b) respectively.

Substituting equation (1) into equation (3) and differentiating equation (3) twice with respect to time, we get the absolute accelerations with respect to the fixed system of axes:

$$\begin{Bmatrix} \ddot{X} \\ \ddot{Y} \\ \ddot{Z} \end{Bmatrix} = \underset{\sim}{S} \begin{Bmatrix} \ddot{u} \\ \ddot{v} \\ \ddot{w} \end{Bmatrix} + 2 \underset{\sim}{\mathring{S}} \begin{Bmatrix} \mathring{u} \\ \dot{v} \\ \dot{w} \end{Bmatrix} + \underset{\sim}{\ddot{S}} \begin{Bmatrix} \xi + u \\ v \\ w \end{Bmatrix} +$$

$$+ \left(\underset{\sim}{\ddot{S}} \underset{\sim}{F} + 2 \underset{\sim}{\dot{S}} \underset{\sim}{\dot{F}} + \underset{\sim}{S} \underset{\sim}{\ddot{F}} \right) \begin{Bmatrix} 0 \\ \eta \\ \zeta \end{Bmatrix}$$

$$+ \Omega^2 e_o \begin{Bmatrix} -\cos \Omega t \cos \beta \\ -\sin \Omega t \sin \beta \\ 0 \end{Bmatrix} \tag{25}$$

Resolving these accelerations along the x,y,z system of axes we get the required components

$$\begin{Bmatrix} \alpha_x \\ \alpha_y \\ \alpha_z \end{Bmatrix} = \underset{\sim}{S}^T \begin{Bmatrix} \ddot{X} \\ \ddot{Y} \\ \ddot{Z} \end{Bmatrix} = \begin{Bmatrix} \ddot{u} \\ \ddot{v} \\ \ddot{w} \end{Bmatrix} + 2 \underset{\sim}{S}^T \underset{\sim}{\mathring{S}} \begin{Bmatrix} \mathring{u} \\ \dot{v} \\ \mathring{w} \end{Bmatrix} +$$

$$+ \underset{\sim}{S}^T \underset{\sim}{\ddot{S}} \begin{Bmatrix} \xi + u \\ v \\ w \end{Bmatrix} + \left(\underset{\sim}{S}^T \underset{\sim}{\ddot{S}} \underset{\sim}{F} + 2 \underset{\sim}{S}^T \underset{\sim}{\mathring{S}} \underset{\sim}{\dot{F}} + \right.$$

$$\left. + \underset{\sim}{\ddot{F}} \right) \begin{Bmatrix} 0 \\ \eta \\ \zeta \end{Bmatrix} + \Omega^2 e_o \begin{Bmatrix} -\cos(\beta + \delta) \cos \beta \\ 0 \\ \sin(\beta + \delta) \cos \beta \end{Bmatrix} \tag{26}$$

where

$$
\underset{\sim}{S}^T \underset{\sim}{\mathring{\mathring{S}}}\,\underset{\sim}{F} + 2\underset{\sim}{S}^T \underset{\sim}{\mathring{S}}\,\underset{\sim}{\mathring{F}} + \underset{\sim}{\mathring{\mathring{F}}} =
\left[\begin{array}{l:l:l}
\begin{array}{l} -\Omega^2\cos^2(\beta+\delta) \\ +\Omega^2\sin(\beta+\delta)\cos(\beta+\delta)w' \\ -2\Omega\cos(\beta+\delta)\mathring{v}' \end{array} &
\begin{array}{l} \Omega^2\cos^2(\beta+\delta)[w'\sin\phi_0 + v'\cos\phi_0] \\ +\Omega^2\sin(\beta+\delta)\cos(\beta+\delta)[\sin\phi_0 + \phi\cos\phi_0] \\ +2\Omega\mathring{\phi}\sin\phi_0\cos(\beta+\delta) - \mathring{\mathring{w}}'\sin\phi_0 - \\ -\mathring{\mathring{v}}'\cos\phi_0 \end{array} &
\begin{array}{l} \Omega^2\cos^2(\beta+\delta)[w'\cos\phi_0 - v'\sin\phi_0] \\ +\Omega^2\sin(\beta+\delta)\cos(\beta+\delta)[\cos\phi_0 \\ -\phi\sin\phi_0] + 2\Omega\mathring{\phi}\cos\phi_0\cdot \\ \cdot\cos(\beta+\delta) - \mathring{\mathring{w}}'\cos\phi_0 + \mathring{\mathring{v}}'\sin\phi_0 \end{array} \\ \hdashline
\begin{array}{l} -\Omega^2 v' + 2\Omega\cos(\beta+\delta) \\ -2\Omega\sin(\beta+\delta)\mathring{w}' \\ +\mathring{\mathring{v}}' \end{array} &
\begin{array}{l} \Omega^2\phi\sin\phi_0 - \Omega^2\cos\phi_0 - 2\Omega\cos(\beta+\delta)\cdot \\ \cdot[\mathring{w}'\sin\phi_0 + \mathring{v}'\cos\phi_0] - 2\Omega\sin(\beta+\delta)\cdot \\ \cdot\mathring{\phi}\cos\phi_0 - \mathring{\mathring{\phi}}\sin\phi_0 \end{array} &
\begin{array}{l} \Omega^2\sin\phi_0 + \Omega^2\phi\cos\phi_0 + 2\Omega\cdot \\ \cdot\cos(\beta+\delta)[-\mathring{w}'\cos\phi_0 + \mathring{v}'\sin\phi_0] \\ +2\Omega\mathring{\phi}\sin\phi_0\sin(\beta+\delta) - \\ -\mathring{\mathring{\phi}}\cos\phi_0 \end{array} \\ \hdashline
\begin{array}{l} \Omega^2\sin(\beta+\delta)\cos(\beta+\delta) \\ -\Omega^2\sin^2(\beta+\delta)w' \\ +2\Omega\sin(\beta+\delta)\mathring{v}' \\ +\mathring{\mathring{w}}' \end{array} &
\begin{array}{l} \Omega^2\sin(\beta+\delta)\cos(\beta+\delta)[-w'\sin\phi_0 - \\ -v'\cos\phi_0] - \Omega^2\sin^2(\beta+\delta)[\sin\phi_0 \\ +\phi\cos\phi_0] - 2\Omega\mathring{\phi}\sin\phi_0\sin(\beta+\delta) \\ +\mathring{\mathring{\phi}}\cos\phi_0 \end{array} &
\begin{array}{l} \Omega^2\sin(\beta+\delta)\cos(\beta+\delta)[-w'\cos\phi_0 \\ +v'\sin\phi_0] - \Omega^2\sin^2(\beta+\delta)\cdot \\ \cdot[\cos\phi_0 - \phi\sin\phi_0] - 2\Omega\mathring{\phi}\cos\phi_0\cdot \\ \cdot\sin(\beta+\delta) - \mathring{\mathring{\phi}}\sin\phi_0 \end{array}
\end{array}\right]
$$

$$
\underset{\sim}{S}^T \underset{\sim}{\mathring{S}} = \Omega\left[\begin{array}{c:c:c} 0 & -\cos(\beta+\delta) & 0 \\ \hdashline \cos(\beta+\delta) & 0 & -\sin(\beta+\delta) \\ \hdashline 0 & \sin(\beta+\delta) & 0 \end{array}\right], \quad
\underset{\sim}{S}^T \underset{\sim}{\mathring{\mathring{S}}} = \Omega^2\left[\begin{array}{c:c:c} -\cos^2(\beta+\delta) & 0 & \sin(\beta+\delta)\cdot\cos(\beta+\delta) \\ \hdashline 0 & -1 & 0 \\ \hdashline \sin(\beta+\delta)\cdot\cos(\beta+\delta) & 0 & -\sin^2(\beta+\delta) \end{array}\right]
$$

( ) D'Alambert Forces and Moments

Since the components of the absolute acceleration vector have been found, we can now proceed to evaluate the inertia loading thus induced on the structure.

Assume that a point on the elastic axis of the blade is allowed to be displaced by a set of small virtual displacements δu, δv, δw and $\delta\phi$ due to the action of the real inertia loadings. These virtual displacements will create a virtual change at the x,y,z coordinates of any point A on the cross-section, i.e., δx, δy, δz respectively. These virtual changes will be obtained by taking the first variation of equation (1) and using the F matrix as given in equation (2a). The expressions thus obtained are listed below:

$$\begin{aligned}
\delta x &= \delta u - \Big[\big[\eta\cos(\phi_0+\phi) - \zeta\sin(\phi_0+\phi)\big]w' + \big[-\eta\sin(\phi_0+\phi) - \\
&\qquad -\zeta\cos(\phi_0+\phi)\big]v'\Big]\delta\phi - \big[\eta\sin(\phi_0+\phi) + \zeta\cos(\phi_0+\phi)\big]\delta w' \\
&\qquad -\big[\eta\cos(\phi_0+\phi) - \zeta\sin(\phi_0+\phi)\big]\delta v' \\
\delta y &= \delta v + \big[-\eta\sin(\phi_0+\phi) - \zeta\cos(\phi_0+\phi)\big]\delta\phi \\
\delta z &= \delta w + \big[\eta\cos(\phi_0+\phi) - \zeta\sin(\phi_0+\phi)\big]\delta\phi
\end{aligned} \tag{27}$$

The virtual work done then by the inertia loading during the above virtual change of coordinates δx, δy, δz will be

$$\delta W = \iiint_{V}\left\{(-\alpha_x)\delta x + (-\alpha_y)\delta y + (-\alpha_z)\delta z\right\}\rho_b\, d\xi\, d\eta\, d\zeta \tag{28}$$

where the minus sign of the acceleration components is to make them inertia components.

Substitution of equations (27) for δx, δy, δz into the virtual work equation (28) will give

$$\delta W = \int_0^R \left\{ p_x \delta u + p_y \delta v + p_z \delta w + q_\xi \delta \phi + q_y \delta w' + q_z \delta v' \right\} d\xi \tag{29}$$

where the inertia loadings will be

$$\begin{aligned}
p_x &= \iint_A \rho_b(-\alpha_x)\, d\eta\, d\zeta \\
p_y &= \iint_A \rho_b(-\alpha_y)\, d\eta\, d\zeta \\
p_z &= \iint_A \rho_b(-\alpha_z)\, d\eta\, d\zeta \\
q_\xi &= \iint_A \rho_b(-\alpha_x)\left[(v-y)w' + (z-w)v'\right] d\eta\, d\zeta + \iint_A \rho_b(-\alpha_y)(w \\
&\quad - z)\, d\eta\, d\zeta + \iint_A \rho_b(-\alpha_z)(y-v)\, d\eta\, d\zeta \\
q_y &= \iint_A \rho_b(-\alpha_x)(w-z)\, d\eta\, d\zeta \\
q_z &= \iint_A \rho_b(-\alpha_x)(v-y)\, d\eta\, d\zeta .
\end{aligned} \tag{30}$$

Substituting the equations (26) for α_x, α_y, α_z previously found, into equations (30) for the loadings, deleting all non-linear terms and all u terms, since u and its derivatives are much smaller than v,w, ϕ and their derivatives, we get the equations of the six loadings as presented in Appendix A.

(c) Blade Absolute Velocity Vector

To be able to perform flutter analysis, we must know the aerodynamic forces exerted on the blade during its rotary and vibratory motion, which means that we have to know the velocity field induced around the blade. This velocity field will be different at different points on the cross-section of the blade. To avoid this difficulty we will take as a reference value for the velocity, the value at the aerodynamic center which is at the elastic axis in our case, i.e., at

$$\eta = \zeta = 0 \tag{31}$$

Similarly, as before, allowing a point A on the elastic axis to be displaced by u,v,w and then the cross-section to be rotated by ϕ , the global coordinates of this point will be, using equations (1), (3) and (31),

$$\begin{Bmatrix} X \\ Y \\ Z \end{Bmatrix} = \underset{\sim}{S} \begin{Bmatrix} \xi + u \\ v \\ w \end{Bmatrix} + e_o \begin{Bmatrix} \cos\Omega t \cos\beta \\ \sin\Omega t \cos\beta \\ \sin\beta \end{Bmatrix} \tag{32}$$

Differentiating the above expression with respect to time we can obtain the absolute blade velocity with respect to the global system of axes

$$\begin{Bmatrix} \overset{\circ}{X} \\ \overset{\circ}{Y} \\ \overset{\circ}{Z} \end{Bmatrix} = \underset{\sim}{S} \begin{Bmatrix} \overset{\circ}{u} \\ \overset{\circ}{v} \\ \overset{\circ}{w} \end{Bmatrix} + \overset{\circ}{\underset{\sim}{S}} \begin{Bmatrix} \xi + u \\ v \\ w \end{Bmatrix} + e_o \begin{Bmatrix} -\Omega \sin\Omega t \cos\beta \\ \Omega \cos\Omega t \cos\beta \\ 0 \end{Bmatrix} \tag{33}$$

where S was given in equation (4).

This absolute blade velocity is due to the vibratory and rotary motion of the blade and it is taken positive along the direction of the unit vectors $\vec{I}\ \vec{J}\ \vec{K}$. Hence, the equivalent air velocity to this blade motion will be equal in magnitude with the blade velocity but taken positive along the direction opposite to $\vec{I}\ \vec{J}\ \vec{K}$ (see Figure 4a).

Allowing the air free stream to have velocity components U_w, V_w, and W_w with respect to the X Y Z system of axes and the induced velocity v_i to be in a direction opposite to W_w (see Figure 4b for positive directions of all air velocities), then

$$\text{Total air velocity} = \text{Blade velocity} + \text{Free air velocity} - \text{Induced velocity}$$

$$= \begin{Bmatrix} \mathring{X} \\ \mathring{Y} \\ \mathring{Z} \end{Bmatrix} + \begin{Bmatrix} U_w \\ V_w \\ W_w \end{Bmatrix} - \begin{Bmatrix} 0 \\ 0 \\ v_i \end{Bmatrix} \tag{34}$$

Resolving the total air velocity of the above expression along the xyz system of axes, according to equation (6b) we get

$$\begin{Bmatrix} U_x \\ U_y \\ U_z \end{Bmatrix} = \underset{\sim}{S}^T \begin{Bmatrix} \mathring{X} + U_w \\ \mathring{Y} + V_w \\ \mathring{Z} + W_w - v_i \end{Bmatrix} \tag{35}$$

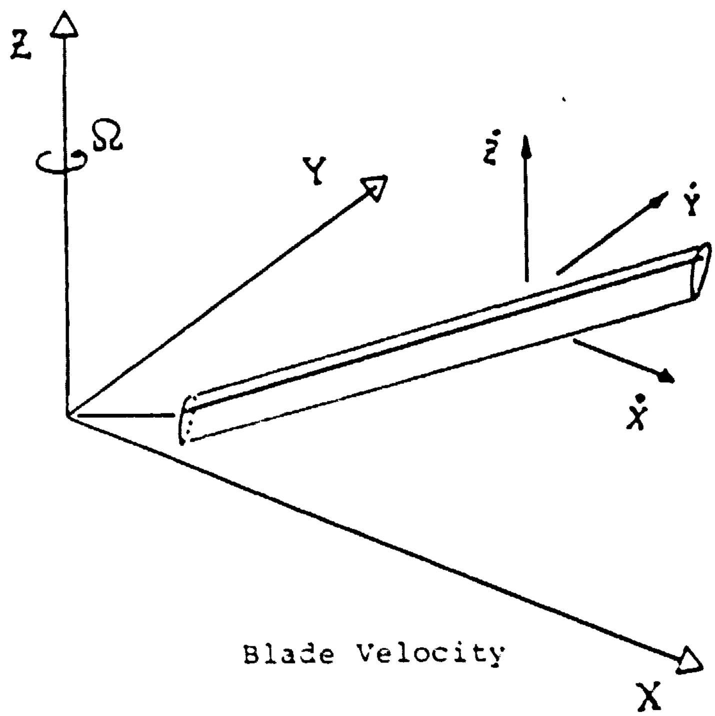

Blade Velocity

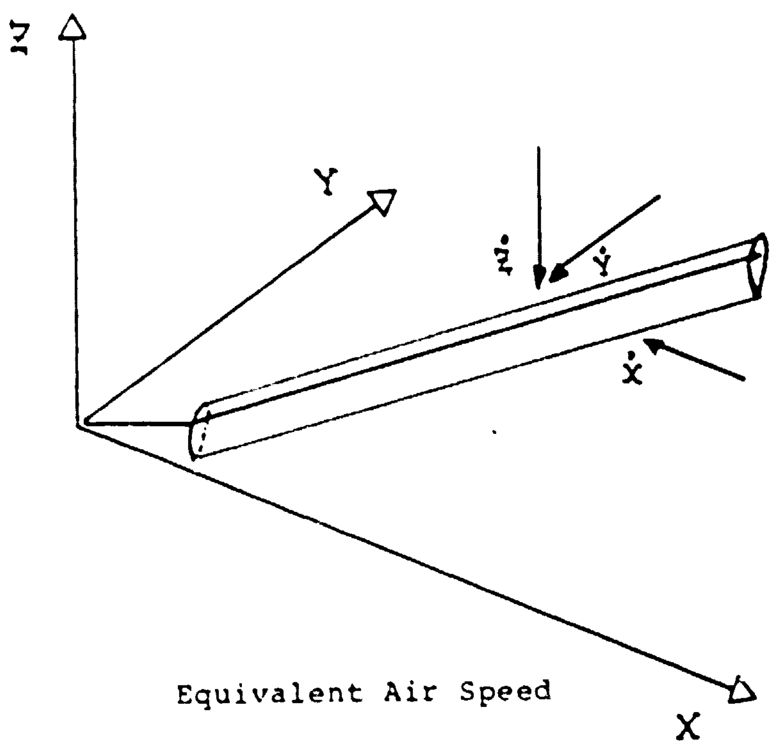

Equivalent Air Speed

Figure 4a

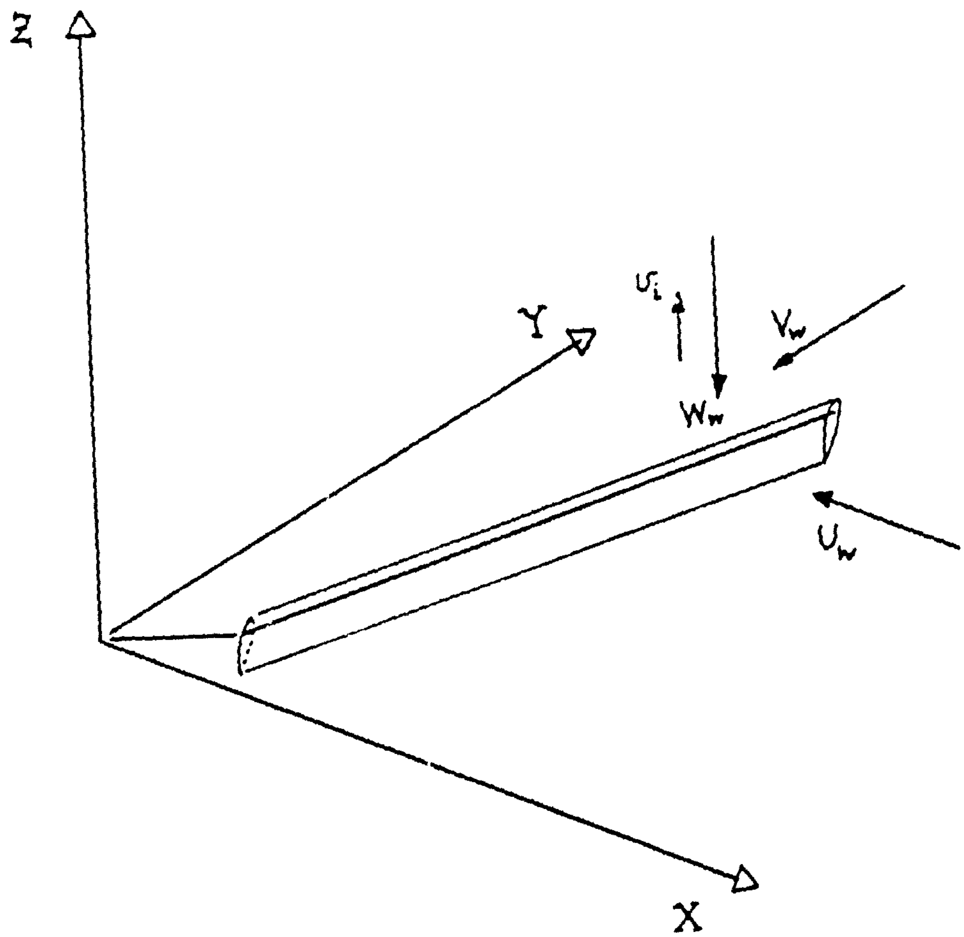

Figure 4b

Further on we will have to resolve these components along the deformed blade since we are interested in the aerodynamic loads after deformation of the blade. Air velocities U_ξ, U_η and U_ζ are going to be taken positive along the negative $\vec{i}_\xi$ $\vec{i}_\eta$ $\vec{i}_\zeta$ unit vectors. Hence according to equation (6a)

$$\begin{Bmatrix} U_\xi \\ U_\eta \\ U_\zeta \end{Bmatrix} = \underset{\sim}{F}^T \begin{Bmatrix} U_x \\ U_y \\ U_z \end{Bmatrix} \tag{36}$$

where

U_ξ = radial component of velocity

U_η = tangential component of velocity

U_ζ = perpendicular component of velocity

Substituting equations (33) and (35) into equation (36) we get

$$\begin{Bmatrix} U_\xi \\ U_\eta \\ U_\zeta \end{Bmatrix} = \underset{\sim}{F}^T \begin{Bmatrix} \dot{u} \\ \dot{v} \\ \dot{w} \end{Bmatrix} + \underset{\sim}{F}^T \underset{\sim}{S}^T \dot{\underset{\sim}{S}} \begin{Bmatrix} u+\xi \\ v \\ w \end{Bmatrix} + \underset{\sim}{F}^T \underset{\sim}{S}^T \begin{Bmatrix} U_w \\ V_w \\ W_w - v_i \end{Bmatrix}$$

$$+ \underset{\sim}{F}^T \underset{\sim}{S}^T e_o \begin{Bmatrix} -\Omega \sin\Omega t \cos\beta \\ \Omega \cos\Omega t \cos\beta \\ 0 \end{Bmatrix} \tag{37}$$

where $\underset{\sim}{F}$ is given in equation (6a)

Since the radial component of velocity is much smaller than the perpendicular and tangential ones we can neglect its contribution to the aerodynamic forces. Also the u displacement and all its derivatives are much smaller than the corresponding v and w ones. Hence all the u terms and their derivatives can be neglected in the U_η and U_ζ equations.

Presenting U_η and U_ζ explicitely (after nonlinear terms have been deleted) we have

$$\begin{aligned} U_\eta = {} & \cos\phi_0\,\mathring{v} + \sin\phi_0\,\mathring{w} + \Omega\sin(\beta+\delta)\sin\phi_0\,v - \Omega\sin(\beta+\delta)\cdot \\ & \cdot\cos\phi_0\,w - \Omega\sin\phi_0\left\{\xi\cos(\beta+\delta) + e_0\cos\beta\right\}\phi + \Omega\,\xi\cos(\beta \\ & +\delta)\cos\phi_0 + \Omega e_0\cos\beta\cos\phi_0 + U_w\Big\{-\cos\Omega t\cos(\beta+\delta)\cdot \\ & (w'\sin\phi_0 + v'\cos\phi_0) - \sin\Omega t(\cos\phi_0 - \phi\sin\phi_0) - \cos\Omega t\cdot \\ & \cdot\sin(\beta+\delta)(\sin\phi_0 + \phi\cos\phi_0)\Big\} + V_w\Big\{-\sin\Omega t\cos(\beta+\delta)(w'\cdot \\ & \sin\phi_0 + v'\cos\phi_0) + \cos\Omega t(\cos\phi_0 - \phi\sin\phi_0) - \sin\Omega t\sin(\beta+\delta)\cdot \\ & (\sin\phi_0 + \phi\cos\phi_0)\Big\} + (W_w - v_i)\Big\{-\sin(\beta+\delta)(w'\sin\phi_0 + \\ & + v'\cos\phi_0) + \cos(\beta+\delta)(\sin\phi_0 + \phi\cos\phi_0)\Big\} \end{aligned} \quad (38$$

$$\begin{aligned} U_\zeta = {} & -\sin\phi_0\,\mathring{v} + \cos\phi_0\,\mathring{w} + \Omega\sin(\beta+\delta)\cos\phi_0\,v + \Omega\sin(\beta+\delta)\cdot \\ & \sin\phi_0\,w - \Omega\cos\phi_0\left\{\xi\cos(\beta+\delta) + e_0\cos\beta\right\}\phi - \Omega\,\xi\cos(\beta \\ & +\delta)\sin\phi_0 - \Omega e_0\cos\beta\sin\phi_0 + U_w\Big\{\cos\Omega t\cos(\beta+\delta)\cdot \\ & \cdot(-w'\cos\phi_0 + v'\sin\phi_0) + \sin\Omega t(\sin\phi_0 + \phi\cos\phi_0) - \cos\Omega t\cdot \\ & \cdot\sin(\beta+\delta)(\cos\phi_0 - \phi\sin\phi_0)\Big\} + V_w\Big\{\sin\Omega t\cos(\beta+\delta)(-w'\cdot \\ & \cdot\cos\phi_0 + v'\sin\phi_0) - \cos\Omega t(\sin\phi_0 + \phi\cos\phi_0) - \sin\Omega t\cdot \\ & \cdot\sin(\beta+\delta)(\cos\phi_0 - \phi\sin\phi_0)\Big\} + (W_w - v_i)\Big\{\sin(\beta+\delta)\cdot \\ & (-w'\cos\phi_0 + v'\sin\phi_0) + \cos(\beta+\delta)(\cos\phi_0 - \phi\sin\phi_0)\Big\} \end{aligned} \quad (38$$

Also since the blade is allowed to pitch to the free stream, we can define this pitch to be ϵ taken positive in the clockwise direction. Then the rate of pitch $\mathring{\epsilon}$, which is along the $\vec{l}_\xi$ direction, to first order terms, will be obtained from

$$[\omega_\xi \;\; \omega_\eta \;\; \omega_\zeta]\begin{Bmatrix}\vec{i}_\xi\\ \vec{i}_\eta\\ \vec{i}_\zeta\end{Bmatrix} = [\overset{\circ}{\phi}\;0\;0]\begin{Bmatrix}\vec{i}_\xi\\ \vec{i}_\eta\\ \vec{i}_\zeta\end{Bmatrix} + [0\; -\overset{\circ}{w}'\; \overset{\circ}{v}']\begin{Bmatrix}\vec{i}_x\\ \vec{i}_y\\ \vec{i}_z\end{Bmatrix} + [0\;0\;\Omega]\begin{Bmatrix}\vec{I}\\ \vec{J}\\ \vec{K}\end{Bmatrix}$$

$$= \left([\overset{\circ}{\phi}\;0\;0] + [0\; -\overset{\circ}{w}'\; \overset{\circ}{v}']\underset{\sim}{F} + [0\;0\;\Omega]\underset{\sim}{S}\,\underset{\sim}{F}\right)\begin{Bmatrix}\vec{i}_\xi\\ \vec{i}_\eta\\ \vec{i}_\zeta\end{Bmatrix}$$

Hence, to first order terms

$$\overset{\circ}{\epsilon} = \omega_\xi = \overset{\circ}{\phi} + \Omega\sin(\beta+\delta) + \Omega\cos(\beta+\delta)w' \tag{39}$$

(d) Aerodynamic Forces and Moments

The aerodynamic loads are formulated according to strip theory; i.e., assuming that only the velocity components perpendicular to the ξ axis (deformed elastic axis) influence the aerodynamic loads.

The convention used for positive air velocities U_η, U_ζ angle of incidence α, lift L, drag D, and pitching moment M. is displayed in figure 5, according to which all velocities and forces are taken positive along the opposite $\vec{i}_\eta$, $\vec{i}_\zeta$ directions while α and M are taken anticlockwise as positive (nose-up).

Assuming that the blade is vertically displaced with velocity $\overset{\circ}{h}$, being positive downwards, and is pitched up at an angle ϵ to the free stream, the total lift and aerodynamic moment will be respectively

$$\begin{aligned} L &= L_c + L_{NC} \\ M &= M_c + M_{NC} \end{aligned} \tag{40}$$

in terms of their Circulatory and Non-Circulatory components.

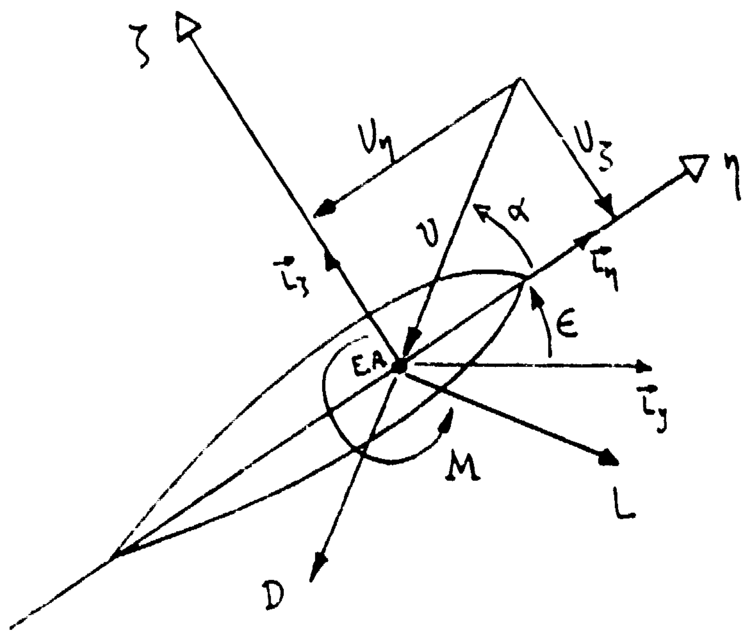

Figure 5

Greenberg theory provides the values for L_c , L_{NC}, M_c and M_{NC} for two dimensional oscillating airfoil in a pulsating incompressible flow V, the airfoil being pivoted about the quarter-chord point which is the aerodynamic centre and the elastic axis (See Ref. (71)).

$$
\begin{aligned}
L_c &= -\frac{1}{2}\rho\alpha c V\left(\dot{h} + V\epsilon + \frac{c}{2}\dot{\epsilon}\right) \\
L_{NC} &= -\frac{1}{2}\rho\alpha c \frac{c}{4}\left(\ddot{h} + V\dot{\epsilon} + \dot{V}\epsilon + \frac{c}{4}\ddot{\epsilon}\right) \\
M_c &= -\frac{1}{2}\rho\alpha c\left(\frac{c}{4}\right)^2 V\dot{\epsilon} \\
M_{NC} &= -\frac{c}{4}L_{NC} - \frac{1}{2}\rho\alpha c\left(\frac{c}{4}\right)^3\frac{\ddot{\epsilon}}{2}
\end{aligned}
\tag{41}
$$

Since the blade is moving with speed $\dot{h}$ downwards then the equivalent air speed will be V_h upwards where

$$V_h = \dot{h}$$

Allowing the free air to approach the blade with velocity V (see figure 6), then projecting V and V_h along the η and ζ axes and applying the conventions for positive velocities stated before we get

$$
\begin{aligned}
U_\eta &= V\cos\epsilon - V_h\sin\epsilon \\
U_\zeta &= -V_h\cos\epsilon - V\sin\epsilon
\end{aligned}
$$

For small angles ϵ , $\cos\epsilon \approx 1$, $\sin\epsilon \approx \epsilon$ and since $V_h < V$, one has

$$
\begin{aligned}
U_\eta &\cong V \\
U_\zeta &\cong -\dot{h} - V\epsilon
\end{aligned}
\tag{42}
$$

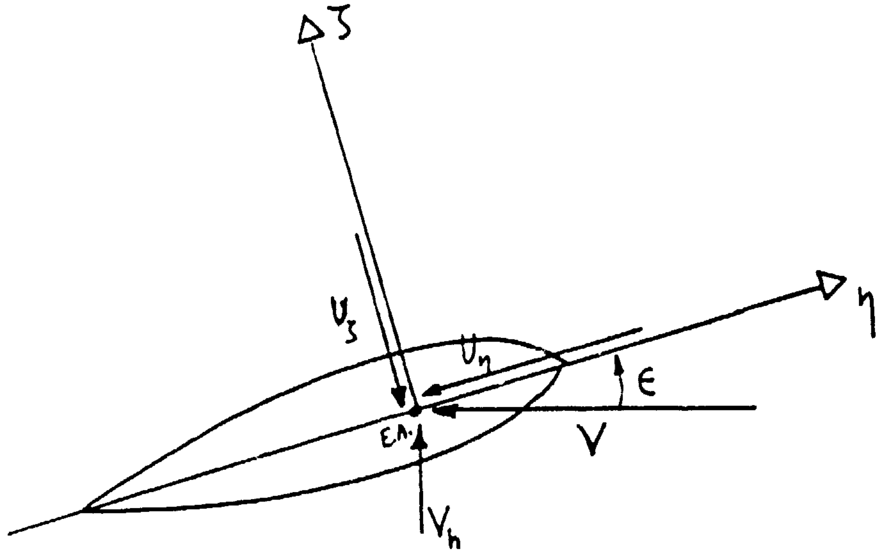

Figure 6

Also, since

$$U_\zeta < U_\eta \qquad \therefore \qquad U_\zeta^2 << U_\eta^2$$

then
$$U = \sqrt{U_\zeta^2 + U_\eta^2} \approx U_\eta \approx V$$

substituting equation (42) into the lift equation (41) we get

$$\begin{aligned} L_c &= -\frac{1}{2}\rho a c\, U\left(-U_\zeta + \frac{c}{2}\mathring{\epsilon}\right) \\ L_{NC} &= -\frac{1}{2}\rho a c\,\frac{c}{4}\left(-\mathring{U}_\zeta + \frac{c}{4}\mathring{\mathring{\epsilon}}\right) \end{aligned} \tag{43}$$

The drag force D will be

$$D = \frac{1}{2}\rho a c\,\frac{C_{d_0}}{a}U^2 \tag{44}$$

Constructing then figure 7, we can write force equilibrium equations for forces F_η and F_ζ exerted on the blade and being positive along the positive $\vec{L}_\eta$ and $\vec{L}_\zeta$ directions.

$$\begin{aligned} F_\eta &= L_c \sin\alpha - D\cos\alpha \\ F_\zeta &= -L_c\cos\alpha - D\sin\alpha - L_{NC} \end{aligned} \tag{45}$$

and

$$\cos\alpha = \frac{U_\eta}{U} \qquad \sin\alpha = \frac{U_\zeta}{U}$$

Hence substituting equations (43) and (44) into equations (45) we get

$$F_\zeta = \frac{1}{2}\rho a c\left[-\frac{c}{4}\mathring{U}_\zeta + \left(\frac{c}{4}\right)^2\mathring{\mathring{\epsilon}} - \left(1+\frac{C_{d_0}}{a}\right)U_\zeta U_\eta + \frac{c}{2}U_\eta\mathring{\epsilon}\right] \tag{46a}$$

$$F_\eta = \frac{1}{2}\rho a c\left[U_\zeta^2 - \frac{c}{2}\mathring{\epsilon}U_\zeta - \frac{C_{d_0}}{a}U_\eta^2\right] \tag{46b}$$

$$M = \frac{1}{2}\rho a c\left(\frac{c}{4}\right)^2\left[U_\eta\mathring{\epsilon} - \mathring{U}_\zeta + \frac{3c}{8}\mathring{\mathring{\epsilon}}\right] \tag{46c}$$

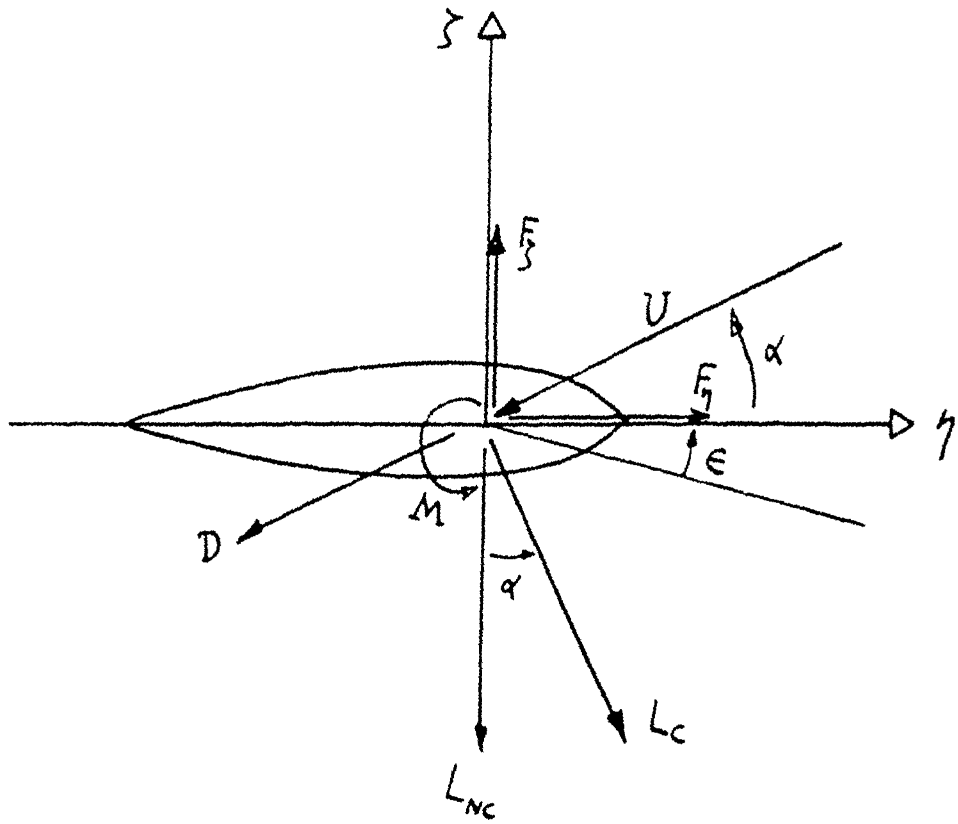

Figure 7

The convention used in this report for positive forces $p_x\ p_y\ p_z$ and moments $q_\xi\ q_y\ q_z$ along the xyz system of axes, is displayed in figure (8).

Transforming equations (46 a,b,c) from the ξ, η, ζ axes to the xyz axes using equation (6a) we get for the forces

$$\begin{Bmatrix} p_x \\ p_y \\ p_z \end{Bmatrix} = \underset{\sim}{E} \begin{Bmatrix} 0 \\ F_\eta \\ F_\zeta \end{Bmatrix}$$

or for the complete loading

$$\begin{aligned}
p_x &= \left(-w'\sin\phi_o - v'\cos\phi_o\right)F_\eta + \left(-w'\cos\phi_o + v'\sin\phi_o\right)F_\zeta \\
p_y &= \left(\cos\phi_o - \phi\sin\phi_o\right)F_\eta + \left(-\sin\phi_o - \phi\cos\phi_o\right)F_\zeta \\
p_z &= \left(\sin\phi_o + \phi\cos\phi_o\right)F_\eta + \left(\cos\phi_o - \phi\sin\phi_o\right)F_\zeta \\
q_\xi &= M \simeq q_x \\
q_y &= -Mv' \\
q_z &= Mw'
\end{aligned} \tag{47}$$

Note the negative sign on q_y due to the convention for q_y adopted in figure 8.

Substituting equations (38a,b) and (39) into equations (46a,b,c) and then into equations (47) we can express all the six loadings listed above, in the following general form

$$\begin{aligned}
\text{(Loading)} = {} & (\text{Coef})_1 \ddot{v} + (\text{Coef})_2 \ddot{w} + (\text{Coef})_3 \ddot{\phi} + (\text{Coef})_4 \mathring{v} \\
& + (\text{Coef})_5 \mathring{w} + (\text{Coef})_6 \mathring{\phi} + (\text{Coef})_7 v + (\text{Coef})_8 w \\
& + (\text{Coef})_9 \phi + (\text{Coef})_{10} \mathring{v}' + (\text{Coef})_{11} \mathring{w}' + (\text{Coef})_{12} v' \\
& + (\text{Coef})_{13} w' + (\text{Coef})_{14}
\end{aligned}$$

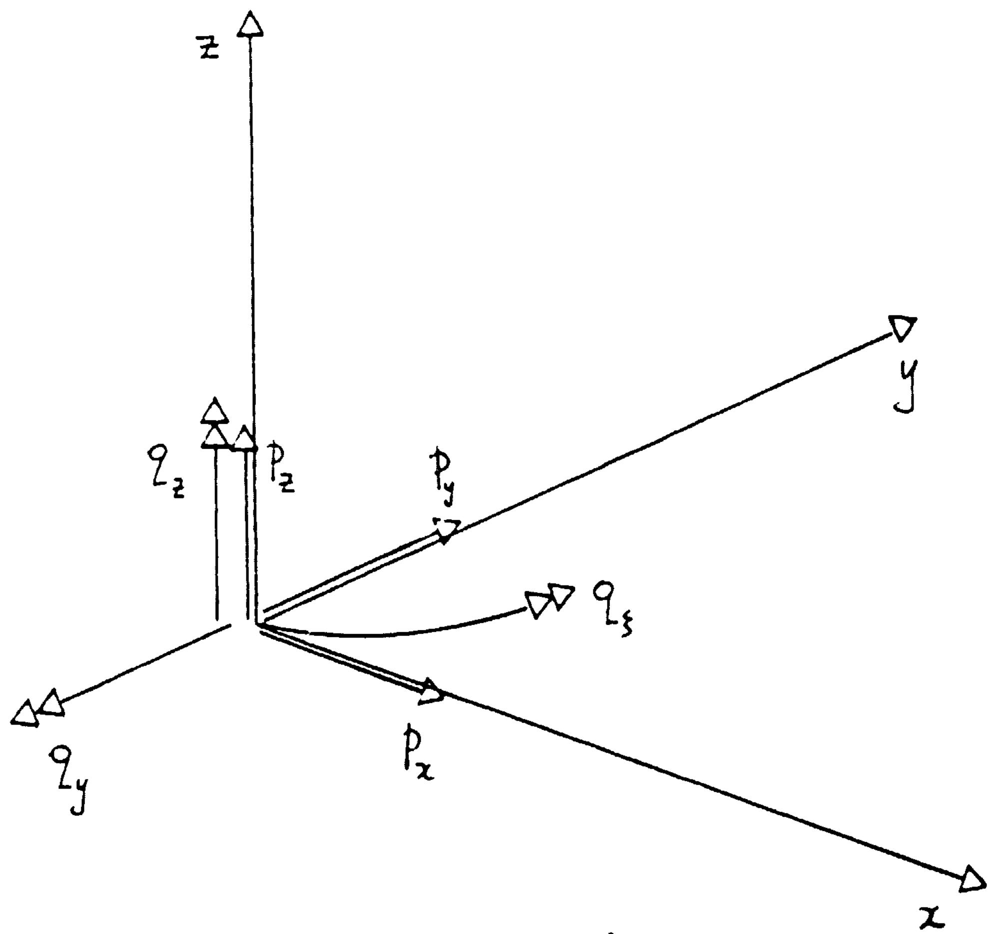

Figure 8

where the 14 coefficients for each loading are presented in appendix B.

It has to be noted that many of the terms in these coefficients are shown to have negligible contribution in the loading terms and hence they can be neglected.

2.4 Order of Magnitude Approximations

Throughout the analysis the following ordering scheme was adopted

Quantity	Order of Magnitude
e	0(1)
e_0	0(1)
e_A	0(1)
c	0(1)
$\sin(\beta+\delta)$	0(1)
ξ	0(0)
C_{d_0}/α	0(1)
u	0(2)
v	0(1)
w	0(1)
ϕ	0(1)
$K_{m_1}^2$	0(2)
$K_{m_2}^2$	0(2)
K_m^2	0(2)
K_A^2	0(2)
everything else	0(0)

It can be seen from the above table that u displacement is one order of magnitude higher than v and w. This is why terms including u and its derivatives have been neglected everywhere in our analysis.

Further on, the equations of equilibrium resulting after the first variation of the total potential energy of the blade, were kept up to second order terms 0(2) except in the torsion equation which was allowed to go up to third order terms 0(3) due to lack of first order terms 0(1). Doing this, the stiffness matrix of the structure became unsymmetric. To preserve symmetry, we had to allow up to third order terms in ϕ, in the v and w equations.

More explicitly, for all the inertia and aerodynamic loadings we have :

In the p_x loading

0(0) terms were kept together with up to 0(2) terms in v and w (all their derivatives have been neglected)

In the p_y, p_z, q_y, q_z loadings

Up to 0(2) terms in v and w and up to 0(3) terms in ϕ were kept.

In the q_ξ loading

Up to 0(3) terms were kept in v, w and ϕ.

Using the above approximations, many terms could be neglected from the inertia and aerodynamic laodings (See appendices A and B).

2.5 Finite Element Formulation

The blade was discretised into a number N of finite elements. In each element, the field variables were interpolated according to piecewise continuous interpolation functions. To satisfy the compatibility and completeness requirement for monotonic convergence to the true answer as the element size decreases (see Reference (9)), we had to prescribe v, v', w, w' and ϕ on each node of the structure. (See figure 9). The corresponding interpolation functions were:

Zeroth Order Hermitean Interpolation function H^0 for ϕ, and First Order Hermitean Interpolation function H^1 for v and w.

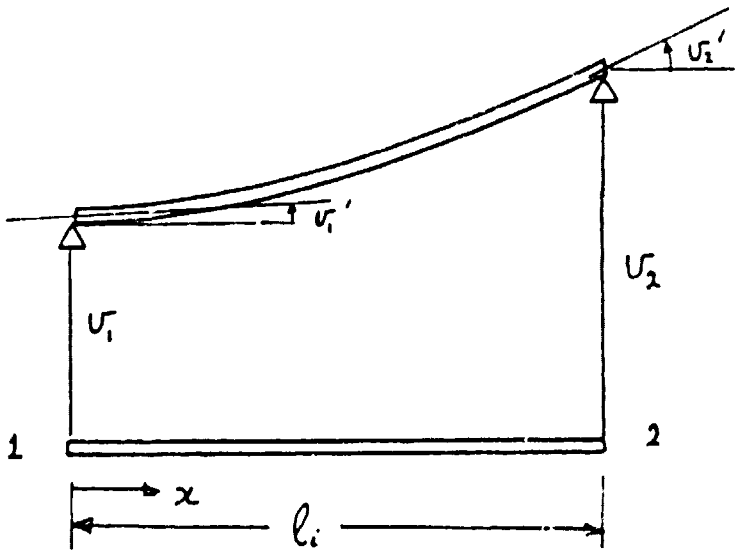

Similarly for w

Figure 9

Then

$$\begin{Bmatrix} v \\ w \\ \phi \end{Bmatrix} = \begin{bmatrix} \underset{\sim}{H}_1 & \underset{\sim}{0} & \underset{\sim}{0} \\ \underset{\sim}{0} & \underset{\sim}{H}_1 & \underset{\sim}{0} \\ \underset{\sim}{0} & \underset{\sim}{0} & \underset{\sim}{H}_0 \end{bmatrix} \begin{Bmatrix} \underset{\sim}{q}_v \\ \underset{\sim}{q}_w \\ \underset{\sim}{q}_\phi \end{Bmatrix} \tag{48}$$

$$\begin{aligned} \underset{\sim}{q}_v^T &= \left[v_1 \; v_1' \; v_2 \; v_2' \right] \\ \underset{\sim}{q}_w^T &= \left[w_1 \; w_1' \; w_2 \; w_2' \right] \\ \underset{\sim}{q}_\phi^T &= \left[\phi_1 \; \phi_2 \right] \end{aligned} \tag{49}$$

$$\begin{aligned} \underset{\sim}{H}_1 &= \left[H_{01}^1 \; H_{11}^1 \; H_{02}^1 \; H_{12}^1 \right] \\ \underset{\sim}{H}_0 &= \left[H_{01}^0 \; H_{02}^0 \right] \\ H_{01}^1 &= 2\left(\frac{x}{l_i}\right)^3 - 3\left(\frac{x}{l_i}\right)^2 + 1 \\ H_{11}^1 &= l_i\left[\left(\frac{x}{l_i}\right)^3 - 2\left(\frac{x}{l_i}\right)^2 + \frac{x}{l_i}\right] \\ H_{02}^1 &= -2\left(\frac{x}{l_i}\right)^3 + 3\left(\frac{x}{l_i}\right)^2 \\ H_{12}^1 &= l_i\left[\left(\frac{x}{l_i}\right)^3 - \left(\frac{x}{l_i}\right)^2\right] \\ H_{01}^0 &= 1 - \frac{x}{l_i} \\ H_{02}^0 &= \frac{x}{l_i} \end{aligned} \tag{50}$$

Substituting equations (48),(49) and (50) into (24) for the minimum total potential energy and taking the variation with respect to $\underset{\sim}{q}$ where

$$\underset{\sim}{q}^T = \sum_{\text{All N elements}} \left[\underset{\sim}{q}_v^T \; \underset{\sim}{q}_w^T \; \underset{\sim}{q}_\phi^T \right]$$

we get

$$(\underset{\sim}{K}_s + \underset{\sim}{K}_G)\,\underset{\sim}{q} = \underset{\sim}{Q} \tag{51}$$

where

K_s : Structural Stiffness Matrix (Assembled)

K_G : Geometric Stiffness Matrix (Assembled)

Q : Loading Vector (Assembled)

and

$$\underset{\sim}{K}_s = \sum_{\text{all N elem.}} \begin{bmatrix} b_1 \underset{\sim}{L}_1 & b_3 \underset{\sim}{L}_1 & b_4 \underset{\sim}{L}_2 \\ & b_2 \underset{\sim}{L}_1 & b_5 \underset{\sim}{L}_2 \\ \text{SYM} & & b_6 \underset{\sim}{L}_3 \end{bmatrix}$$

$$\underset{\sim}{K}_G = \sum_{\text{all N elem}} \left(\int_x^R p_x \, dx \right) \begin{bmatrix} \underset{\sim}{L}_4 & \underset{\sim}{0} & b_7 \underset{\sim}{L}_5 \\ & \underset{\sim}{L}_4 & b_8 \underset{\sim}{L}_5 \\ \text{SYM} & & b_9 \underset{\sim}{L}_3 \end{bmatrix}$$

$$\underset{\sim}{Q} = \sum_{\text{all N elem}} \left[\begin{array}{c} e_A \cos\phi_0 \int_x^R p_x \, dx \int_0^{l_i} \underset{\sim}{H}_1''^T d\xi + \int_0^{l_i} \underset{\sim}{H}_1^T p_y \, dx + \int_0^{l_i} H_1'^T q_z \, dx \\ \hdashline e_A \sin\phi_0 \int_x^R p_x \, dx \int_0^{l_i} H_1''^T d\xi + \int_0^{l_i} \underset{\sim}{H}_1^T p_z \, dx + \int_0^{l_i} \underset{\sim}{H}_1'^T q_y \, dx \\ \hdashline -K_A^2 \phi_0' \int_x^R p_x \, dx \int_0^{l_i} \underset{\sim}{H}_0'^T d\xi + \int_0^{l_i} \underset{\sim}{H}_0^T q_\xi \, d\xi \end{array} \right]$$

where the $\underset{\sim}{L}_i$ matrices are presented in appendix C and the b_i coefficients are

$$b_1 = EI_1 \cos^2\phi_o + EI_2 \sin^2\phi_o$$
$$b_2 = EI_1 \sin^2\phi_o + EI_2 \cos^2\phi_o$$
$$b_3 = (EI_2 - EI_1)\cos\phi_o \sin\phi_o$$
$$b_4 = -EB_2 \cos\phi_o (\phi_o')$$
$$b_5 = -EB_2 \sin\phi_o (\phi_o')$$
$$b_6 = GJ + EB_1 (\phi_o')^2$$
$$b_7 = e_A \sin\phi_o$$
$$b_8 = -e_A \cos\phi_o$$
$$b_9 = K_A^2$$

Substituting the reduced loading equations presented in appendices A and B into equation (51) we get

$$(\underset{\sim}{M}_A + \underset{\sim}{M}_S)\ddot{\underset{\sim}{q}} + (\underset{\sim}{C}_A + \underset{\sim}{C}_G)\dot{\underset{\sim}{q}} + \\ + (\underset{\sim}{K}_A + \underset{\sim}{K}_S + \underset{\sim}{K}_G + \underset{\sim}{K}_M)\underset{\sim}{q} = \underset{\sim}{Q}_{steady} \tag{52}$$

where

$\underset{\sim}{M}_A$ = Aerodynamic Mass Matrix
$\underset{\sim}{M}_S$ = Structural Mass Matrix
$\underset{\sim}{C}_A$ = Aerodynamic Damping Matrix
$\underset{\sim}{C}_G$ = Gyroscopic Matrix
$\underset{\sim}{K}_A$ = Aerodynamic Stiffness Matrix
$\underset{\sim}{K}_S$ = Structural Stiffness Matrix
$\underset{\sim}{K}_G$ = Geometric Stiffness Matrix

$\tilde{K}_M$ = Structural "Mass" Stiffness Matrix

$\tilde{Q}_{Steady}$ = Steady Load Vector

$$\tilde{M}_A = \sum_{all\ N_{elem.}} \begin{bmatrix} B_1 \tilde{L}_6 & B_2 \tilde{L}_6 & B_3 \tilde{L}_9^T \\ & \Gamma_2 \tilde{L}_6 & \Gamma_3 \tilde{L}_9^T \\ SYM & & \tilde{0} \end{bmatrix}$$

$$\tilde{M}_s = \sum_{all\ N_{elem}} \begin{bmatrix} \alpha_1 \tilde{L}_6 & \tilde{0} & \alpha_3 \tilde{L}_9^T \\ & \alpha_1 \tilde{L}_6 & \alpha_4 \tilde{L}_9^T \\ SYM & & \alpha_2 \tilde{L}_8 \end{bmatrix}$$

$$\tilde{C}_A = \sum_{all\ N_{elem.}} \left[\begin{array}{c:c:c} B_4 \tilde{L}_6 + B_{12} \tilde{L}_7 & B_5 \tilde{L}_6 + B_{13} \tilde{L}_7 & B_6 \tilde{L}_9^T \\ \hdashline \Gamma_4 \tilde{L}_6 + \Gamma_{12} \tilde{L}_7 & \Gamma_5 \tilde{L}_6 + \Gamma_{13} \tilde{L}_7 & \Gamma_6 \tilde{L}_9^T \\ \hdashline \Delta_{12} \tilde{L}_{10} & \Delta_{13} \tilde{L}_{10} & \Delta_6 \tilde{L}_8 \end{array}\right]$$

$$\tilde{C}_G = \sum_{all\ N_{elem.}} \left[\begin{array}{c:c:c} \tilde{0} & -\alpha_5 \tilde{L}_6 - \alpha_6 \tilde{L}_7 & -\alpha_{16} \tilde{L}_9^T - \alpha_{17} \tilde{L}_{10}^T \\ \hdashline \alpha_5 \tilde{L}_6 + \alpha_6 \tilde{L}_7 & \tilde{0} & -\alpha_{18} \tilde{L}_9^T - \alpha_{19} \tilde{L}_{10}^T \\ \hdashline \alpha_{16} \tilde{L}_9 + \alpha_{17} \tilde{L}_{10} & \alpha_{18} \tilde{L}_9 + \alpha_{19} \tilde{L}_{10} & \tilde{0} \end{array}\right]$$

K_s, K_G matrices were defined on page 56.

$$\underset{\sim}{K}_A = \sum_{\text{all } N \text{ elem.}} \left[\begin{array}{c:c:c} B_8 \underset{\sim}{L}_6 + B_{14} \underset{\sim}{L}_7 & B_9 \underset{\sim}{L}_6 + B_{15} \underset{\sim}{L}_7 + \Delta_{16} \underset{\sim}{L}_4 & B_{10} \underset{\sim}{L}_9^T \\ \hdashline \Gamma_8 \underset{\sim}{L}_6 + \Gamma_{14} \underset{\sim}{L}_7 - \Delta_{16} \underset{\sim}{L}_4 & \Gamma_9 \underset{\sim}{L}_6 + \Gamma_{15} \underset{\sim}{L}_7 & \Gamma_{10} \underset{\sim}{L}_9^T \\ \hdashline \Delta_{14} \underset{\sim}{L}_{10} & \Delta_{15} \underset{\sim}{L}_{10} & \Delta_{10} \underset{\sim}{L}_8 \end{array}\right]$$

$$\underset{\sim}{K}_M = \sum_{\text{all } N \text{ elem.}} \begin{bmatrix} \alpha_7 \underset{\sim}{L}_6 & \underset{\sim}{0} & \alpha_9 \underset{\sim}{L}_9^T - \alpha_{10} \underset{\sim}{L}_{10}^T \\ & \underset{\sim}{0} & \alpha_{11} \underset{\sim}{L}_{10}^T \\ \text{SYM} & & \alpha_8 \underset{\sim}{L}_8 \end{bmatrix}$$

$$Q_{steady} = \sum_{\text{all } N \text{ elem.}} \left[\begin{array}{l} e_A \cos\phi_0 \int_x^R p_x\, dx \int_0^{l_i} \underset{\sim}{H}_1''^T d\xi + (\alpha_{12} - B_{16}) \int_0^{l_i} \underset{\sim}{H}_1^T dx + \alpha_{11} \int_0^{l_i} \underset{\sim}{H}_1'^T dx \\ \hdashline e_A \sin\phi_0 \int_x^R p_x\, dx \int_0^{l_i} \underset{\sim}{H}_1''^T d\xi + (\alpha_{13} - \Gamma_{16}) \int_0^{l_i} \underset{\sim}{H}_1^T dx + \alpha_{14} \int_0^{l_i} \underset{\sim}{H}_1'^T dx \\ \hdashline -K_A^2 \phi_0' \int_x^R p_x\, dx \int_0^{l_i} \underset{\sim}{H}_0'^T d\xi + (\alpha_{15} - \Delta_{16}) \int_0^{l_i} \underset{\sim}{H}_0^T d\xi \end{array}\right]$$

where the α_i coefficients are

$$\alpha_1 = m$$
$$\alpha_2 = m K_m^2$$
$$\alpha_3 = -me\sin\phi_0$$
$$\alpha_4 = me\cos\phi_0$$
$$\alpha_5 = 2m\Omega\sin(\beta+\delta)$$
$$\alpha_6 = 2m\Omega e\cos(\beta+\delta)\sin\phi_0$$
$$\alpha_7 = -m\Omega^2$$
$$\alpha_8 = m\Omega^2\cos(\beta+\delta)\Big[(K_{m_2}^2 - K_{m_1}^2)\cos(\beta+\delta)\cos 2\phi_0 - e\xi\sin\phi_0 \cdot \sin(\beta+\delta)\Big]$$
$$\alpha_9 = m\Omega^2 e\sin\phi_0$$

$$\alpha_{10} = me\Omega^2\left[\xi\cos^2(\beta+\delta) + e_o\cos(\beta+\delta)\cos\beta\right]\sin\phi_o$$

$$\alpha_{11} = me\Omega^2\left[\xi\cos^2(\beta+\delta) + e_o\cos(\beta+\delta)\cos\beta\right]\cos\phi_o$$

$$\alpha_{12} = me\Omega^2\cos\phi_o$$

$$\alpha_{13} = -m\Omega^2\sin(\beta+\delta)\left[\xi\cos(\beta+\delta) + e_o\cos\beta\right]$$

$$\alpha_{14} = -me\Omega^2\left[\xi\cos^2(\beta+\delta) + e_o\cos(\beta+\delta)\cos\beta\right]$$

$$\alpha_{15} = -m\Omega^2\cos\phi_o\Big[(K_{m_2}^2-K_{m_1}^2)\cos^2(\beta+\delta)\sin\phi_o + e\xi\sin(\beta+\delta)\cdot \\ \cdot\cos(\beta+\delta) + ee_o\sin(\beta+\delta)\cos\beta\Big]$$

$$\alpha_{16} = 2me\Omega\sin(\beta+\delta)\cos\phi_o$$

$$\alpha_{17} = 2m\Omega(K_{m_2}^2-K_{m_1}^2)\cos(\beta+\delta)\cos\phi_o\sin\phi_o$$

$$\alpha_{18} = 2me\Omega\sin(\beta+\delta)\sin\phi_o$$

$$\alpha_{19} = 2m\Omega(K_{m_2}^2\sin^2\phi_o + K_{m_1}^2\cos^2\phi_o)\cos(\beta+\delta)$$

The B_i, Γ_i and Δ_i coefficients relate to the aerodynamic forces and are listed in appendix B with opposite sign since they have been obtained from the loadings directly. Hence, in order to be substituted in the matrices $\underset{\sim}{M}_A$, $\underset{\sim}{C}_A$ and $\underset{\sim}{K}_A$ appearing in equation (52) their signs have to be changed since these matrices have been transfered from the right-hand-side to the left-hand-side of the equilibrium equations.

2.6 Static Analysis

To perform static analysis of the structure we set

$$\ddot{\underset{\sim}{q}} = 0$$

$$\dot{\underset{\sim}{q}} = 0$$

then the equilibrium equations (52) will be

$$\underset{\sim}{K}\,\underset{\sim}{q} = \underset{\sim}{Q}_{steady} \tag{53}$$

and

$$\underset{\sim}{K} = \underset{\sim}{K}_A + \underset{\sim}{K}_S + \underset{\sim}{K}_G + \underset{\sim}{K}_M$$

The solution of equation (53) will give the generalized displacements $\underset{\sim}{q}$, where

$$\underset{\sim}{q}^T = \sum_{\text{all } N \text{ elem.}} \left[v_1 \; v_1' \; v_2 \; v_2' \; w_1 \; w_1' \; w_2 \; w_2' \; \phi_1 \; \phi_2 \right]$$

To obtain the shear forces V_y and V_z and the bending moments M_y and M_z of the blade we used the same conventions for their positive directions that are shown in figure 8 for the loadings p_y, p_z, q_y, q_z, respectively.

The shear forces V_y V_z for each element can be obtained from the equilibrium equations, using force summation method (see Reference (1))

$$\frac{\partial V_y}{\partial x} = -p_y \tag{54a}$$

$$\frac{\partial V_z}{\partial x} = -p_z \tag{54b}$$

Approximating the above derivatives for the i^{th} element

$$\frac{\partial V_y}{\partial x} = \frac{V_{y_{i+1}} - V_{y_i}}{l_i}$$
$$\frac{\partial V_z}{\partial x} = \frac{V_{z_{i+1}} - V_{z_i}}{l_i} \tag{55}$$

then, the nodal values of V_y and V_z for each element will be obtained from

$$V_{y_{i+1}} = V_{y_i} - p_{y_i} l_i \tag{56a}$$

$$V_{z_{i+1}} = V_{z_i} - p_{z_i} l_i \tag{56b}$$

with the condition that $V_{y\,(\text{free end})} = V_{z\,(\text{free end})} = 0$

It has to be noted that in equations (54a,b) we have

$$p_{y_i} = \left(p_{y_i}\right)_{Aerodynamic} + \left(p_{y_i}\right)_{Structural}$$

$$p_{z_i} = \left(p_{z_i}\right)_{Aerodynamic} + \left(p_{z_i}\right)_{Structural}$$

where the "aerodynamic" and "structural" parts can be obtained from appendices B and A, respectively, by setting all the time derivatives to zero and then substituting the solution for $\underset{\sim}{q}$ (which is a function of v, w, ϕ and their derivatives).

To obtain the bending moments M_y and M_z for each element we use the mode displacement method where (see Reference (1)).

$$M_y = \left(EI_1\cos^2\phi_0 + EI_2\sin^2\phi_0\right)w'' + \left(EI_2 - EI_1\right)\sin\phi_0\cos\phi_0 v'' - \left(Te_A + EB_2\phi_0'\phi'\right)\sin\phi_0 - Te_A\phi\cos\phi_0 \quad (57a$$

$$M_z = \left(EI_2 - EI_1\right)\sin\phi_0\cos\phi_0 w'' + \left(EI_1\sin^2\phi_0 + EI_2\cos^2\phi_0\right)v'' - \left(Te_A + EB_2\phi_0'\phi'\right)\cos\phi_0 + Te_A\phi\sin\phi_0 \quad (57b$$

and $$\frac{\partial T}{\partial x} = -p_x \quad (58)$$

In this case we cannot substitute directly into the moment equations the solution for $\underset{\sim}{q}$ since they contain curvature terms that are not represented explicitly in $\underset{\sim}{q}$. Nevertheless, we can approximate the curvatures for the i^{th} element, like

$$w'' = \frac{\partial(w')}{\partial x} = \frac{w'_{i+1} - w'_i}{l_i}$$

$$v'' = \frac{\partial(v')}{\partial x} = \frac{v'_{i+1} - v'_i}{l_i} \quad (59)$$

$$\phi' = \frac{\partial(\phi)}{\partial x} = \frac{\phi_{i+1} - \phi_i}{l_i}$$

and then substitute the solution for $\underset{\sim}{q}$. It has also to be noted that since the equation (58) has similar form as equation (54a or b) we can express T in the following form (for the

i^{th} element)

$$T_{i+1} = T_i - p_{x_i} \ell_i \tag{60}$$

with $\quad T_{free\ end} = 0$

where $\quad p_{x_i} = \left(p_{x_i}\right)_{aerodynamic} + \left(p_{x_i}\right)_{structural}$

and the "aerodynamic" and "structural" components can be obtained in an exactly similar way with p_{y_i} and p_{z_i} discussed before.

Finally, after all the nodal values of T have been found using equation (60) we will have to average them for each element; i.e.,

$$T = T_{av_i} = \frac{T_{i+1} + T_i}{2}$$

and then substitute it in equations (57a,b) together with equations (59) and the solution for $\underset{\sim}{q}$ to obtain the bending mements M_y and M_z.

2.7 Vibration Analysis

To perform the vibration analysis of the structure we set

$$\overset{\circ}{\underset{\sim}{q}} = 0$$

all aerodynamic terms = 0

$$\underset{\sim}{Q}_{steady} = 0$$

Then equation (52) will become

$$\underset{\sim}{M}_s \overset{\circ\circ}{\underset{\sim}{q}} + \left(\underset{\sim}{K}_s + \underset{\sim}{K}_G + \underset{\sim}{K}_M\right)\underset{\sim}{q} = 0$$

The above equation can be solved as a generalised eigenvalue problem (see Ref. (10)) of the following form

$$(\underset{\sim}{K}_S + \underset{\sim}{K}_G + \underset{\sim}{K}_M)\underset{\sim}{\Phi} = \underset{\sim}{M}_S \underset{\sim}{\Phi} \underset{\sim}{\Lambda}$$

if

$$\underset{\sim}{q} = \underset{\sim}{\Phi}\,\bar{\underset{\sim}{q}} \quad \text{and} \quad \bar{\underset{\sim}{q}} = \bar{\underset{\sim}{q}}_0 \left\{e^{wt}\right\}$$

where

$$\underset{\sim}{\Lambda} = \begin{bmatrix} \omega_1^2 & & & \\ & \omega_2^2 & & \\ & & \ddots & \\ & & & \omega_m^2 \end{bmatrix} \quad \text{is the eigenvalue matrix } (m \times m)$$

and

$$\underset{\sim}{\Phi} = \left[\, \underset{\sim}{\Phi}_1 \; \underset{\sim}{\Phi}_2 \; \ldots \; \underset{\sim}{\Phi}_m \,\right] \quad \text{is the eigenvector matrix } (m \times m)$$

for m degrees of freedom (generalised coordinates)

(a) <u>Uniform Cantilever Beam</u>

The lowest 6 vibration modes were obtained for a non-rotating uniform beam cantilever, discretised into 10 elements, using subspace iteration.

The frequencies corresponding to these 6 modes were also obtained theoretically using

$$\omega_{Flap} = \alpha_n \sqrt{\frac{EI_1}{m\ell^4}} \qquad \omega_{Lag} = \alpha_n \sqrt{\frac{EI_2}{m\ell^4}}$$

$$\omega_{Torsion} = b_n \sqrt{\frac{GJ}{m K_m^2 \ell^2}} \tag{61}$$

where the blade properties, the coefficients α_n and b_n together with the theoretical and numerical vibration frequencies, are presented in appendix D.

The agreement between the theoretical and numerical results is very good.

Also, in the same appendix, the vibration frequencies for the same cantilever, rotating with Ω = 4.191 rad/s, are listed, for the lowest 6 modes.

(b) NASA MOD-0 100KW Wind Turbine Blade

The above blade was discretised into 10 elements with non-uniform properties which are listed in appendix E.

The vibration mode-shapes and frequencies for the lowest 10 modes were obtained.

Figures 10, 11 and 12 present a comparison between the first flap, first lag and second flap rotating mode shapes, respectively (Ω= 4.191 rad/s) as obtained numerically using subspace iteration with our analysis, versus numerical results presented by Lockheed California Company.

The agreement is very good.

(c) Investigation of the Direction of Motion -
- Flat Plate

In figure 13, the direction of motion θ_M of the MOD-0 blade during the first flap, non-rotating mode shape is presented versus the pretwist ϕ_o , where

$$\theta_M = \tan^{-1} \frac{w}{v}$$

It has to be noted that according to figure 13, although the blade is pretwisted from the root to the tip by as much as 26°, the direction of motion doesn't seem to be affected a lot.

ORIGINAL PAGE IS
OF POOR QUALITY

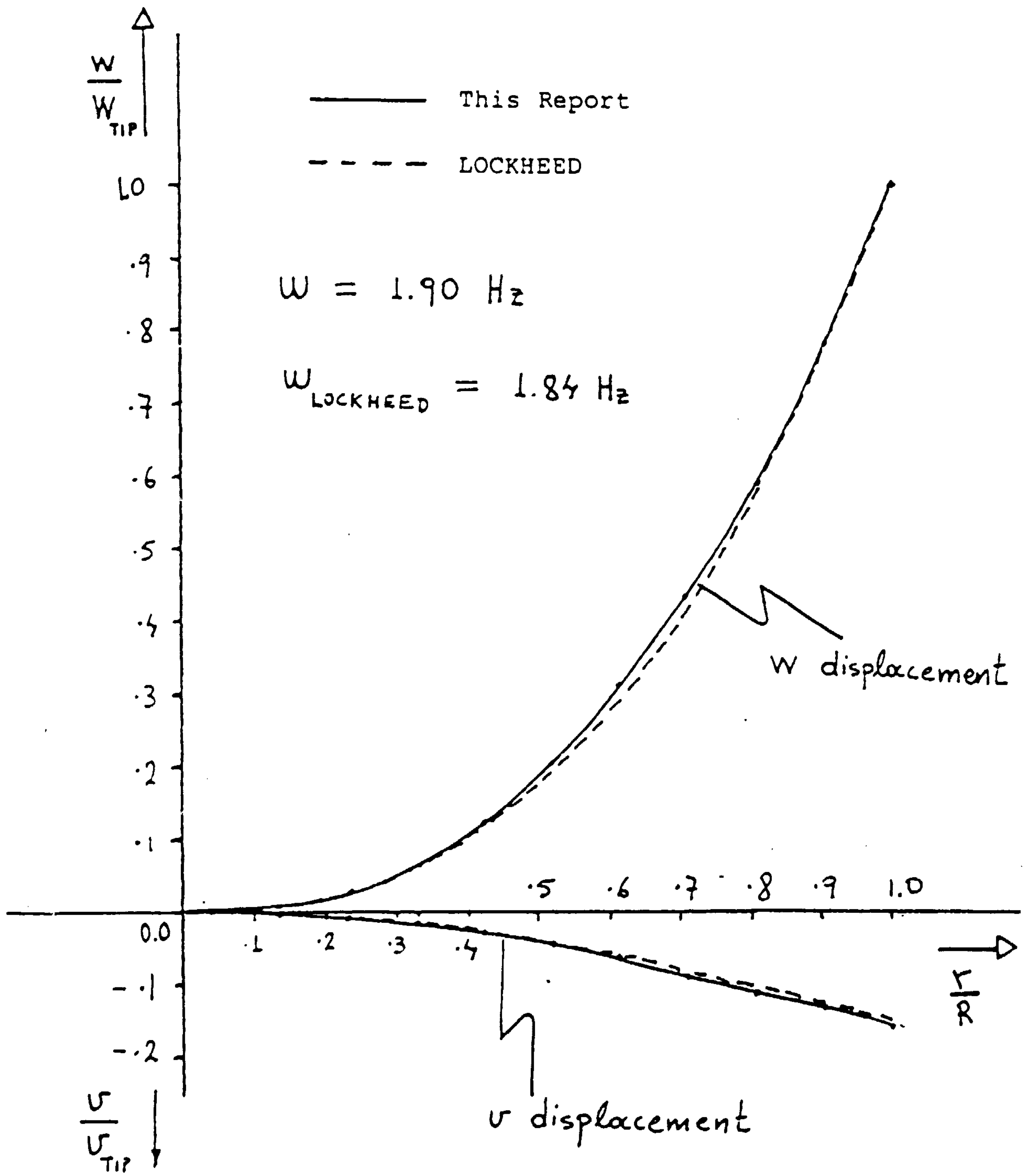

MOD-O First Out-of-Plane (Flap) Mode Shape

Figure 10

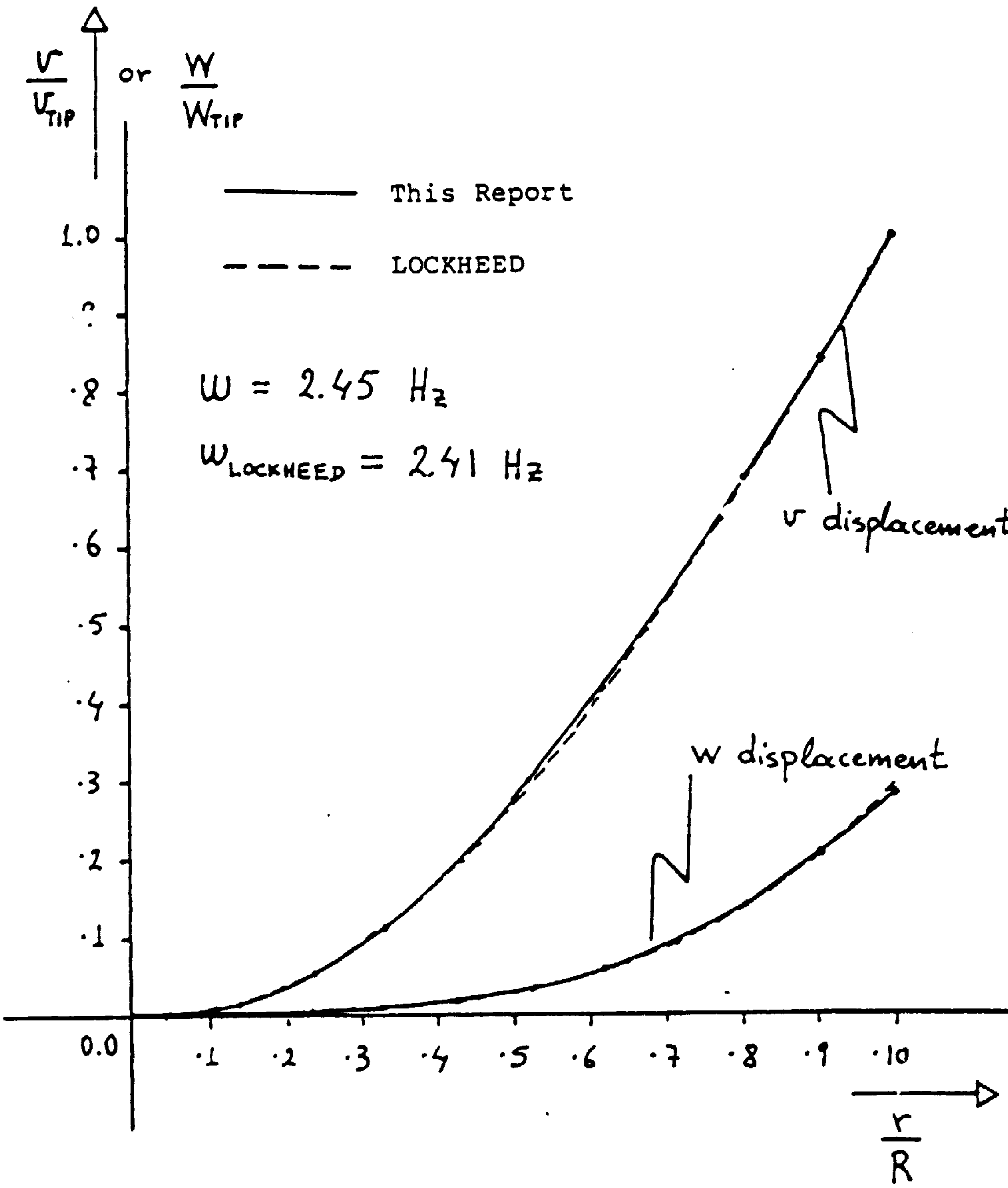

MOD-O First In-Plane (Lag) Mode Shape

Figure 11

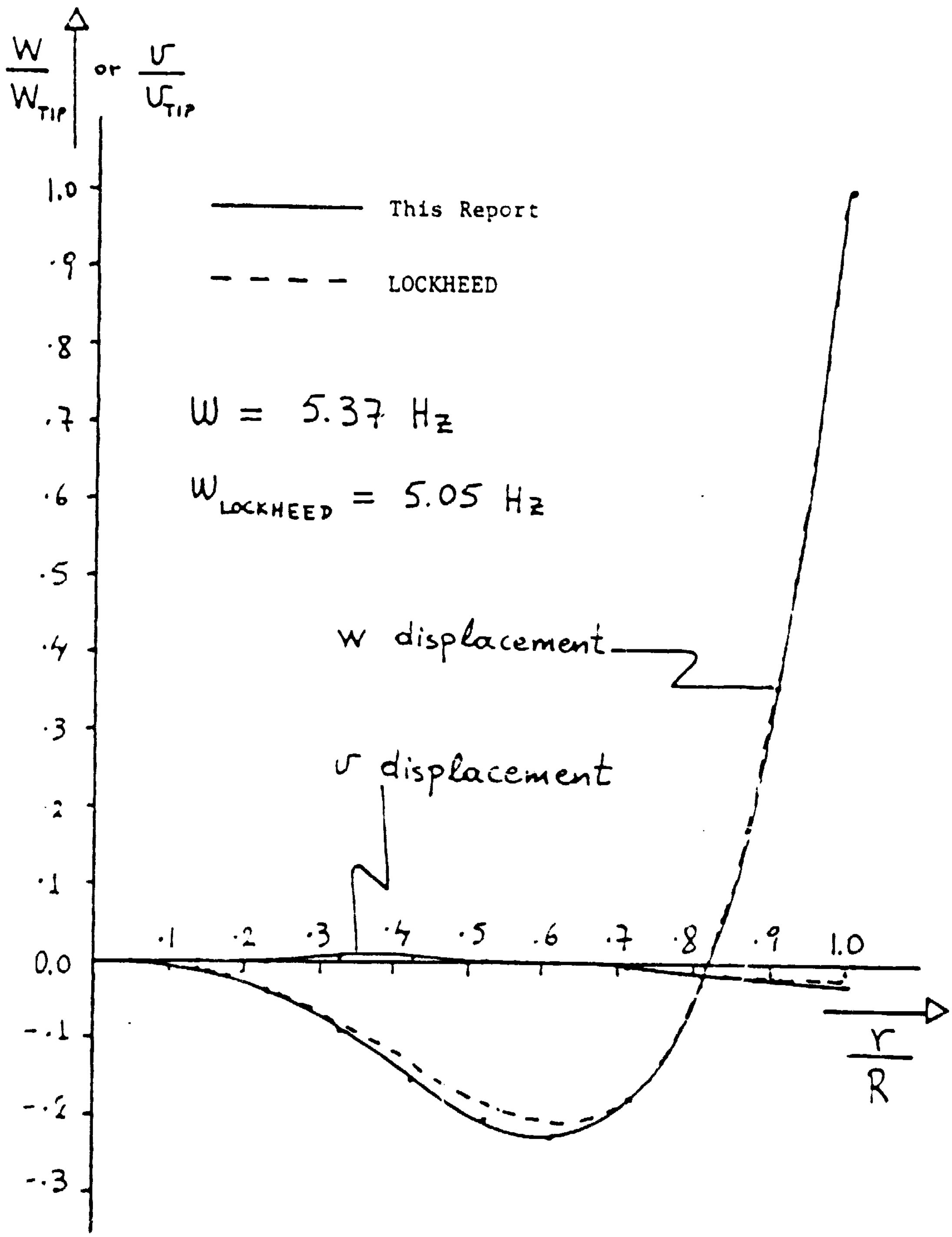

MOD-O Second Out-Of-Plane Mode Shape

Figure 12

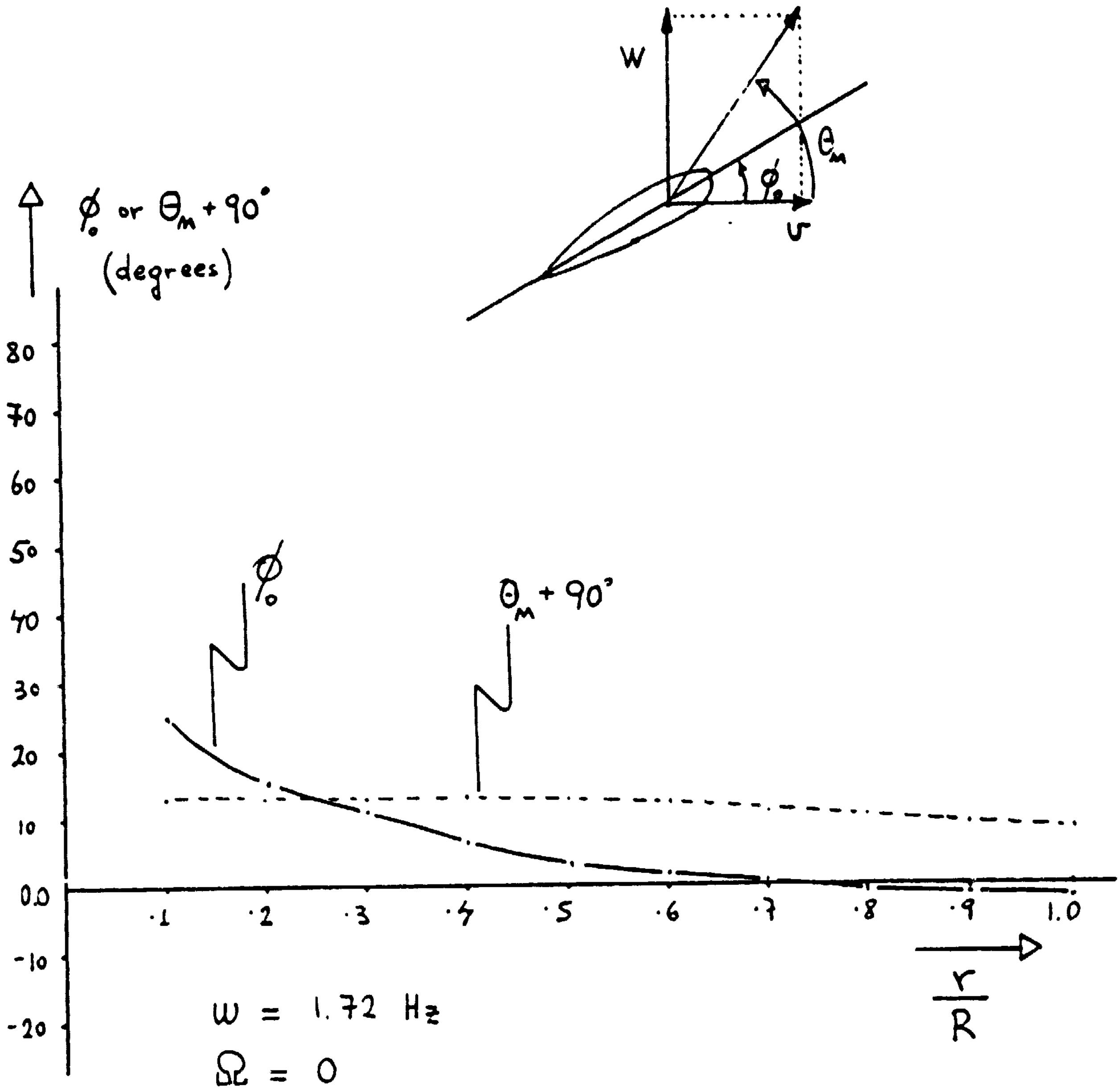

MOD-O First Flap Mode Shape Direction of Motion

Figure 13

In fact, the blade appears vibrating in most of its span along the direction normal to the chord at the section around 30-35% of the span.

Similar behaviour is exhibited in the North Wind Turbine (figure 14) with total pretwist 14°, and in the McCauley Propeller (figure 15) with total pretwist 22°.

Examining the former three blades for the direction of motion during the first lag non-rotating mode shape (figures 16, 17 and 18) no such behaviour is encountered.

In an effort to see how far we can stretch the direction of motion concept, we examined the vibration modes of a non-rotating very thin uniform plate, which has been treated as a cantilever beam. (See appendix F). The plate was given a very high bending stiffness in the lag direction, with a very small bending stiffness in the flap direction (ill-conditioned problem). The first flap and first lag modes we examined for 30°, 60° and 90° root to tip pretwist and the direction of motion was plotted versus the total pretwist in each case (figures 19, 20, 21, 22).

For the first flap mode shape a similar behaviour was encountered where the blade appeared to move throughout most of its span, in the direction normal to the chord of the section around 15-20% of the span (figures 19, 20, 21).

No such behaviour is encountered during the first lag mode shape (figure 22).

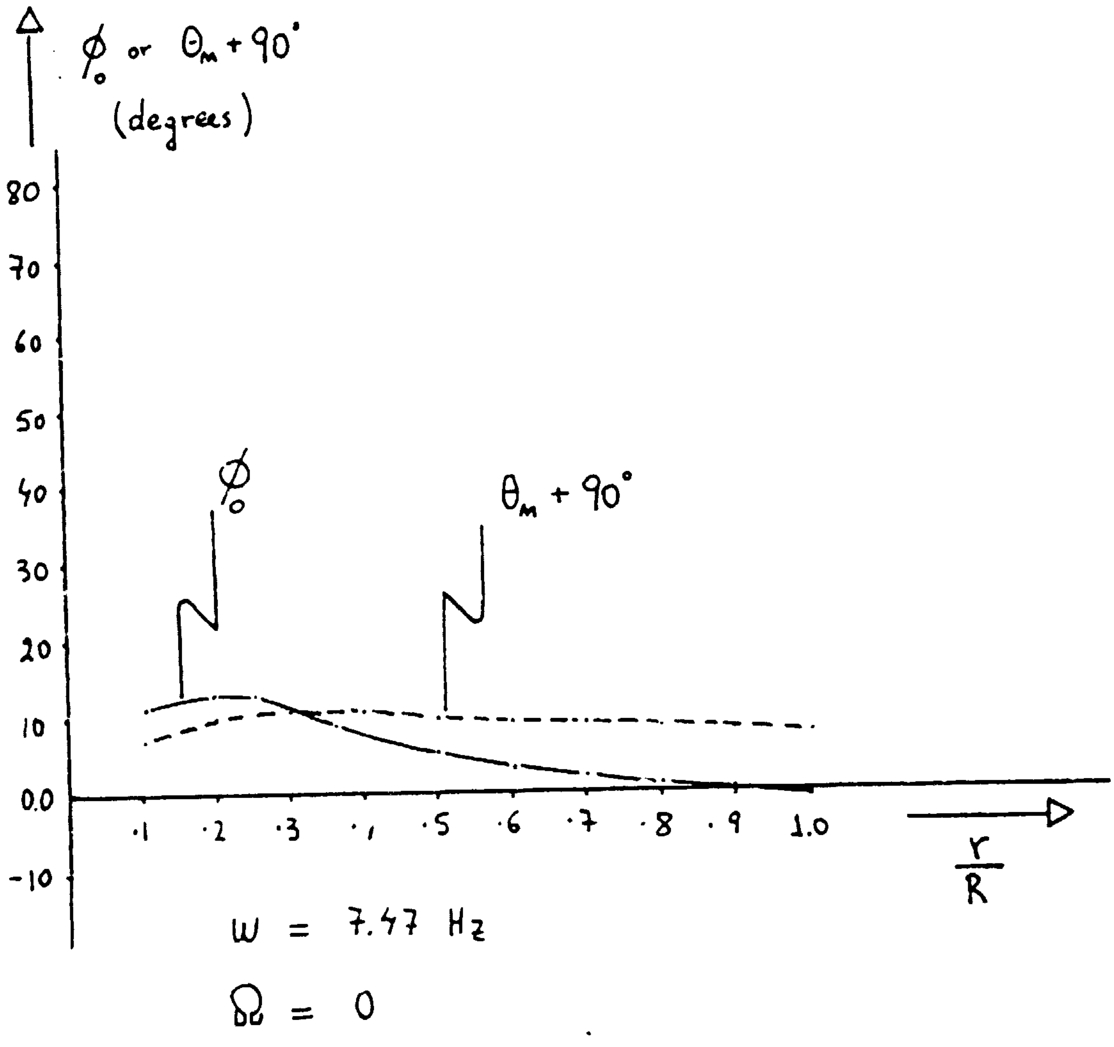

North Wind Turbine First Flap Mode Shape Direction of Motion

Figure 14

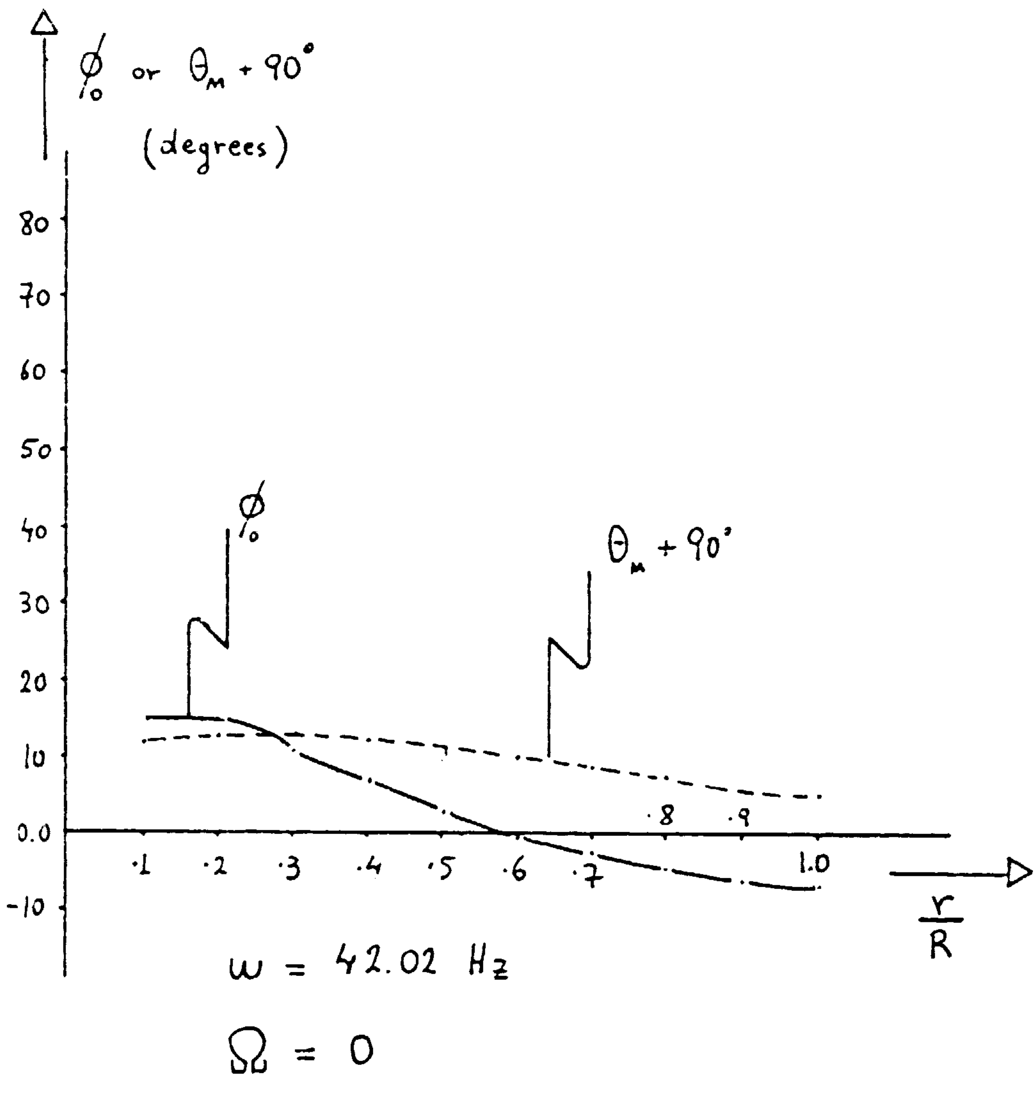

McCauley Propell r First Flap Mode Shape Direction of Motion

Figure 15

ORIGINAL PAGE IS
OF POOR QUALITY

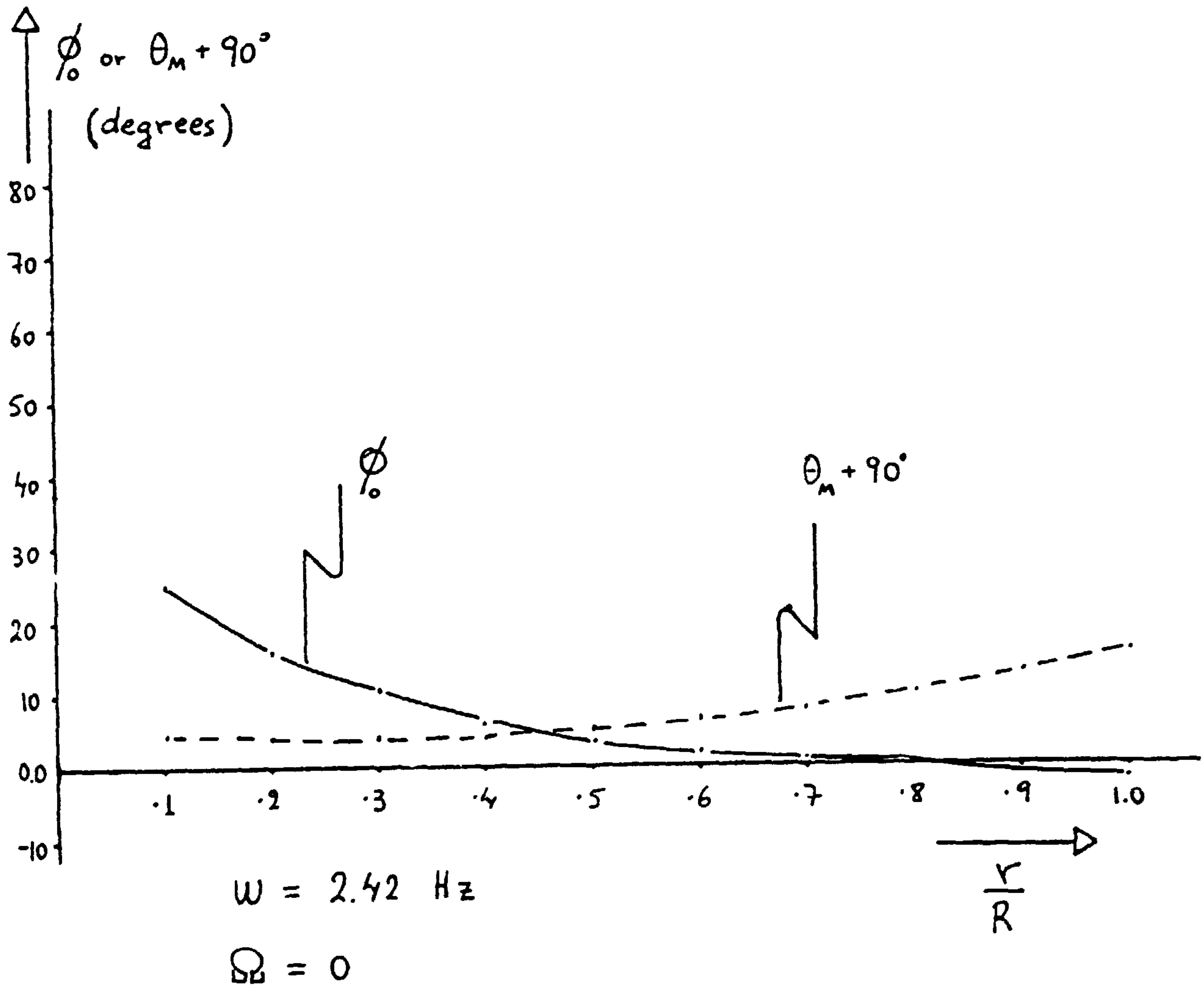

MOD-O First Lag Mode Shape Direction of Motion

Figure 16

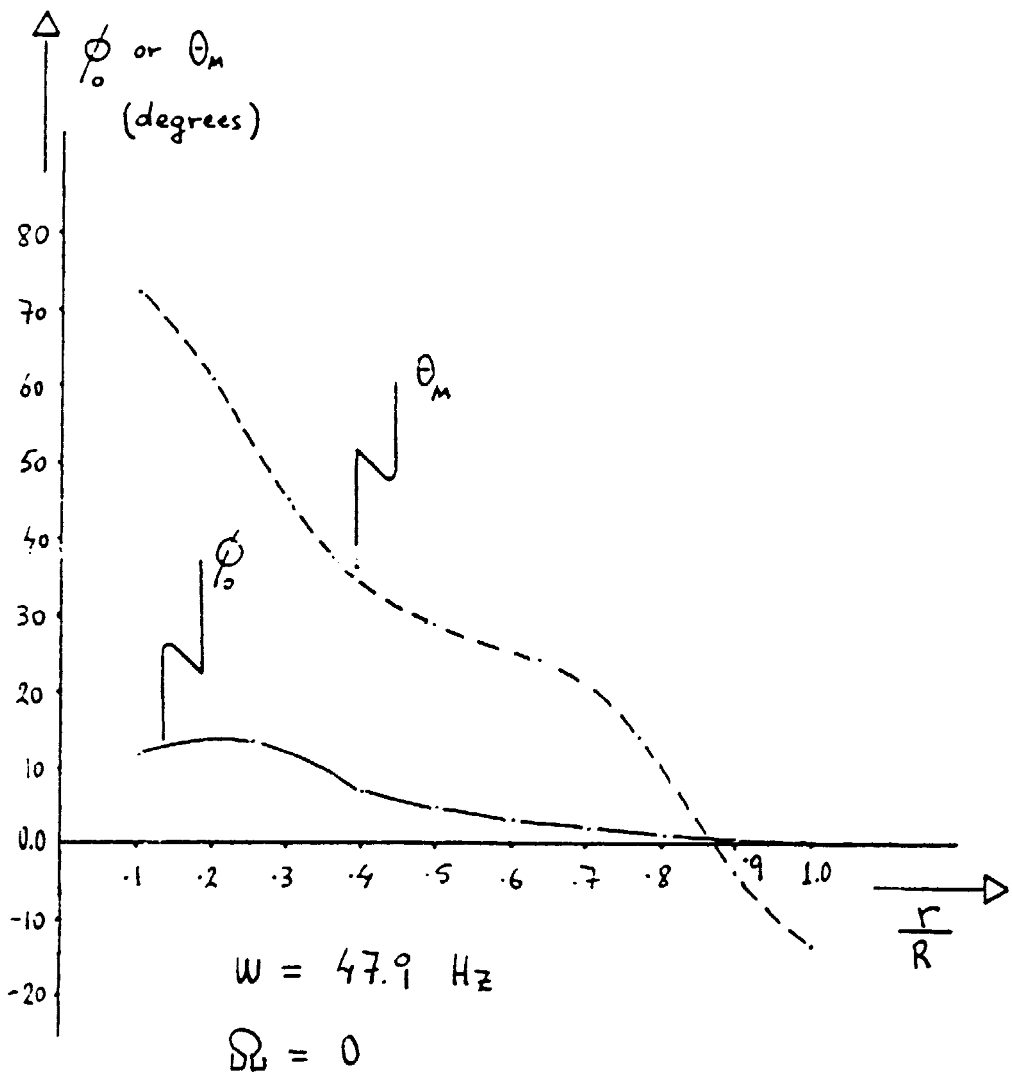

North Wind Turbine First Lag Mode Shape Direction of Motion

Figure 17

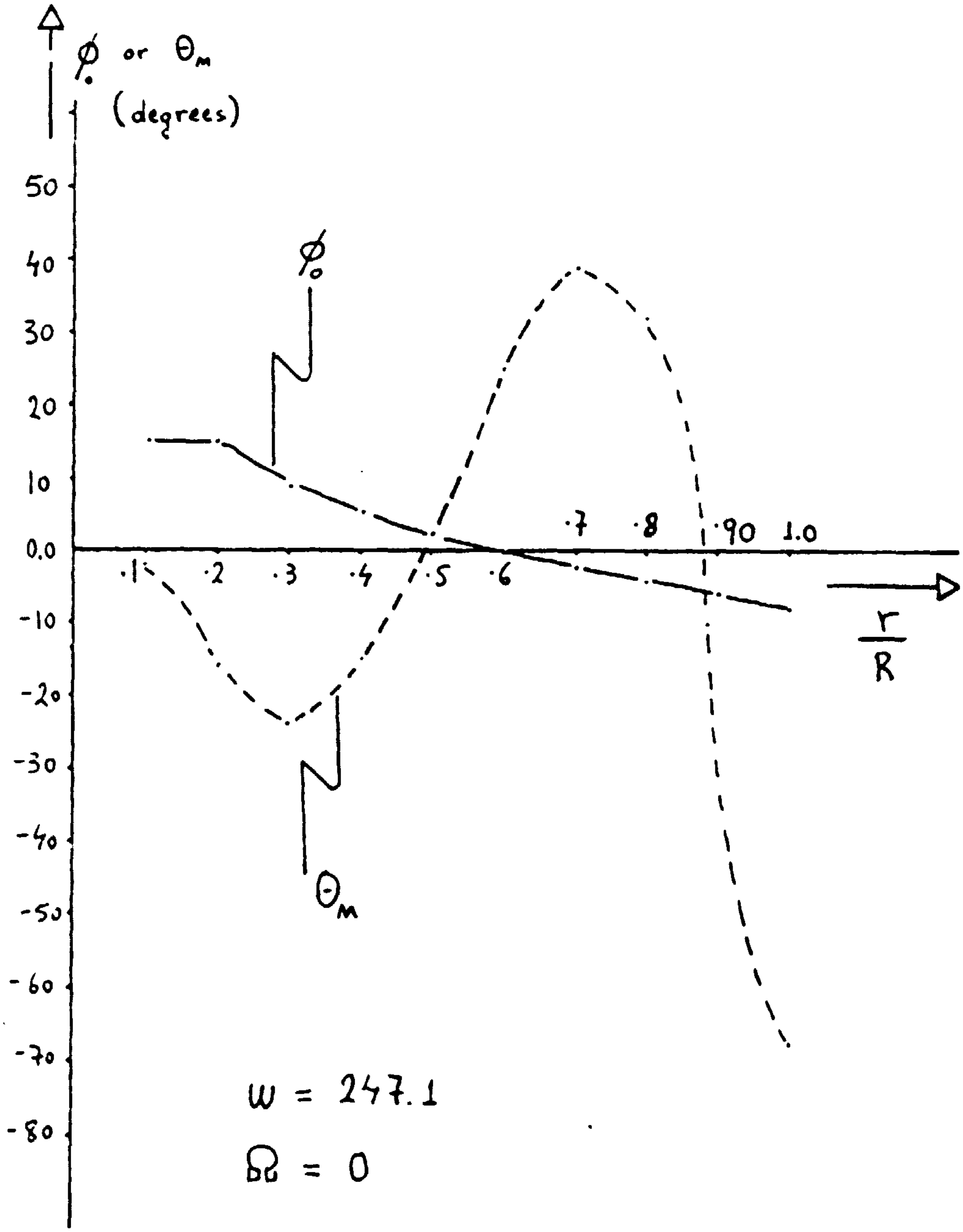

McCauley Propeller First Lag Mode Shape Direction of Motion

Figure 18

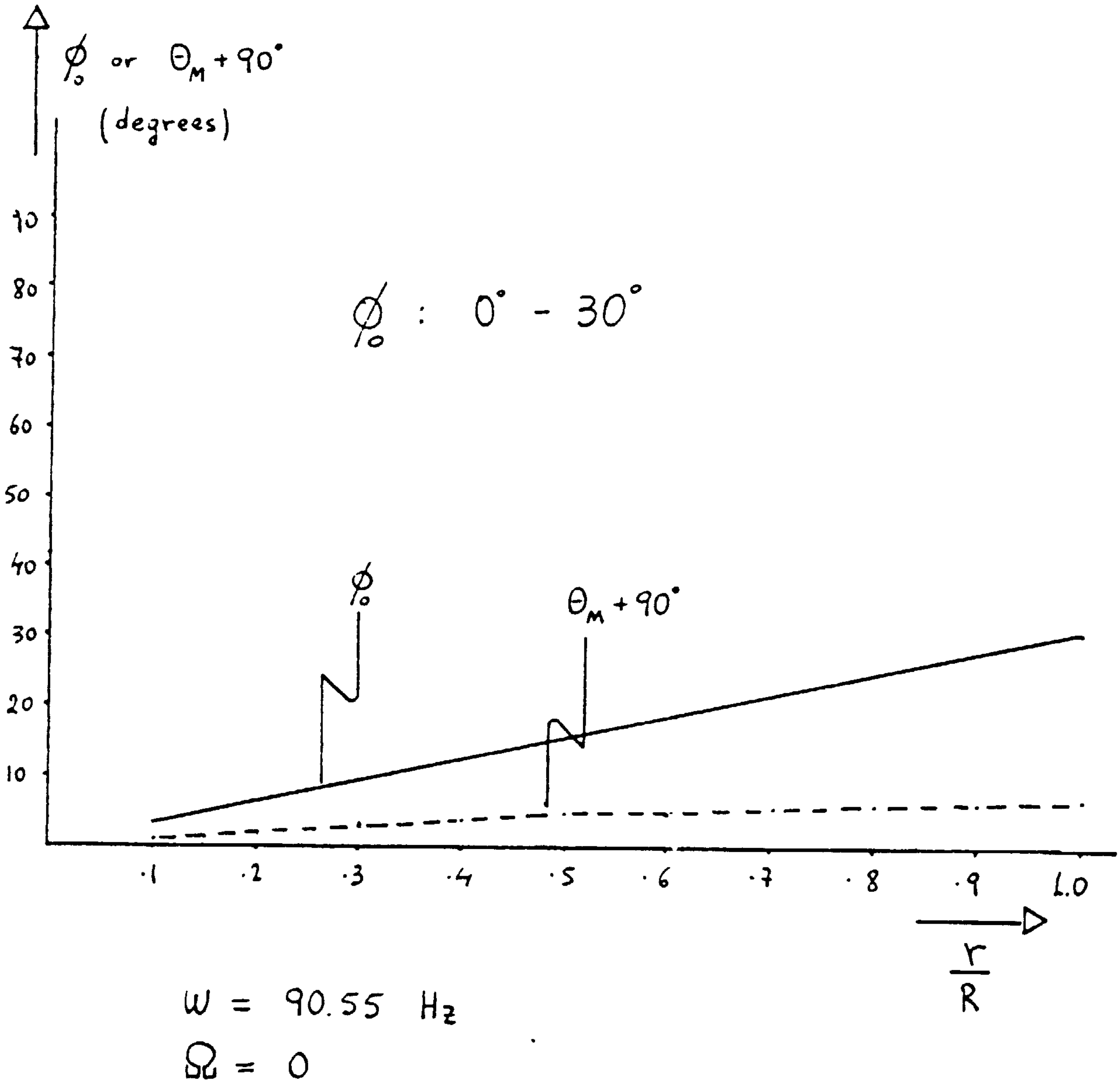

Flat Plate First Flap Mode Shape Direction of Motion

Figure 19

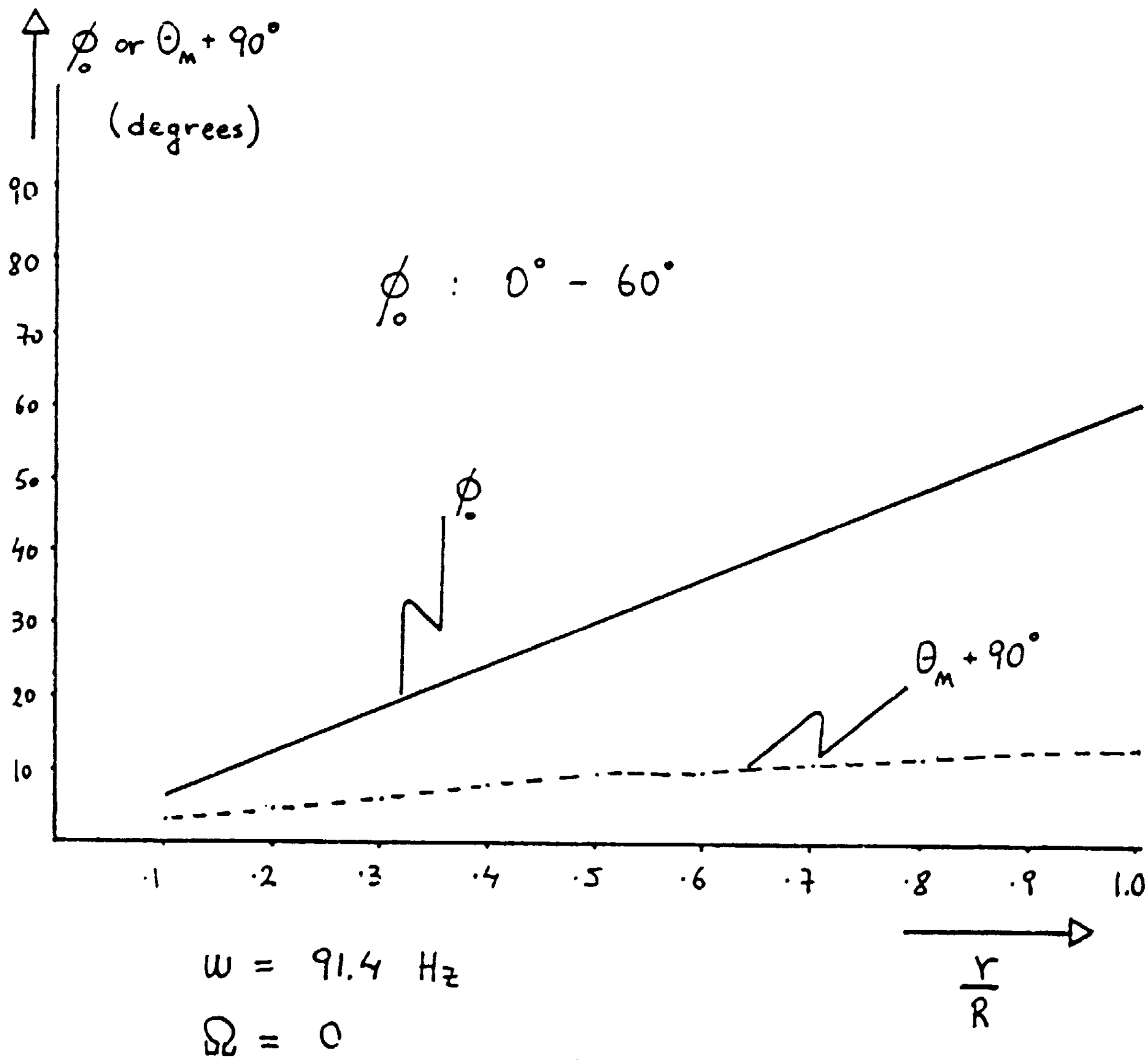

Flat Plate First Flap Mode Shape Direction of Motion

Figure 20

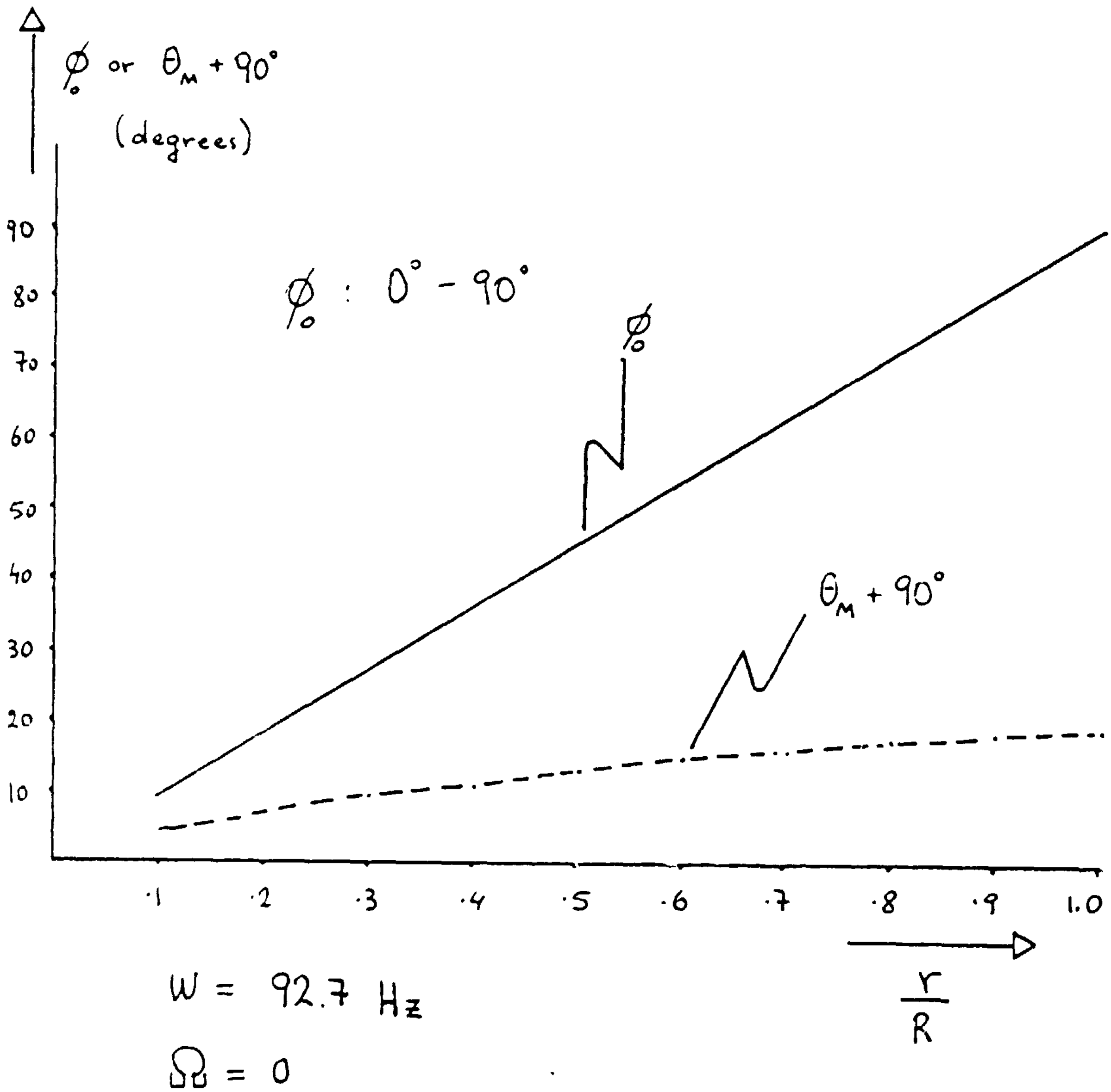

Flat Plate First Flap Mode Shape Direction of Motion

Figure 21

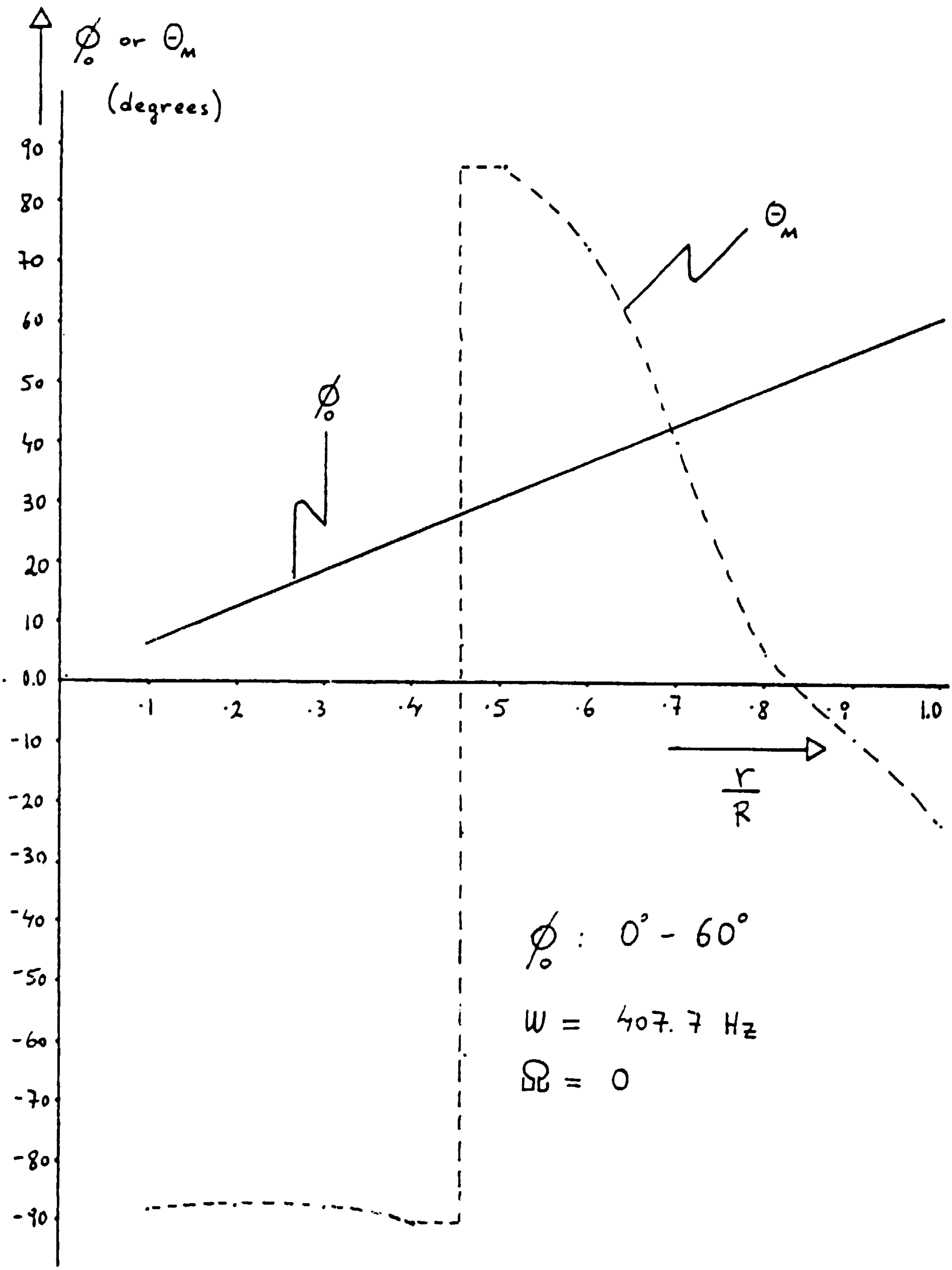

Flat Plate First Lag Mode Shape Direction of Motion

Figure 22

2.8 Flutter Analysis

To perform flutter analysis of the structure we set

$$\underset{\sim}{Q}_{steady} = \underset{\sim}{0}$$

and hence we have

$$\underset{\sim}{M}\,\ddot{\underset{\sim}{q}} + \underset{\sim}{C}\,\dot{\underset{\sim}{q}} + \underset{\sim}{K}\,\underset{\sim}{q} = 0$$

with

$$\underset{\sim}{M} = \underset{\sim}{M}_A + \underset{\sim}{M}_S$$

$$\underset{\sim}{C} = \underset{\sim}{C}_A + \underset{\sim}{C}_G$$

$$\underset{\sim}{K} = \underset{\sim}{K}_A + \underset{\sim}{K}_S + \underset{\sim}{K}_G + \underset{\sim}{K}_M$$

Doing a modal analysis, we can select a number of modes p out of a total of m (see Vibration Analysis) and then transform the above equations into this reduced modal space, through the following relation

$$\underset{\sim}{q} = \bar{\underset{\sim}{\Phi}}_p\,\bar{\underset{\sim}{q}}_p$$

to obtain

$$\bar{\underset{\sim}{M}}\,\ddot{\bar{\underset{\sim}{q}}}_p + \bar{\underset{\sim}{C}}\,\dot{\bar{\underset{\sim}{q}}}_p + \bar{\underset{\sim}{K}}\,\bar{\underset{\sim}{q}}_p = 0$$

with

$$\bar{\underset{\sim}{M}} = \bar{\underset{\sim}{\Phi}}_p^T\,\underset{\sim}{M}\,\bar{\underset{\sim}{\Phi}}_p$$

$$\bar{\underset{\sim}{C}} = \bar{\underset{\sim}{\Phi}}_p^T\,\underset{\sim}{C}\,\bar{\underset{\sim}{\Phi}}_p$$

$$\bar{\underset{\sim}{K}} = \bar{\underset{\sim}{\Phi}}_p\,\underset{\sim}{K}\,\bar{\underset{\sim}{\Phi}}_p$$

Further on, setting

$$\underset{\sim}{\Psi} = \begin{Bmatrix} \bar{\underset{\sim}{q}} \\ \dot{\bar{\underset{\sim}{q}}} \end{Bmatrix}$$

we obtain

$$\dot{\underset{\sim}{\Psi}} = \underset{\sim}{\Xi}\,\underset{\sim}{\Psi} \qquad (62)$$

where

$$\underset{\sim}{\Xi} = \begin{bmatrix} \underset{\sim}{0} & \underset{\sim}{I} \\ -\bar{\underset{\sim}{M}}^{-1}\bar{\underset{\sim}{K}} & -\bar{\underset{\sim}{M}}^{-1}\bar{\underset{\sim}{C}} \end{bmatrix}$$

Equation (62) is much more handy from the computational point of view due to the appreciable saving in computer storage that results. For instance, in a typical modal analysis of a cantilever blade, the assembled, damping and stiffness matrices are 55 x 55 in size (for 10 beam elements). Picking up 5 normal modes; i.e., first and second flap, first and second la- and first torsion, (p = 5) then the resulting $\underset{\sim}{\Xi}$ matrix will be 10 x 10 in size.

Equation (62) can be solved as a complex eigenvalue problem. For

$$\underset{\sim}{\Psi} = \underset{\sim}{\Phi}_c \, \underset{\sim}{\bar{\Psi}} \qquad \text{and} \qquad \underset{\sim}{\bar{\Psi}} = \underset{\sim}{\bar{\Psi}}_o \left\{ e^{\lambda t} \right\}$$

equation (62) will be

$$\underset{\sim}{\Phi}_c \, \underset{\sim}{\Lambda}_c = \underset{\sim}{\Xi} \, \underset{\sim}{\Phi}_c$$

where

$$\underset{\sim}{\Phi}_c = \left[\underset{\sim}{\Phi}_{c_1} \; \underset{\sim}{\Phi}_{c_2} \cdots \underset{\sim}{\Phi}_{c_{2p}} \right] \qquad (2p \times 2p)$$

being the complex eigenvector matrix

and

$$\underset{\sim}{\Lambda}_c = \begin{bmatrix} \lambda_1 & & & & \\ & \lambda_2 & & & \\ & & \lambda_3 & & \\ & & & \ddots & \\ & & & & \lambda_{2p} \end{bmatrix} \qquad (2p \times 2p)$$

being the complex eigenvector matrix

i.e., a complex eigenvalue will be

$$\lambda = \mu \pm i\omega$$

μ represents the damping associated with a given mode while ω is the frequency of that mode.

When μ is zero we have flutter, while when it becomes positive we have dynamic instability.

Three numerical cases were examined, concerning cantilever beams, as a comparison test between results obtained from this analysis and results presented in the following papers, respectively:

Ref. (3) by Kottapalli, Friedmann and Rosen

Ref. (6) by Stephens, Hodges, Avila and Kung

Ref. (8) by Sivaneri and Chopra

In all cases, the vibration analysis of the beam was done with the beam having been discretised into 10 finite elements.

(a) <u>Ref. (3) by Kottapalli, Friedmann and Rosen</u>

In this case the response of the NASA/DOE MOD-0 WIND TURBINE blade was examined. The blade was allowed to experience aerodynamic loads due to a constant wind velocity W_w along the $\vec{K}$ direction, while rotating at an angular velocity Ω = 4.191 rad/s. Note that according to our convention for wind velocity in figure 4b, W_w for this case has to be negative.

Vibration analysis was first performed and 5 natural modes were obtained (first and second flap, first and second lag and first torsion).

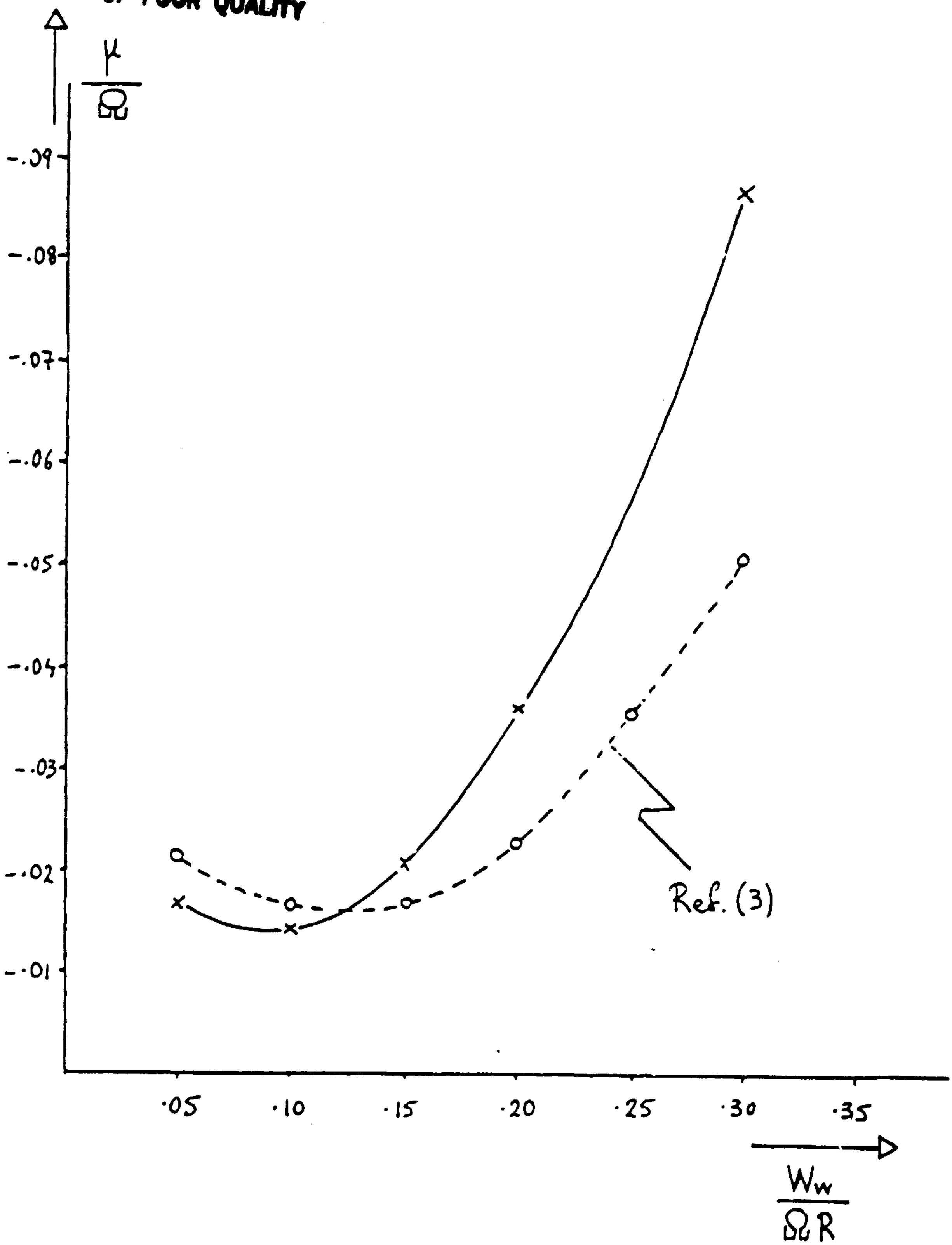

MOD-O Lag Stability

Figure 23

Flutter analysis was then done, using the above five modes, for the following wind cases:

$$U_w = 0$$

$$V_w = 0$$

and $$W_w = -157,\ -313,\ -470,\ -627 \text{ and } -940.5\ \text{in/s}$$

The real part of the complex eigenvalue of the first lag mode i.e., μ_{LAG} was nondimensionalised with Ω and plotted against the nondimensional wind velocity $\frac{W_w}{\Omega R}$, where R is the radius of the MOD-0 blade (see figure 23). On the same plot, results presented in Ref. (3) are also shown.

The agreement between the two curves is good, considering the fact that in Reference (3) the input used was based on data concerning a much earlier design of the MOD-0. The blade was found to be stable for all the W_w cases examined. The lag stability was found to increase with W_w velocity.

(b) Ref. (6) by Stephens, Hodges, Avila and Kung

A uniform cantilever blade was examined, with properties as listed in the above Ref. (6) as "Reference [1] Configuration."

Two distinct cases were examined, the soft-in-plane and the stiff-in-plane case, both for zero pretwist. The properties associated with these cases are listed in appendix G.

The lowest six rotating mode shapes were obtained from a vibration analysis; i.e., the first, second and third flap, first and second lag and first torsion.

Flutter analysis was then performed using the above six modes. The complex eigenvalues obtained were non-dimensionalised with the rotation speed Ω and then compared with the ones presented in Reference (6). The comparison between the first flap, first lag and first torsion modes is presented in appendix G.

It can be seen that all the eigenvalues, except the real part in the lag, have very good agreement for both soft and stiff-in-plane cases.

The blade was found to be generally stable for both cases. It can be seen also that the stiff-in-plane blade is more stable in flap and less stable in lag than the soft-in-plane blade.

(c) Ref. (8) by Sivaneri and Chopra

A uniform cantilever beam was examined, with the properties given by Ref. (8) and listed in appendix H.

The blade was examined at

$$\frac{C_T}{\sigma} = 0.1$$

where C_T = rotor thrust coefficient

σ = solidity ratio

which is equivalent to the blade having been set at a pitch angle of 12.7°.

Vibration analysis was performed and 5 normal modes were obtained; i.e., first and second flap, first and second lag and first torsion. The 5 corresponding eigenvalues were non-dimensionalised by Ω, the rotation speed, and then compared with results presented in Reference (8). The comparison is good and is presented in appendix H.

Flutter analysis was then performed with the previous five normal modes and the complex eigenvalues thus obtained were non-dimensionalised by Ω and then compared with the ones of Ref. (8). The comparison is good and is shown in appendix H.

The same process was repeated for

$$\frac{C_T}{\sigma} = 0.0$$

or blade pitch = 0°.

The comparison of the complex eigenvalues is good.

When the blade was set at

$$\frac{C_T}{\sigma} = 0.3$$

or blade pitch = 29.3°

the results obtained failed to predict the instability in lag which is shown in both Ref. (8) and Ref. (2).

3. NON-STRAIGHT ELASTIC AXIS ANALYSIS

3.1 Mathematical Model

A blade with a non-straight elastic axis can be modeled as an assembly of a finite number of straight elastic axis elements with different inclinations $\hat{\alpha}$ and $\hat{\beta}$ with respect to the $x\,y\,z$ system of axes of the previous section.

Or more explicitly, we define again a global fixed in space system of axes XYZ in an identical manner with the straight elastic axis case. (See figure 24).

We define an xyz system of axes at an offset e_o from the Z axis and being inclined at angles β and δ from the $X\,Y$ plane. β is the precone angle and δ the droop angle (See figure 25).

A local system of axes $x_L\ y_L\ z_L$ is then defined for every element (See figure 26). The direction of these axes can be obtained from the $x\,y\,z$ system of axes if we rotate it about the z-axis by an angle $\hat{\alpha}$ and then about the y-axis by an angle $\hat{\beta}$, the angles $\hat{\alpha}$ and $\hat{\beta}$ being different for each element. The x_L-axis is the elastic axis of this element in the undeformed blade.

The position of a point A in the blade can be defined by the blade coordinates $\xi\,\eta\,\zeta$ associated with the blade element to which this point belongs. The position of this point with respect to the $x_L\ y_L\ z_L$ system of axes of this element will be (see figure 26)

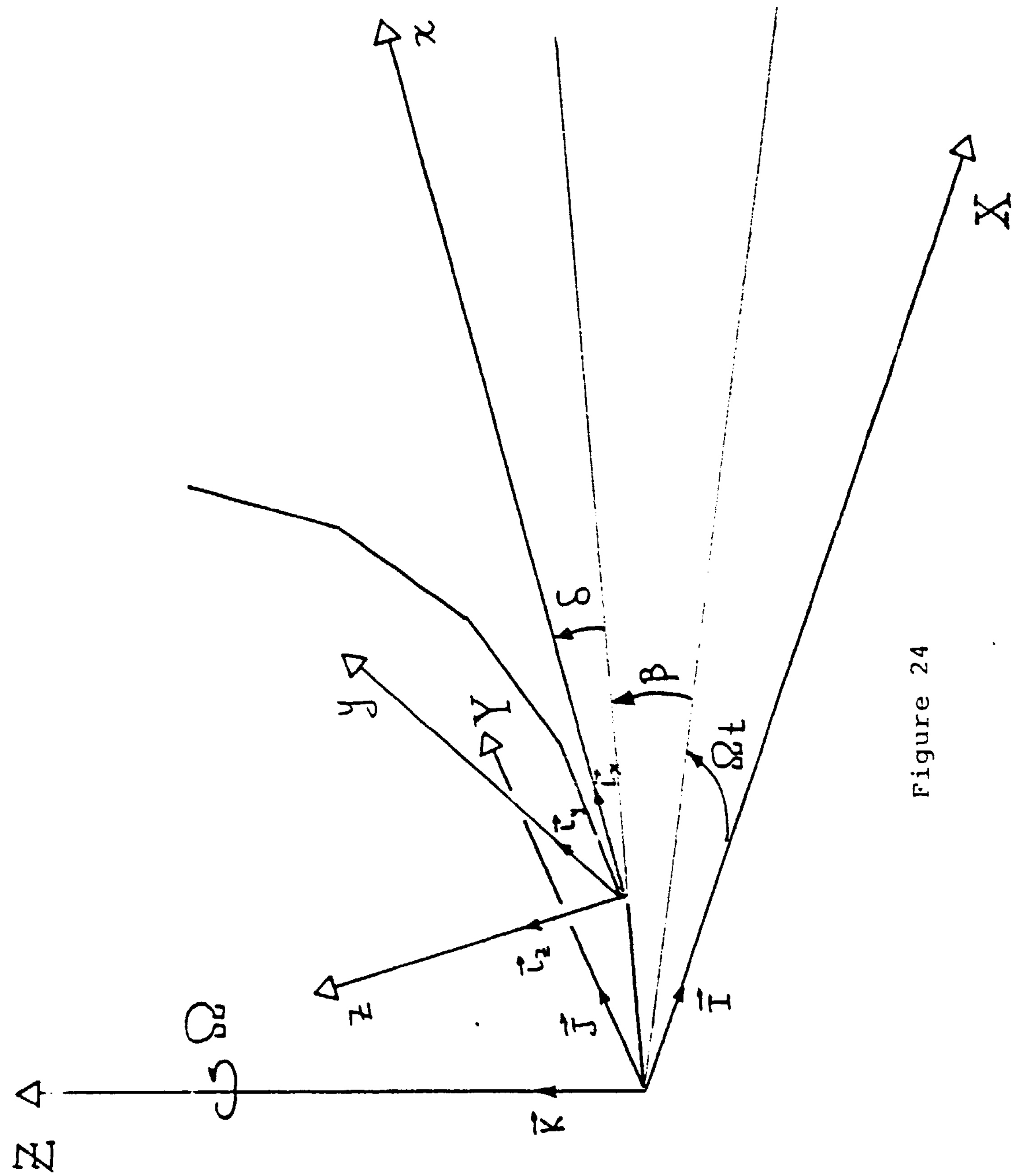

Figure 24

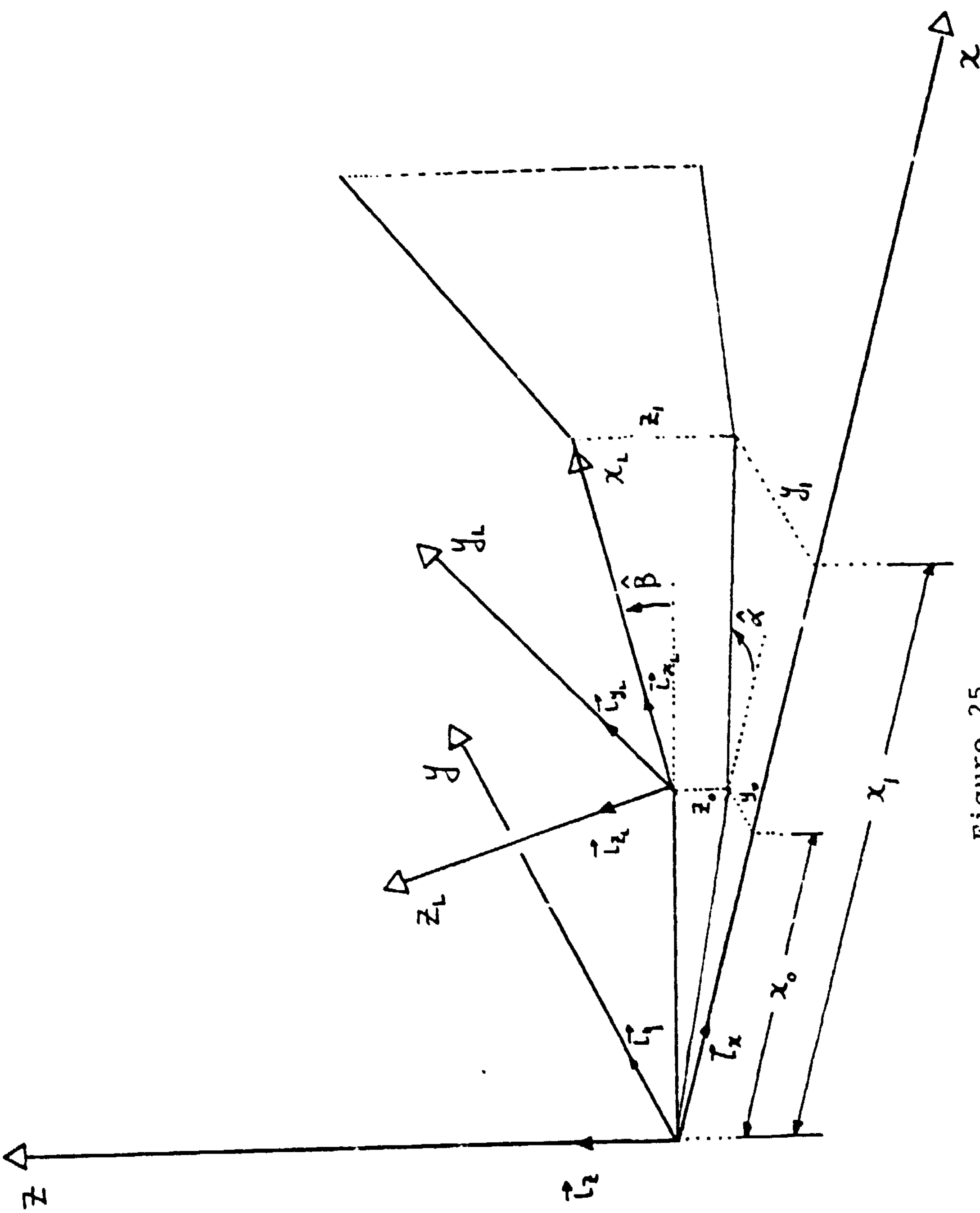

Figure 25

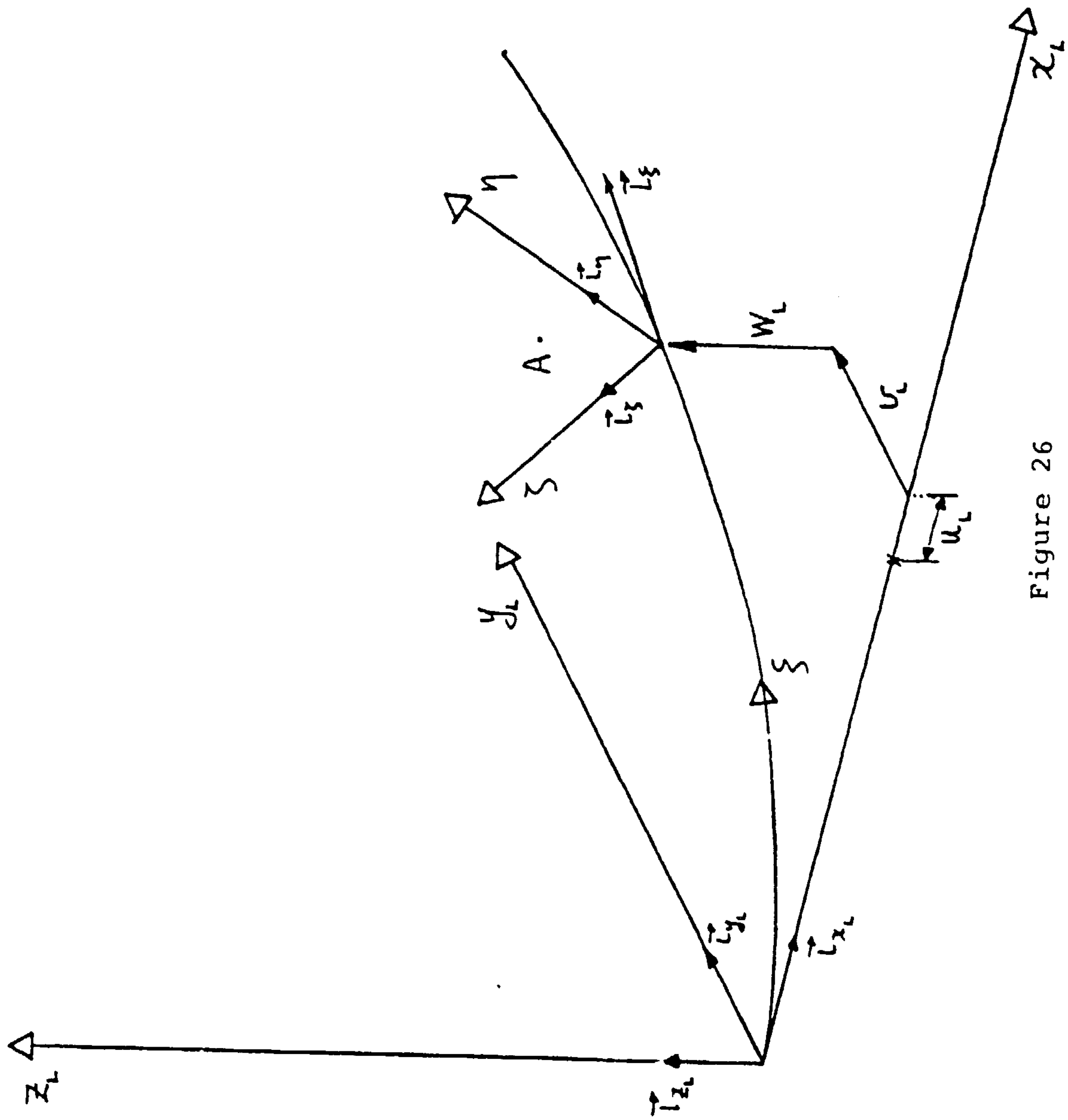

Figure 26

$$\begin{Bmatrix} x_L \\ y_L \\ z_L \end{Bmatrix} = \begin{Bmatrix} \xi + u_L \\ v_L \\ w_L \end{Bmatrix} + \underset{\sim}{F} \begin{Bmatrix} 0 \\ \eta \\ \zeta \end{Bmatrix} \tag{63}$$

where

u_L, v_L, w_L and ϕ_L are elastic axis displacements and cross-section rotations of the blade element in question, u_L, v_L and w_L being positive along the positive $\vec{L}_{x_L}$ $\vec{L}_{y_L}$ $\vec{L}_{z_L}$ directions, respectively, ϕ_L along the ξ direction . ξ is equal to the x_L axis coordinate of point A in the undeformed blade element, and

$$\underset{\sim}{F} = \begin{bmatrix} 1 & -v_L' \cos(\phi_0+\phi_L) - w_L' \sin(\phi_0+\phi_L) & v_L' \sin(\phi_0+\phi_L) - w_L' \cos(\phi_0+\phi_L) \\ v_L' & \cos(\phi_0+\phi_L) & -\sin(\phi_0+\phi_L) \\ w_L' & \sin(\phi_0+\phi_L) & \cos(\phi_0+\phi_L) \end{bmatrix} \tag{64}$$

The position of this point A with respect to the $x\ y\ z$ system of axes will be

$$\begin{Bmatrix} x \\ y \\ z \end{Bmatrix} = \begin{Bmatrix} x_0 \\ y_0 \\ z_0 \end{Bmatrix} + \underset{\sim}{T} \begin{Bmatrix} x_L \\ y_L \\ z_L \end{Bmatrix} \tag{65}$$

where

$$\underset{\sim}{T} = \begin{bmatrix} \cos\hat{\alpha}\cos\hat{\beta} & -\sin\hat{\alpha} & -\sin\hat{\beta}\cos\hat{\alpha} \\ \sin\hat{\alpha}\cos\hat{\beta} & \cos\hat{\alpha} & \sin\hat{\beta}\sin\hat{\alpha} \\ \sin\hat{\beta} & 0 & \cos\hat{\beta} \end{bmatrix} \tag{66}$$

and $x_o\ y_o\ z_o$ are the $x\,y\,z$ coordinates of the left-hand-side node of the element in question in the undeformed blade, defined as

$$\begin{Bmatrix} x_o \\ y_o \\ z_o \end{Bmatrix} = \sum_{\substack{\text{all previous} \\ \text{elements}}} \underset{\sim}{T} \begin{Bmatrix} \ell_i \\ 0 \\ 0 \end{Bmatrix} \tag{67}$$

ℓ_i = element length

The position of point A with respect to the $X\,Y\,Z$ system of axes will be

$$\begin{Bmatrix} X \\ Y \\ Z \end{Bmatrix} = \underset{\sim}{S} \begin{Bmatrix} x \\ y \\ z \end{Bmatrix} + e_o \begin{Bmatrix} \cos\Omega t \cos\phi_o \\ \sin\Omega t \cos\phi_o \\ \sin\phi_o \end{Bmatrix} \tag{68}$$

where

$$\underset{\sim}{S} = \begin{bmatrix} \cos\Omega t \cos(\beta+\delta) & -\sin\Omega t & -\cos\Omega t \sin(\beta+\delta) \\ \sin\Omega t \cos(\beta+\delta) & \cos\Omega t & -\sin\Omega t \sin(\beta+\delta) \\ \sin(\beta+\delta) & 0 & \cos(\beta+\delta) \end{bmatrix} \tag{69}$$

It should also be noted that

$$\begin{aligned} \underset{\sim}{S}^{-1} &= \underset{\sim}{S}^{T} \\ \underset{\sim}{F}^{-1} &= \underset{\sim}{F}^{T} \\ \underset{\sim}{T}^{-1} &= \underset{\sim}{T}^{T} \end{aligned} \tag{70}$$

and

$$\begin{Bmatrix} \vec{i}_{x_L} \\ \vec{i}_{y_L} \\ \vec{i}_{z_L} \end{Bmatrix} = \underset{\sim}{F} \begin{Bmatrix} \vec{i}_{\xi} \\ \vec{i}_{\eta} \\ \vec{i}_{\zeta} \end{Bmatrix} \tag{71a}$$

$$\begin{Bmatrix} \vec{i}_{x} \\ \vec{i}_{y} \\ \vec{i}_{z} \end{Bmatrix} = \underset{\sim}{T} \begin{Bmatrix} \vec{i}_{x_L} \\ \vec{i}_{y_L} \\ \vec{i}_{z_L} \end{Bmatrix} \tag{71b}$$

$$\begin{Bmatrix} \vec{I} \\ \vec{J} \\ \vec{K} \end{Bmatrix} = \underset{\sim}{S} \begin{Bmatrix} \vec{i}_{x} \\ \vec{i}_{y} \\ \vec{i}_{z} \end{Bmatrix} \tag{71c}$$

The rest of the blade properties are identical with the straight elastic axis case.

Finally, once the displacements u v w and ϕ along the x y z system of axes are found, then the new coordinates $(x\ y\ z)_{NEW}$ of the nodes of the blade, the new element lengths $(l_i)_{NEW}$ their new inclinations $(\hat{\alpha})_{NEW}$ and $(\hat{\beta})_{NEW}$ and the new pretwist of the blade $(\phi_o)_{NEW}$ will be obtained as follows

$$\begin{Bmatrix} x \\ y \\ z \end{Bmatrix}_{NEW} = \begin{Bmatrix} u \\ v \\ w \end{Bmatrix} + \begin{Bmatrix} x \\ y \\ z \end{Bmatrix}_{OLD}$$

$$(\ell_i)_{NEW} = \left\{ \sqrt{(x_1 - x_0)^2 + (y_1 - y_0)^2 + (z_1 - z_0)^2} \right\}_{NEW}$$

(See figure 25)

$$(\hat{\alpha})_{NEW} = \tan^{-1}\left(\frac{y_1 - y_0}{x_1 - x_0}\right)_{NEW}$$

$$(\hat{\beta})_{NEW} = \sin^{-1}\left(\frac{z_1 - z_0}{\ell_i}\right)_{NEW}$$

$$(\phi_0)_{NEW} = (\phi_0)_{OLD} + \phi$$

3.2 Minimum Total Potential Energy Formulation

Defining the functional π where

$$\pi = \text{(Strain Energy)} - \text{(Work of External Loads)} \tag{72}$$

and

$$\text{Strain Energy} = \frac{1}{2} \iiint_{\forall} \left(E\epsilon_{xx}^2 + G\gamma_{xy}^2 + G\gamma_{xz}^2 \right) dx\,dy\,dz$$

$$= \frac{1}{2} \sum_{\text{all elements}} \iiint_{\forall} \left(E\epsilon_{\xi\xi}^2 + G\gamma_{\xi\eta}^2 + G\gamma_{\xi\zeta}^2 \right) d\eta\, d\zeta\, d\xi \qquad ($$

where $\forall$ = volume of the blade

$$\text{Work of External Loads} = \sum_{\text{all elements}} \left\{ \int_0^{l_i} \frac{T_c}{A} \iint_A \epsilon_{\xi\xi}\, d\eta\, d\zeta\, d\xi \right.$$

$$+ \int_0^{l_i} p_{y_L} v_L\, dx_L + \int_0^{l_i} p_{z_L} w_L\, dx_L + \int_0^{l_i} q_\xi \phi_L\, d\xi$$

$$\left. + \int_0^{l_i} q_{y_L} w_L'\, dx_L + \int_0^{l_i} q_{z_L} v_L'\, dx_L \right\} \qquad (74)$$

The strain equations that have been obtained in the previous chapter (equations (12), (18), (19)) are applicable here since the energy equation (72) is written as an assembly of straight elastic axis element contributions.

Since we intend to preserve u_L as a separate degree of freedom, we will not use the tension equation to reduce it in favor of v_L, w_L and ϕ_L but we will keep it in the strain equations. Hence

$$\epsilon_{\xi\xi} = u_L' - \eta\left(v_L'' \cos\phi_o + w_L'' \sin\phi_o\right) - \zeta\left(-v_L'' \sin\phi_o + w_L'' \cos\phi_o\right)$$
$$+ \left(\eta^2 + \zeta^2\right) \phi_o' \phi_L'$$

$$\gamma_{\xi\eta} = -\zeta \phi_L'$$

$$\gamma_{\xi\zeta} = \eta \phi_L'$$

By substituting the above into equations (73) and (74) respectively, we get:

$$\text{Strain Energy} = \frac{1}{2}\sum_{\text{all elements}}\int_0^{l_i}\Big\{EA(u_L')^2 + \big[EI_1\sin^2\phi_0 + \overline{EI}_2\cos^2\phi_0\big](v_L'')^2 + \big[EI_1\cos^2\phi_0 + \overline{EI}_2\sin^2\phi_0\big](w_L'')^2 + 2\big[\overline{EI}_2 - EI_1\big]\cdot v_L''w_L''\sin\phi_0\cos\phi_0 + \big[GJ + \overline{EB}_1\cdot(\phi_0')^2\big](\phi_L')^2 - 2EA\big[e_A\cos\phi_0 v_L'' + e_A\sin\phi_0 w_L'' - K_A^2\phi_0'\phi'\big]u_L' - 2\overline{EB}_2\big[v_L''\cos\phi_0 + w_L''\sin\phi_0\big]\phi_0'\phi_L'\Big\}d\xi$$

where

$$\overline{EI}_2 = EI_2 + EAe_A^2$$

$$\overline{EB}_1 = EB_1 + EAK_A^4$$

$$\overline{EB}_2 = EB_2 + EAK_A^2e_A$$

$$\text{Work of External Loads} = \sum_{\text{all elements}}\Big\{\int_0^{l_i}T_c\Big\{-u_L' - \frac{1}{2}\big[(v_L')^2 + (w_L')^2\big] + e_A\big[v_L''\cos\phi_0 + w_L''\sin\phi_0\big] - e_A\phi_L\big[v_L''\sin\phi_0 - w_L''\cos\phi_0\big] - K_A^2\big[\tfrac{1}{2}(\phi_L')^2 + \phi_0'\phi_L'\big]\Big\}d\xi$$

$$+\int_0^{l_i}\left\{p_{y_L} v_L + p_{z_L} w_L + q_{y_L} w_L' + q_{z_L} v_L'\right\} dx_L + \int_0^{l_i} q_\xi \phi_L \, d\xi \Bigg]$$

or

$$\begin{aligned}\Pi = \sum_{\text{all elements}} \Bigg[\frac{1}{2}\int_0^{l_i} & \Big\{ EA(u_L')^2 + [EI_1 \sin^2\phi_0 + \overline{EI}_2 \cos^2\phi_0](v_L'')^2 \\ & + [EI_1 \cos^2\phi_0 + \overline{EI}_2 \sin^2\phi_0](w_L'')^2 + \\ & + 2[\overline{EI}_2 - EI_1] v_L'' w_L'' \sin\phi_0 \cos\phi_0 + \\ & + [GJ + \overline{EB}_1(\phi_0')^2](\phi_L')^2 - 2EA \cdot \\ & \cdot [e_A \cos\phi_0 v_L'' + e_A \sin\phi_0 w_L'' - K_A^2 \phi_0' \phi_L'] u_L' \\ & - 2\overline{EB}_2 [v_L'' \cos\phi_0 + w_L'' \sin\phi_0] \phi_0' \phi_L' \Big\} d\xi \\ - \int_0^{l_i} T_c & \Big\{ -u_L' - \frac{1}{2}[(v_L')^2 + (w_L')^2] + e_A [v_L'' \cos\phi_0 \\ & + w_L'' \sin\phi_0] - e_A \phi_L [v_L'' \sin\phi_0 - w_L'' \cos\phi_0] \\ & - K_A^2 [\tfrac{1}{2}(\phi_L')^2 - \phi_0' \phi_L'] \Big\} d\xi \\ - \int_0^{l_i} & \Big\{ p_{y_L} v_L + p_{z_L} w_L + q_{y_L} w_L' + q_{z_L} v_L' \Big\} dx_L \\ - \int_0^{l_i} & q_\xi \phi_L \, d\xi \Bigg]\end{aligned} \tag{75a}$$

and $$T_c = \int_{x_i}^{l_i} p_{x_L}\, dx_L + P_x \cos\hat{\alpha}\cos\hat{\beta} + P_y \sin\hat{\alpha}\cos\hat{\beta} + P_z \sin\hat{\beta} \qquad (75b)$$

where

$$\begin{Bmatrix} P_x \\ P_y \\ P_z \end{Bmatrix} = \sum_{\substack{\text{rest of elements} \\ \text{along +ve } \vec{i}_x \\ \text{direction}}} \underset{\sim}{T} \begin{Bmatrix} \int_0^{l_i} p_{x_L}\, dx_L \\ \int_0^{l_i} p_{y_L}\, dx_L \\ \int_0^{l_i} p_{z_L}\, dx_L \end{Bmatrix}$$

3.3 Forces and Moments Applied on the Blade

(a) Blade Absolute Acceleration Vector

Assume a point on the undeformed elastic axis to be displaced by u_L, v_L, w_L and then the cross-section to be rotated by ϕ_L.

The global coordinates X, Y, Z of a point A on the above cross-section will be, according to equation (68)

$$\begin{Bmatrix} X \\ Y \\ Z \end{Bmatrix} = \underset{\sim}{S} \begin{Bmatrix} x \\ y \\ z \end{Bmatrix} + e_o \begin{Bmatrix} \cos\Omega t \cos\phi_o \\ \sin\Omega t \cos\phi_o \\ \sin\phi_o \end{Bmatrix}$$

where from equation (65) $$\begin{Bmatrix} x \\ y \\ z \end{Bmatrix} = \begin{Bmatrix} x_o \\ y_o \\ z_o \end{Bmatrix} + \underset{\sim}{T} \begin{Bmatrix} x_L \\ y_L \\ z_L \end{Bmatrix}$$

and from equation (63) $$\begin{Bmatrix} x_L \\ y_L \\ z_L \end{Bmatrix} = \begin{Bmatrix} \xi + u_L \\ v_L \\ w_L \end{Bmatrix} + \underset{\sim}{F} \begin{Bmatrix} 0 \\ \eta \\ \zeta \end{Bmatrix}$$

Substituting equation (63) into (65), then into (68) and differentiating the result twice with respect to time we get the absolute acceleration at point A with respect to the fixed system of axes

$$\begin{Bmatrix} \ddot{X} \\ \ddot{Y} \\ \ddot{Z} \end{Bmatrix} = \underset{\sim}{S}\,\underset{\sim}{T} \begin{Bmatrix} \ddot{u}_L \\ \ddot{v}_L \\ \ddot{w}_L \end{Bmatrix} + 2\,\dot{\underset{\sim}{S}}\,\underset{\sim}{T} \begin{Bmatrix} \dot{u}_L \\ \dot{v}_L \\ \dot{w}_L \end{Bmatrix} + \ddot{\underset{\sim}{S}} \left(\begin{Bmatrix} x_0 \\ y_0 \\ z_0 \end{Bmatrix} + \underset{\sim}{T} \begin{Bmatrix} \xi + u_L \\ v_L \\ w_L \end{Bmatrix} \right)$$

$$+ \left(\underset{\sim}{S}\,\underset{\sim}{T}\,\ddot{\underset{\sim}{F}} + 2\,\dot{\underset{\sim}{S}}\,\underset{\sim}{T}\,\dot{\underset{\sim}{F}} + \ddot{\underset{\sim}{S}}\,\underset{\sim}{T}\,\underset{\sim}{F} \right) \begin{Bmatrix} 0 \\ \eta \\ \zeta \end{Bmatrix}$$

$$+ \Omega^2 e_0 \begin{Bmatrix} -\cos\Omega t \cos\beta \\ -\sin\Omega t \cos\beta \\ 0 \end{Bmatrix} \tag{76}$$

Resolving these accelerations along the $x\,y\,z$ system of axes we get the following components

$$\begin{Bmatrix} a_x \\ a_y \\ a_z \end{Bmatrix} = \underset{\sim}{S}^T \begin{Bmatrix} \ddot{X} \\ \ddot{Y} \\ \ddot{Z} \end{Bmatrix} = \underset{\sim}{T} \begin{Bmatrix} \ddot{u}_L \\ \ddot{v}_L \\ \ddot{w}_L \end{Bmatrix} + 2\,\underset{\sim}{S}^T \dot{\underset{\sim}{S}}\,\underset{\sim}{T} \begin{Bmatrix} \dot{u}_L \\ \dot{v}_L \\ \dot{w}_L \end{Bmatrix}$$

$$+ \underset{\sim}{S}^T \ddot{\underset{\sim}{S}} \left(\begin{Bmatrix} x_0 \\ y_0 \\ z_0 \end{Bmatrix} + \underset{\sim}{T} \begin{Bmatrix} \xi + u_L \\ v_L \\ w_L \end{Bmatrix} \right) + \left(\underset{\sim}{T}\,\ddot{\underset{\sim}{F}} + 2\,\underset{\sim}{S}^T \dot{\underset{\sim}{S}}\,\underset{\sim}{T}\,\dot{\underset{\sim}{F}} \right.$$

$$\left. + \underset{\sim}{S}^T \ddot{\underset{\sim}{S}}\,\underset{\sim}{T}\,\underset{\sim}{F} \right) \begin{Bmatrix} 0 \\ \eta \\ \zeta \end{Bmatrix} + \Omega^2 e_0 \begin{Bmatrix} -\cos(\beta+\delta)\cos\beta \\ 0 \\ \sin(\beta+\delta)\cos\beta \end{Bmatrix} \tag{77}$$

Or more explicitly, the equations for α_x, α_y and α_z are presented in appendix I.

(b) D'Alambert Forces and Moments

In an exactly similar manner with the straight elastic axis analysis, we assume that a point on the elastic axis of the undeformed blade is allowed to be displaced by a set of small virtual displacements δu_L, δv_L, δw_L and $\delta \phi_L$ due to the action of the real inertia loadings. These virtual displacements will change the $x\ y\ z$ coordinates of any point A in that cross-section by $\delta x\ \delta y\ \delta z$, respectively. These virtual changes can be found by taking the first variation of the following equation, which can be obtained by substitution of equation (63) into equation (65):

$$\begin{Bmatrix} x \\ y \\ z \end{Bmatrix} = \begin{Bmatrix} x_o \\ y_o \\ z_o \end{Bmatrix} + \underset{\sim}{T} \begin{Bmatrix} \xi + u_L \\ v_L \\ w_L \end{Bmatrix} + \underset{\sim}{T}\,\underset{\sim}{E} \begin{Bmatrix} 0 \\ \eta \\ \zeta \end{Bmatrix}$$

Ignoring higher order terms and applying the following small angle approximation

$$\cos(\phi + \phi_o) \simeq \cos\phi_o - \phi \sin\phi_o$$
$$\sin(\phi + \phi_o) \simeq \sin\phi_o + \phi \cos\phi_o$$

we get

$$
\begin{aligned}
\delta x = {} & \cos\hat{\alpha}\cos\hat{\beta}\,\delta u_L - \sin\hat{\alpha}\,\delta v_L - \sin\hat{\beta}\cos\hat{\alpha}\,\delta w_L + \\
& + \cos\hat{\alpha}\cos\hat{\beta}\left[-\eta(\cos\phi_0 - \phi_L\sin\phi_0) + \zeta(\sin\phi_0 + \phi_L\cos\phi_0)\right]\delta v_L' \\
& + \cos\hat{\alpha}\cos\hat{\beta}\left[-\eta(\sin\phi_0 + \phi_L\cos\phi_0) - \zeta(\cos\phi_0 - \phi_L\sin\phi_0)\right]\delta w_L' \\
& + \Big\{\cos\hat{\alpha}\cos\hat{\beta}\left[-\eta w_L'\cos\phi_0 + \eta v_L'\sin\phi_0 + \zeta w_L'\sin\phi_0\right. \\
& \quad \left. + \zeta v_L'\cos\phi_0\right] + \sin\hat{\alpha}\left[\eta(\sin\phi_0 + \phi_L\cos\phi_0) + \zeta(\cos\phi_0\right. \\
& \quad \left. - \phi_L\sin\phi_0)\right] - \sin\hat{\beta}\cos\hat{\alpha}\left[\eta(\cos\phi_0 - \phi_L\sin\phi_0) - \zeta(\sin\phi_0\right. \\
& \quad \left. + \phi_L\cos\phi_0)\right]\Big\}\,\delta\phi_L \qquad \text{(78a}
\end{aligned}
$$

$$
\begin{aligned}
\delta y = {} & \sin\hat{\alpha}\cos\hat{\beta}\,\delta u_L + \cos\hat{\alpha}\,\delta v_L - \sin\hat{\beta}\sin\hat{\alpha}\,\delta w_L \\
& + \sin\hat{\alpha}\cos\hat{\beta}\left[-\eta(\cos\phi_0 - \phi_L\sin\phi_0) + \zeta(\sin\phi_0 + \phi_L\cos\phi_0)\right]\delta v_L' \\
& + \sin\hat{\alpha}\cos\hat{\beta}\left[-\eta(\sin\phi_0 + \phi_L\cos\phi_0) - \zeta(\cos\phi_0 - \phi_L\sin\phi_0)\right]\delta w_L' \\
& + \Big\{\sin\hat{\alpha}\cos\hat{\beta}\left[-\eta w_L'\cos\phi_0 + \eta v_L'\sin\phi_0 + \zeta w_L'\sin\phi_0 + \zeta v_L'\cos\phi_0\right] \\
& \quad - \cos\hat{\alpha}\left[\eta(\sin\phi_0 + \phi_L\cos\phi_0) + \zeta(\cos\phi_0 - \phi_L\sin\phi_0)\right] - \\
& \quad - \sin\hat{\beta}\sin\hat{\alpha}\left[\eta(\cos\phi_0 - \phi_L\sin\phi_0) - \zeta(\sin\phi_0 + \phi_L\cos\phi_0)\right]\Big\}\,\delta\phi_L \qquad \text{(78b}
\end{aligned}
$$

$$
\begin{aligned}
\delta z = {} & \sin\hat{\beta}\,\delta u_L + \cos\hat{\beta}\,\delta w_L + \sin\hat{\beta}\left[-\eta(\cos\phi_0 - \phi_L\sin\phi_0) + \right. \\
& \left. + \zeta(\sin\phi_0 + \phi_L\cos\phi_0)\right]\delta v_L' + \sin\hat{\beta}\left[-\eta(\sin\phi_0 + \phi_L\cos\phi_0)\right. \\
& \left. - \zeta(\cos\phi_0 - \phi_L\sin\phi_0)\right]\delta w_L' + \Big\{\sin\hat{\beta}\left[-\eta w_L'\cos\phi_0 + \eta v_L'\sin\phi_0\right. \\
& \left. + \zeta w_L'\sin\phi_0 + \zeta v_L'\cos\phi_0\right] + \cos\hat{\beta}\left[\eta(\cos\phi_0 - \phi_L\sin\phi_0)\right. \\
& \left. - \zeta(\sin\phi_0 + \phi_L\cos\phi_0)\right]\Big\}\,\delta\phi_L \qquad \text{(78c}
\end{aligned}
$$

Then the virtual work done by the inertia loading during the above virtual change of coordinates δx, δy, δz will be

$$\delta W = \iiint_{V} \left\{ (-\alpha_x)\delta x + (-\alpha_y)\delta y + (-\alpha_z)\delta z \right\} \rho_b \, dx\,dy\,dz$$

$$= \sum_{\text{all elements}} \iiint_{V_i} \left\{ (-\alpha_x)\delta x + (-\alpha_y)\delta y + (-\alpha_z)\delta z \right\} \rho_b \, d\eta\, d\zeta\, d\xi$$

Substituting equations (78a,b,c) into the above expression for the virtual work we will get

$$\delta W = \sum_{\text{all elements}} \left\{ \int_0^{l_i} \left[p_{x_L} \delta u_L + p_{y_L} \delta v_L + p_{z_L} \delta w_L + q_{y_L} \delta w_L' + q_{z_L} \delta v_L' \right] dx_L + \int_0^{l_i} q_\xi \, \delta\phi_L \, d\xi \right\}$$

where the inertia loadings will be

$$p_{x_L} = \iint_A \left(-\alpha_x \cos\hat{\alpha}\cos\hat{\beta} - \alpha_y \sin\hat{\alpha}\cos\hat{\beta} - \alpha_z \sin\hat{\beta} \right) \rho_b \, d\eta\, d\zeta$$

$$p_{y_L} = \iint_A \left(-\alpha_x \sin\hat{\alpha} - \alpha_y \cos\hat{\alpha} \right) \rho_b \, d\eta\, d\zeta$$

$$p_{z_L} = \iint_A \left(\alpha_x \sin\hat{\beta}\cos\hat{\alpha} + \alpha_y \sin\hat{\beta}\sin\hat{\alpha} - \alpha_z \cos\hat{\beta} \right) \rho_b \, d\eta\, d\zeta \tag{7}$$

$$\begin{aligned} q_\xi = \iint_A \Big\{ & \left(-\eta w' \cos\phi_0 + \eta v' \sin\phi_0 + \zeta w' \sin\phi_0 + \zeta v' \cos\phi_0 \right) \cdot \big(-\alpha_x \cdot \\ & \cdot \cos\hat{\alpha}\cos\hat{\beta} - \alpha_y \sin\hat{\alpha}\cos\hat{\beta} - \alpha_z \sin\hat{\beta} \big) + \big[\eta (\sin\phi_0 + \\ & + \phi\cos\phi_0) + \zeta (\cos\phi_0 - \phi\sin\phi_0) \big] \cdot \left(-\alpha_x \sin\hat{\alpha} + \alpha_y \cos\hat{\alpha} \right) \\ & + \left[\eta (\cos\phi_0 - \phi\sin\phi_0) - \zeta (\sin\phi_0 + \phi\cos\phi_0) \right] \cdot \big(\alpha_x \sin\hat{\beta}\cos\hat{\alpha} \\ & + \alpha_y \sin\hat{\beta}\sin\hat{\alpha} - \alpha_z \cos\hat{\beta} \big) \Big\} \rho_b \, d\eta\, d\zeta \end{aligned}$$

$$q_{y_L} = \iint_A \left[-\eta(\sin\phi_o + \phi\cos\phi_o) - \zeta(\cos\phi_o - \phi\sin\phi_o)\right]\cdot\left(-\alpha_x\cos\hat{\alpha}\cos\hat{\beta} - \alpha_y\sin\hat{\alpha}\cos\hat{\beta} - \alpha_z\sin\hat{\beta}\right)\rho_b\, d\eta\, d\zeta$$

$$q_{z_L} = \iint_A \left[-\eta(\cos\phi_o - \phi\sin\phi_o) + \zeta(\sin\phi_o + \phi\cos\phi_o)\right]\cdot\left(-\alpha_x\cos\hat{\alpha}\cos\hat{\beta} - \alpha_y\sin\hat{\alpha}\cos\hat{\beta} - \alpha_z\sin\hat{\beta}\right)\rho_b\, d\eta\, d\zeta$$

Substituting the expressions for α_x α_y and α_z presented in appendix I into equations (79) and deleting non-linear and higher order terms we get the equations for the six loadings which can be presented in the following general form

$$\begin{aligned}(\text{Loading}) = {} & (Coef)_1\ddot{u} + (Coef)_2\ddot{v} + (Coef)_3\ddot{w} + (Coef)_4\ddot{\phi} \\ & (Coef)_5\ddot{v}' + (Coef)_6\ddot{w}' + (Coef)_7 u + (Coef)_8 u \\ & (Coef)_9 w + (Coef)_{10}\phi + (Coef)_{11} v' + (Coef)_{12} w' \\ & (Coef)_{13}\mathring{u} + (Coef)_{14}\mathring{v} + (Coef)_{15}\mathring{w} + (Coef)_{16}\mathring{\phi} \\ & (Coef)_{17}\mathring{v}' + (Coef)_{18}\mathring{w}' + (Coef)_{19}\end{aligned}$$

where

$$(\text{Loading}) = p_{x_L},\ p_{y_L},\ p_{z_L},\ q_\xi,\ q_{y_L},\ q_{z_L}$$

Since in this report we investigated only the vibration analysis of the non-straight elastic axis beam, all the damping and constant loading terms in the above loading equations were not included. Thus, only the inertia and stiffness loading terms are presented in appendix J.

3.4 Finite Element Formulation

The blade was discretised into a number N of finite elements with straight elastic axis. In each element the field variables were interpolated according to piecewise continuous interpolation functions. Hence, in a similar manner with the straight elastic axis beam analysis, we prescribe on each node u_L, v_L, v_L', w_L, w_L', ϕ_L or

$$\begin{Bmatrix} u_L \\ v_L \\ w_L \\ \phi_L \end{Bmatrix} = \begin{bmatrix} \underset{\sim}{H}_0 & & & \\ & \underset{\sim}{H}_1 & & \\ & & \underset{\sim}{H}_1 & \\ & & & \underset{\sim}{H}_0 \end{bmatrix} \begin{Bmatrix} \underset{\sim}{q}_{u_L} \\ \underset{\sim}{q}_{v_L} \\ \underset{\sim}{q}_{w_L} \\ \underset{\sim}{q}_{\phi_L} \end{Bmatrix} \tag{80}$$

where
$$\underset{\sim}{q}_{u_L}^T = \left\{ u_{L_1} \; u_{L_2} \right\}$$
$$\underset{\sim}{q}_{v_L}^T = \left\{ v_{L_1} \, v_{L_1}' \; v_{L_2} \; v_{L_2}' \right\}$$
$$\underset{\sim}{q}_{w_L}^T = \left\{ w_{L_1} \; w_{L_1}' \; w_{L_2} \; w_{L_2}' \right\}$$
$$\underset{\sim}{q}_{\phi_L}^T = \left\{ \phi_{L_1} \; \phi_{L_2} \right\}$$

and $\underset{\sim}{H}_0$, $\underset{\sim}{H}_1$ are defined as in equations (50).

Setting
$$\underset{\sim}{q}_L^T = \left\{ \underset{\sim}{q}_{u_L}^T \; \underset{\sim}{q}_{v_L}^T \cdot \underset{\sim}{q}_{w_L}^T \; \underset{\sim}{q}_{\phi_L} \right\} \tag{81}$$

substituting equations (80) and (81) into equation (75a) we get

$$\Pi = \sum_{\text{all } N \text{ elements}} \left[\frac{1}{2} \underset{\sim}{q}_L^T \underset{\sim}{K}_L \underset{\sim}{q}_L - \underset{\sim}{q}_L^T \underset{\sim}{P}_L \right] \tag{82}$$

where $$\underset{\sim}{K}_L = \underset{\sim}{K}_s + \underset{\sim}{K}_G$$

$\underset{\sim}{K}_s$ = structural stiffness matrix of the i^{th} element

$\underset{\sim}{K}_G$ = geometric stiffness matrix of the i^{th} element

$\underset{\sim}{P}_i$ = load vector

and

$$\underset{\sim}{K}_s = \begin{bmatrix} \bar{b}_{10}\underset{\sim}{L}_3 & \bar{b}_{11}\underset{\sim}{L}_2^T & \bar{b}_{12}\underset{\sim}{L}_2^T & \bar{b}_{13}\underset{\sim}{L}_3 \\ & \bar{b}_1\underset{\sim}{L}_1 & \bar{b}_3\underset{\sim}{L}_1 & \bar{b}_4\underset{\sim}{L}_2 \\ & & \bar{b}_2\underset{\sim}{L}_1 & \bar{b}_5\underset{\sim}{L}_2 \\ & \text{SYM} & & \bar{b}_6\underset{\sim}{L}_3 \end{bmatrix}$$

$$\underset{\sim}{K}_G = \begin{bmatrix} \underset{\sim}{0} & \underset{\sim}{0} & \underset{\sim}{0} & \underset{\sim}{0} \\ & \underset{\sim}{L}_4 & \underset{\sim}{0} & \bar{b}_7\underset{\sim}{L}_5 \\ & & \underset{\sim}{L}_4 & \bar{b}_8\underset{\sim}{L}_5 \\ & & & \bar{b}_9\underset{\sim}{L}_3 \end{bmatrix}$$

T_c is given in equation (75b)

$$\underset{\sim}{P} = \begin{bmatrix} -\int_0^{l_i} \underset{\sim}{H}_0'^T T_c \, d\xi + \int_0^{l_i} \underset{\sim}{H}_0^T p_{z_L} \, dx_L \\ -\int_0^{l_i} \underset{\sim}{H}_1''^T T_c \bar{b}_8 \, d\xi + \int_0^{l_i} \underset{\sim}{H}_1^T p_{y_L} \, dx_L + \int_0^{l_i} \underset{\sim}{H}_1'^T q_{z_L} \, dx_L \\ \int_0^{l_i} \underset{\sim}{H}_1''^T T_c \bar{b}_2 \, d\xi + \int_0^{l_i} \underset{\sim}{H}_1^T p_{z_L} \, dx_L + \int_0^{l_i} \underset{\sim}{H}_1'^T q_{y_L} \, dx_L \\ -\int_0^{l_i} \underset{\sim}{H}_0'^T T_c K_A^2 \phi_0' \, d\xi + \int_0^{l_i} \underset{\sim}{H}_0^T q_\xi \, d\xi \end{bmatrix}$$

where the $\bar{b}_i$ coefficients are

$$\bar{b}_1 = EI_1 \cos^2\phi_o + \overline{EI}_2 \sin^2\phi_o$$
$$\bar{b}_2 = EI_1 \sin^2\phi_o + \overline{EI}_2 \cos^2\phi_o$$
$$\bar{b}_3 = (\overline{EI}_2 - EI_1) \cos\phi_o \sin\phi_o$$
$$\bar{b}_4 = -\overline{EB}_2 \cos\phi_o (\phi_o')$$
$$b_5 = -EB_2 \sin\phi_o (\phi_o')$$
$$\bar{b}_6 = GJ + \overline{EB}_1 (\phi_o')^2$$
$$\bar{b}_7 = e_A \sin\phi_o$$
$$\bar{b}_8 = -e_A \cos\phi_o$$
$$\bar{b}_9 = K_A^2$$
$$\bar{b}_{10} = EA$$
$$\bar{b}_{11} = EA\, e_A \cos\phi_o$$
$$\bar{b}_{12} = EA\, e_A \sin\phi_o$$
$$\bar{b}_{13} = -EA K_A^2 \phi_o'$$

and the $\underset{\sim}{L}_i$ matrices are given in appendix C.

Substituting the loadings presented in appendix J into equation (82) we get

$$\pi = \sum_{\text{all } N \text{ elements}} \left[\frac{1}{2} \underset{\sim}{q}_i^T \underset{\sim}{K}_i \underset{\sim}{q}_i + \underset{\sim}{q}_i^T \underset{\sim}{m}_i \ddot{\underset{\sim}{q}}_i + \underset{\sim}{q}_i^T \underset{\sim}{K}_m \underset{\sim}{q}_i \right] \qquad (83)$$

where $\underset{\sim}{m}_i$ = mass matrix of the i^{th} element

$\underset{\sim}{K}_m$ = "mass" stiffness matrix of the i^{th} element

ORIGINAL PAGE IS
OF POOR QUALITY

and

$$\mathbf{m}_L = -\begin{bmatrix} E_1\mathbf{L}_8 & E_6\mathbf{L}_{10} & E_7\mathbf{L}_{10} & \mathbf{0} \\ & E_1\mathbf{L}_6 + K_6\mathbf{L}_4 & K_7\mathbf{L}_4 & \Theta_2\mathbf{L}_9^T \\ & & E_1\mathbf{L}_6 + I_7\mathbf{L}_4 & \Theta_3\mathbf{L}_9^T \\ \text{SYM} & & & \Theta_4\mathbf{L}_8 \end{bmatrix}$$

$$\mathbf{K}_m = -\left[\begin{array}{c:c:c:c} E_8\mathbf{L}_8 & E_9\mathbf{L}_9 + E_{13}\mathbf{L}_{10} & E_{10}\mathbf{L}_9 + E_{14}\mathbf{L}_{10} & E_{11}\mathbf{L}_8 \\ \hdashline & \begin{matrix} Z_9\mathbf{L}_6 + Z_{13}\mathbf{L}_7 \\ +K_9\mathbf{L}_7^T + K_{13}\mathbf{L}_4 \end{matrix} & \begin{matrix} Z_{10}\mathbf{L}_6 + Z_{14}\mathbf{L}_7 \\ +K_{10}\mathbf{L}_7^T + K_{14}\mathbf{L}_4 \end{matrix} & \begin{matrix} Z_{11}\mathbf{L}_9^T \\ +K_{11}\mathbf{L}_{10}^T \end{matrix} \\ \hdashline & & \begin{matrix} H_{10}\mathbf{L}_6 + H_{14}\mathbf{L}_7 \\ +I_{10}\mathbf{L}_7^T + I_{14}\mathbf{L}_4 \end{matrix} & \begin{matrix} H_{11}\mathbf{L}_9^T \\ +I_{11}\mathbf{L}_{10}^T \end{matrix} \\ \hdashline \text{SYM} & & & \Theta_{11}\mathbf{L}_8 \end{array}\right]$$

the E_i, Z_i, H_i, Θ_i, K_i, I_i coefficients are given in appendix J. Since the coefficients of the mass matrix $\mathbf{m}_L$ are much simpler than the ones of the stiffness matrix $\mathbf{K}_m$, they are listed below

$$E_1 = -m$$

$$E_6 = me\cos\phi_0$$

$$E_7 = me\sin\phi_0$$

$$K_6 = -m\left(K_{m_1}^2\sin^2\phi_0 + K_{m_2}^2\cos^2\phi_0\right)$$

$$K_7 = -m\left(K_{m_2}^2 - K_{m_1}^2\right)\sin\phi_0\cos\phi_0$$

$$\Theta_2 = me\sin\phi_0$$

$$\Theta_3 = -me\cos\phi_o$$
$$I_2 = -m\left(K_{m_1}^2\cos^2\phi_o + K_{m_2}^2\sin^2\phi_o\right)$$
$$\Theta_4 = -mK_m^2$$

From equations (70) and 71b) we have

$$\begin{Bmatrix} \vec{L}_{x_L} \\ \vec{L}_{y_L} \\ \vec{L}_{z_L} \end{Bmatrix} = \underset{\sim}{T}^T \begin{Bmatrix} \vec{L}_x \\ \vec{L}_y \\ \vec{L}_z \end{Bmatrix}$$

Hence we can write

$$\begin{Bmatrix} u_L \\ v_L \\ w_L \\ \phi_L \\ -w_L' \\ v_L' \end{Bmatrix} = \left[\begin{array}{c|c} \underset{\sim}{T}^T & \\ \hline & \underset{\sim}{T}^T \end{array}\right] \begin{Bmatrix} u \\ v \\ w \\ \phi \\ -w' \\ v' \end{Bmatrix} \tag{94}$$

where $u\ v\ w$ and ϕ are nodal displacements and rotations measured along the $x\,y\,z$ system of axes.

Rearranging the terms in equation (84) and changing the sign of w_L' terms we get

$$\begin{Bmatrix} u_L \\ v_L \\ v_L' \\ w_L \\ w_L' \\ \phi_L \end{Bmatrix} = \underset{\sim}{T}_M \begin{Bmatrix} u \\ v \\ v' \\ w \\ w \\ \phi \end{Bmatrix} \tag{85}$$

where $\underset{\sim}{T}_M$ is a modified transformation matrix obtained from equation (84) and is presented in appendix L.

Rearranging equation (85) to include both nodes of a given finite element we get

$$\underset{\sim}{q}_L = \underset{\sim}{T}_A \underset{\sim}{q} \tag{86}$$

where

$$\underset{\sim}{q}^T = \left\{ u_1\ u_2\ v_1\ v_1'\ v_2\ v_2'\ w_1\ w_1'\ w_2\ w_2'\ \phi_1\ \phi_2 \right\}$$

It has to be noted that for this particular arrangement of displacements and rotations in the $\underset{\sim}{q}$ matrix, the elements of $\underset{\sim}{T}_A$ are related to the elements of $\underset{\sim}{T}_M$ by suitable rearrangement. In appendix L a differently arranged $\underset{\sim}{q}$ matrix is presented which leads into a simpler transformation matrix $\underset{\sim}{T}_B$.

Substituting equation (86) into equation (83) and setting the first variation of π to zero we get

$$\delta\pi = \underset{\sim}{M}\, \ddot{\underset{\sim}{q}}_T + \underset{\sim}{K}\, \underset{\sim}{q}_T = 0 \tag{87}$$

where

$$\underset{\sim}{q}_T = \sum_{\text{all } N \text{ elements}} \underset{\sim}{q}$$

$$K = \sum_{\text{all } N \text{ elements}} \underset{\sim}{T}_A^T (\underset{\sim}{K}_s + \underset{\sim}{K}_G + \underset{\sim}{K}_m) \underset{\sim}{T}_A$$

$$M = \sum_{\text{all } N \text{ elements}} \underset{\sim}{T}_A^T \underset{\sim}{m}_L \underset{\sim}{T}_A$$

3.5 Vibration Analysis

Equation (87) can be solved in an exactly similar manner as in 2.5 Vibration Analysis, as a generalised eigenvalue problem of the following form

$$\underset{\sim}{K} \underset{\sim}{\Phi} = \underset{\sim}{M} \underset{\sim}{\Phi} \underset{\sim}{\Lambda}$$

where $$\Lambda = \begin{bmatrix} \omega_1^2 & & & \\ & \omega_2^2 & & \\ & & \ddots & \\ & & & \omega_m \end{bmatrix}$$ being the eigenvalue matrix

$$\Phi = \left[\underset{\sim}{\Phi}_1 \; \underset{\sim}{\Phi}_2 \; \ldots \; \underset{\sim}{\Phi}_m \right]$$ being the eigenvector matrix

for m degrees of freedom (generalised coordinates).

(a) Uniform Cantilever Curved Beam

A curved cantilever beam with its elastic axis in the shape of a circular arc, was discretised into 7 finite elements with the following inclinations $\hat{\alpha}$ and $\hat{\beta}$.

Element Number	$\hat{\alpha}$	$\hat{\beta}$
1	0°	0°
2	10°	0°
3	20°	0°
4	30°	0°
5	40°	0°
6	50°	0°
7	60°	0°

The free vibration mode shapes of the lowest 5 non-rotating modes were obtained using subspace iteration.

The same cantilever beam but with a straight elastic axis was analysed and the lowest 5 vibration modes and frequencies were obtained. In appendix K a comparison between these frequencies and the ones calculated theoretically, is shown. The agreement is very good.

Figure 27 shows the first out-of-plane vibration mode shape of both straight and circular elastic axis cantilever beams. This mode shape consists primarily of w displacement, the u

and v being almost zero. It can be seen that there is almost no difference between the straight and the circular elastic axis beam mode shapes, the circular one having a slightly higher frequency than the straight,

i.e., $$\omega_{circular} = 1.86 \text{ Hz}$$

$$\omega_{straight} = 1.84 \text{ Hz}$$

Figure 28 shows the first in-plane vibration mode shape for both beams. This mode shape consists primarily of v displacement (upper plot). The lower plot shows the u displacement associated with this mode. ($w \approx 0$) It can be seen that the circular beam exhibits a little different mode shape than the straight one and it has a higher frequency, too.

i.e., $$\omega_{circular} = 1.899 \text{ Hz}$$

$$\omega_{straight} = 1.84 \text{ Hz}$$

Figure 29 shows the second out-of-plane mode shape for both beams. It consists primarily of w displacement ($u \approx v \approx 0$). It has to be noted that the circular beam, although it does not exhibit a big change in the w mode shape, has a lower frequency than the straight one

$$\omega_{circular} = 9.76 \text{ Hz}$$

$$\omega_{straight} = 11.53 \text{ Hz}$$

Figure 30 shows the second in-plane vibration mode shape for both beams. It consists primarily of u displacement (lower plot). The upper plot shows the v displacement associated with

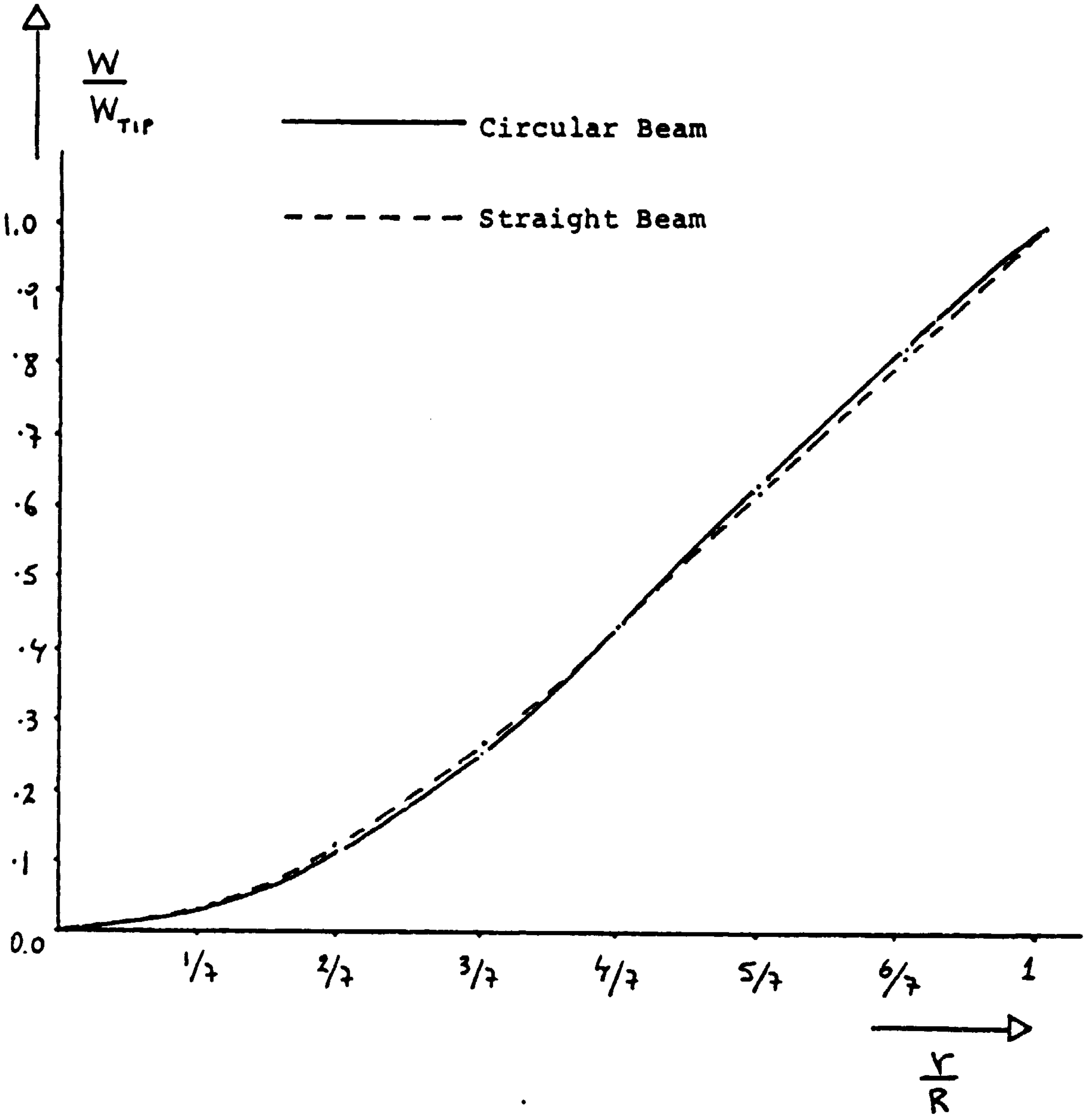

First Out-Of-Plane Mode Shape

Figure 27

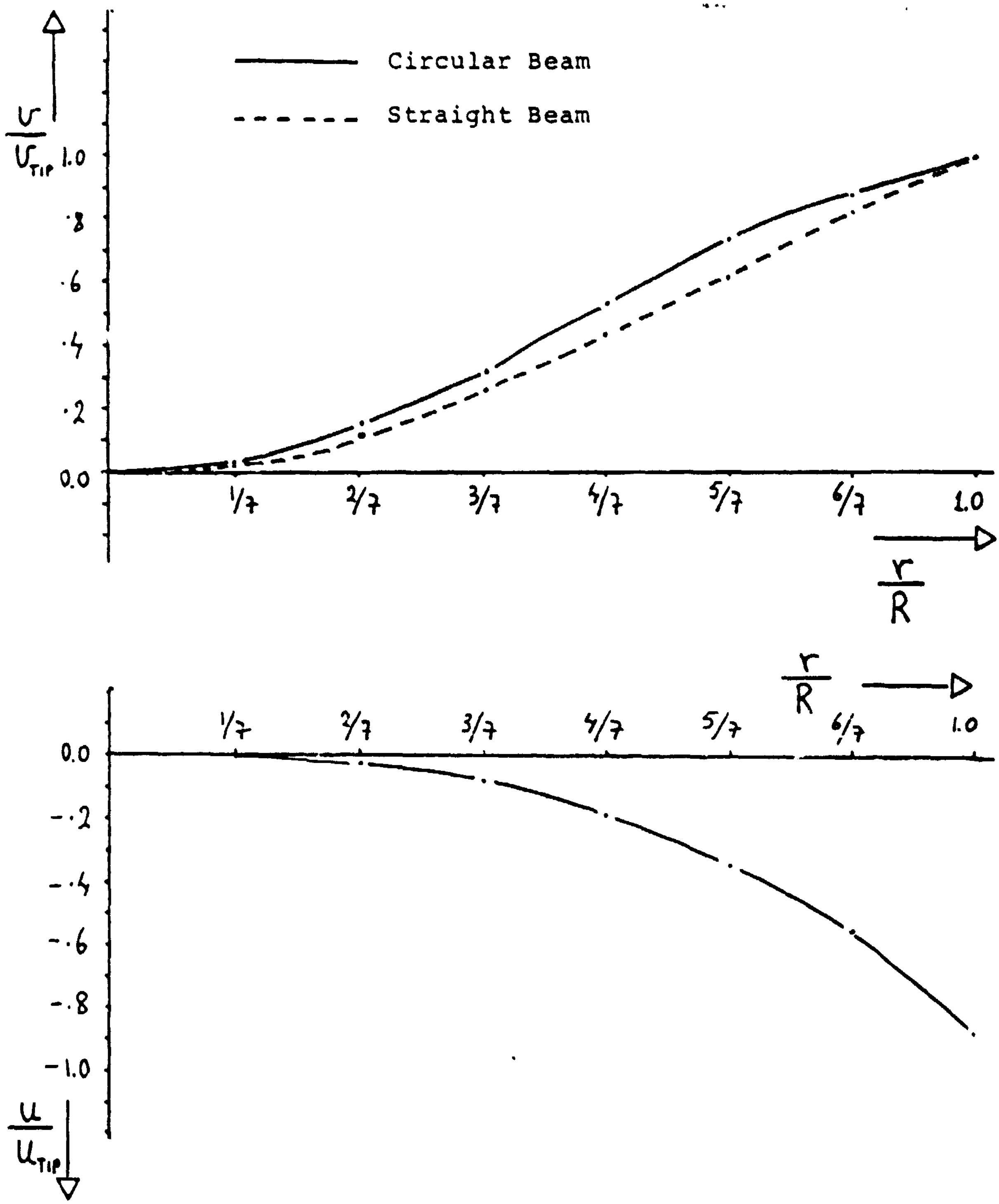

First In-Plane Mode Shape

Figure 28

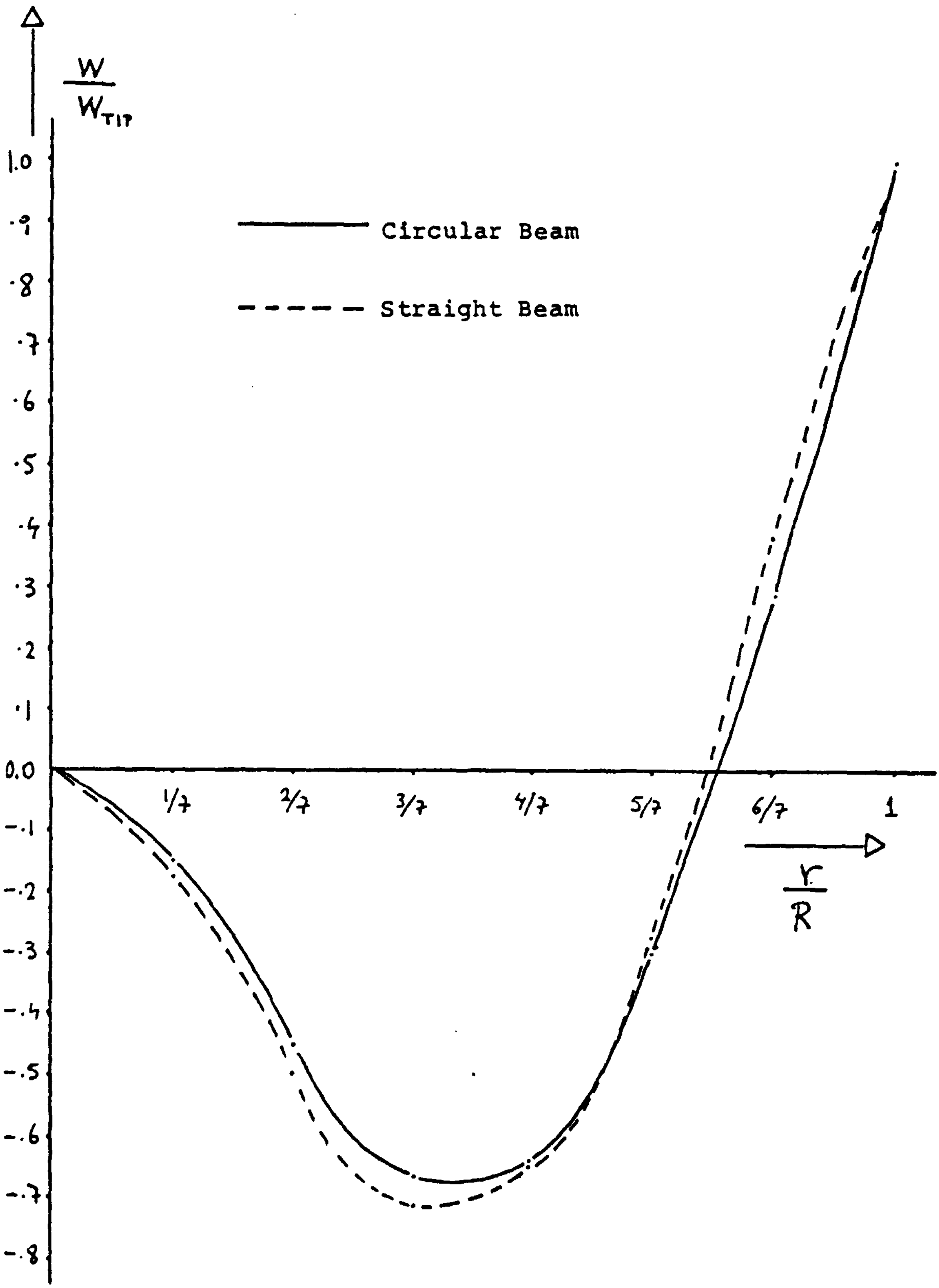

Second Out-Of-Plane Mode Shape

Figure 29

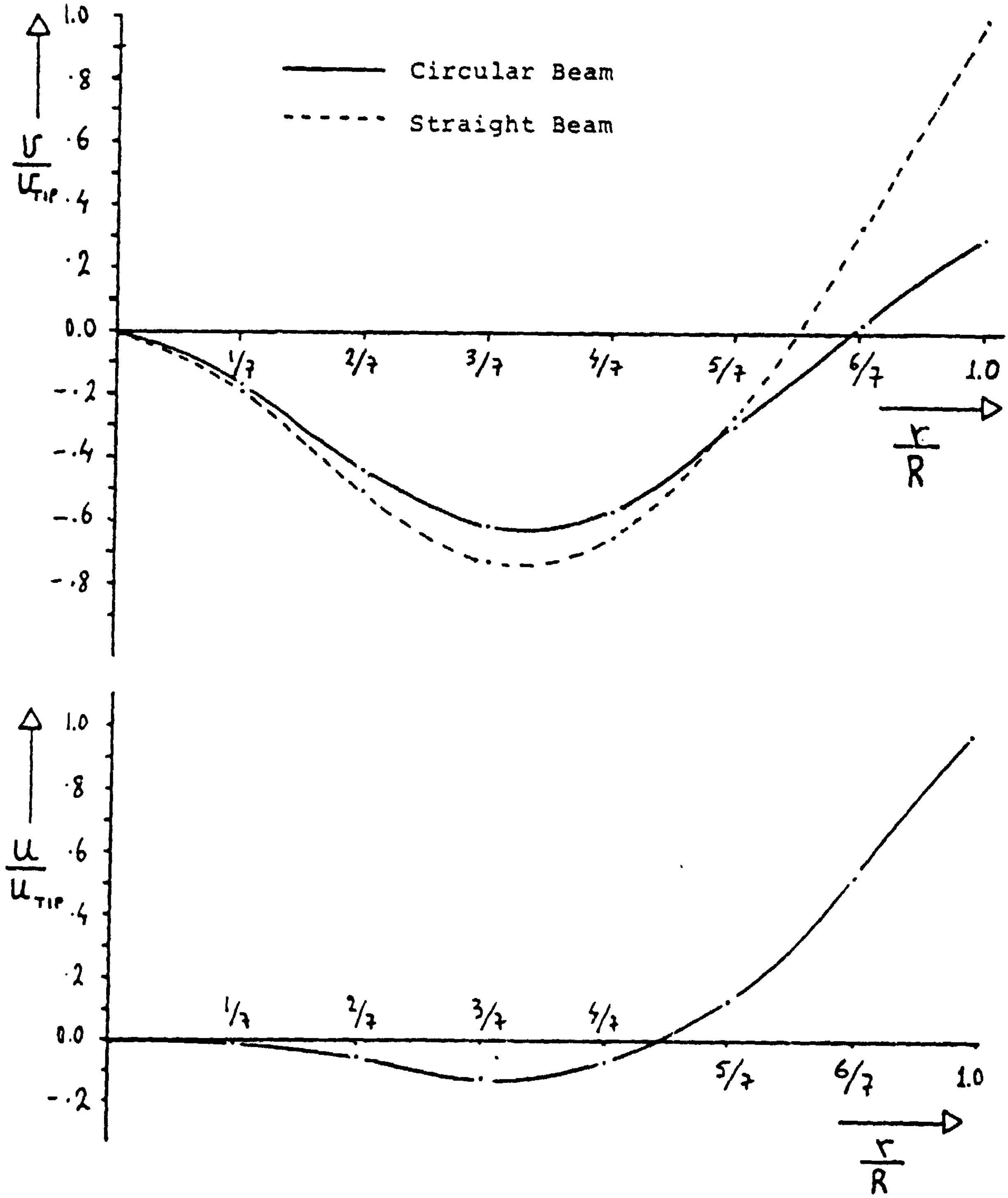

Second In-Plane Mode Shape

Figure 30

this mode ($w \approx 0$). It can be seen that the circular beam has a considerably different v mode shape than the straight one and also a lower frequency

i.e.,
$$\omega_{circular} = 10.01 \text{ Hz}$$
$$\omega_{straight} = 11.54 \text{ Hz}$$

Finally, figures 31 and 32 present a picture of the vibration pattern associated with the first in-plane and second in-plane mode of the circular beam, respectively.

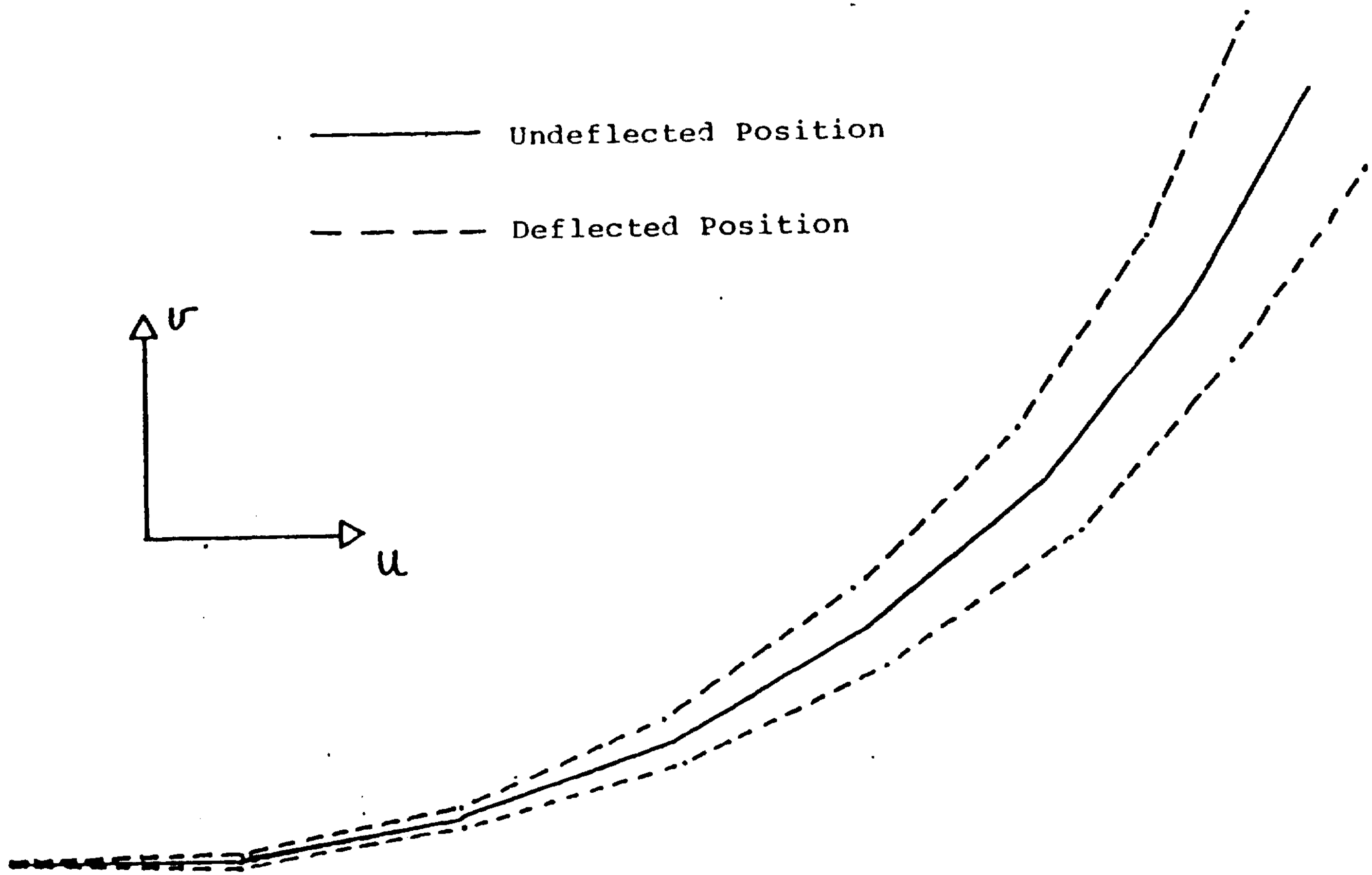

First In-Plane Mode Shape

Figure 31

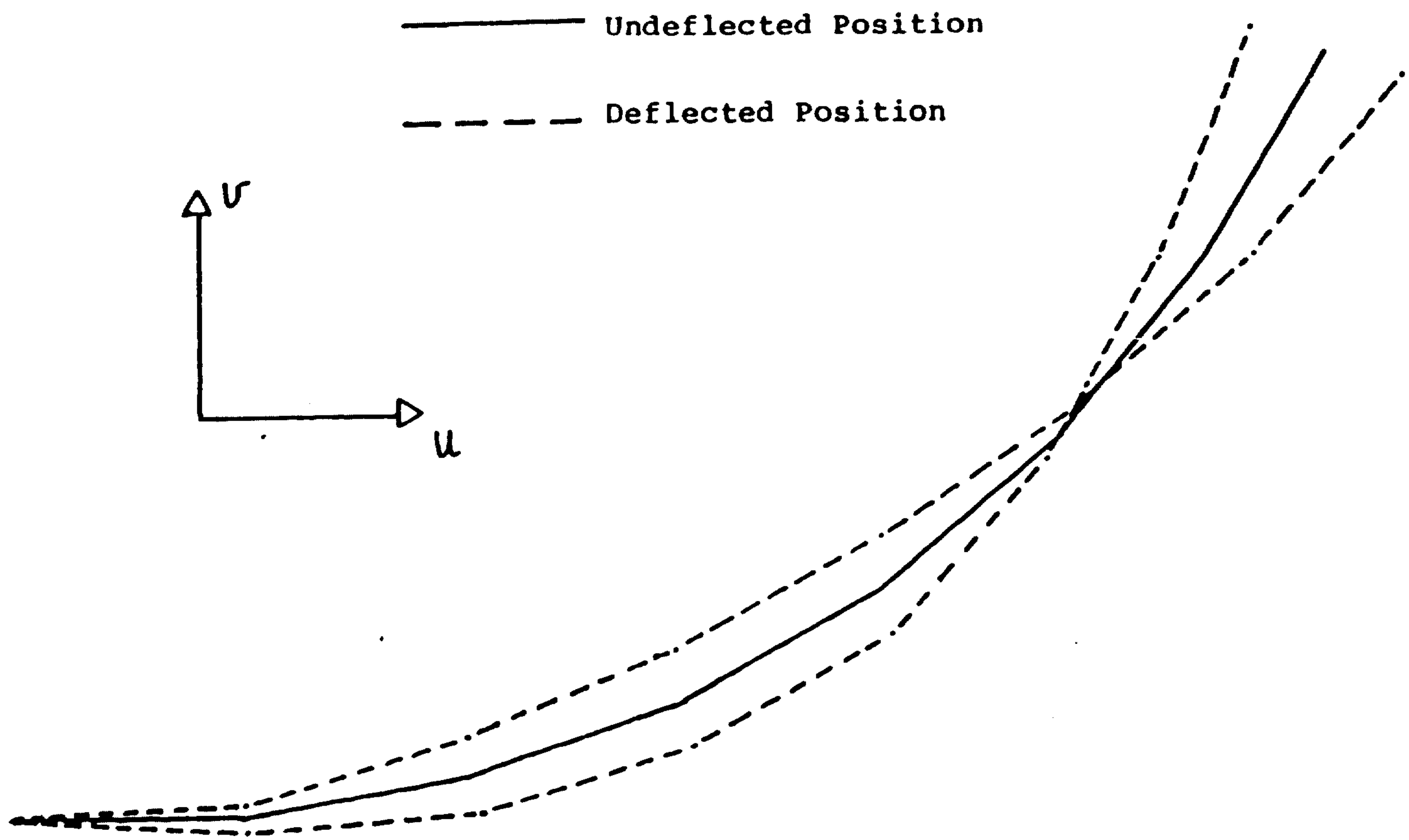

Second In-Plane Mode Shape

Figure 32

4. CONCLUSIONS

In this report, a straight elastic axis blade was represented by an Euler-Bernoulli beam, with generally non-uniform properties. The Total Potential Energy functional Π was formulated in terms of in-plane and out-of-plane displacements and cross-section rotations, based on linear theory of beams.

The blade was allowed to rotate and vibrate in a uniform free air stream in general. The blade absolute acceleration and absolute velocity vectors were found from which the linear, inertia and aerodynamics loads were calculated.

The blade was discretised in a sufficient number of finite beam elements along which the field variables were interpolated according to the Finite Element Method. Static, Vibration and Flutter Analysis were then performed by minimizing the functional Π.

In Vibration Analysis, a uniform cantilever beam was analysed and the mode shapes and frequencies were compared with theoretical ones. The agreement was very good. The lowest three mode shapes and frequencies of the NASA/DOE MOD-O blade were obtained and compared with results from Lockheed-California Company. The agreement was good. The direction of motion of the NASA/DOE MOD-O blade, the McCauley Propeller and the North Wind Turbine blade were investigated for the first out-of-plane and first in-plane modes. All the three blades were found to vibrate, during the first out-of-plane mode, along most of their span in a direction normal to the chord at the section around

30-35% of their span. This behaviour was not generally exhibited during the first in-plane mode. Similar behaviour was encountered on a set of variable-pretwist flat plates treated as cantilever beams and vibrating in the first out-of-plane mode.

In Flutter Analysis, three comparison sets of cases were examined, involving References (3), (6) and (8). The agreement was generally good.

In this report, the Vibration Analysis of a non-straight elastic axis blade was also formulated, based on linear theory of beams. The blade was modeled as an assembly of straight elastic axis elements with different inclination with respect to a common system of axes. The Vibration Analysis was then reduced in a form similar to the straight elastic axis case. Two, non-rotating, uniform cantilever beams with identical properties, one having a straight elastic axis and the other having a circular arc one, were analysed and their lowest two mode shapes and frequencies were compared to each other. It was found that there was very little difference in the mode shapes between the two cantilever beams for the first and second out-of-plane modes, but generally more difference for the in-plane modes. The frequencies were, in general, almost the same between the two cantilever beams for all the modes examined.

Appendix A - Inertia Loadings

Second order terms are shown deleted.

$$
\begin{aligned}
p_x = {} & 2\Omega m \cancel{\cos(\beta+\delta)}\dot{v} - 2\Omega m e \cancel{\cos(\beta+\delta)} \sin\phi_0 \dot{\phi} - \\
& - \Omega^2 m \sin(\beta+\delta)\cos(\beta+\delta) w - \Omega^2 m e \cancel{\sin(\beta+\delta)}\cos(\beta+\delta)\cdot \\
& \cdot \cos\phi_0 \phi + m\Omega^2 \xi \cos^2(\beta+\delta) + m\Omega^2 e_0 \cos(\beta+\delta)\cos\beta \\
& - m\Omega^2 e \sin(\beta+\delta)\cos(\beta+\delta)\sin\phi_0 - m\Omega^2 e \cos^2(\beta+\delta)\cdot \\
& \cdot \cos\phi_0 v' - m\Omega^2 e \cos^2(\beta+\delta)\sin\phi_0 w' + m\cancel{e\cos\phi_0}\ddot{v}' \\
& + m\cancel{e\sin\phi_0}\ddot{w}'
\end{aligned}
$$

$$
\begin{aligned}
p_y = {} & -m\ddot{v} + me\sin\phi_0 \ddot{\phi} + 2m\Omega\sin(\beta+\delta)\dot{w} + 2m\Omega\cdot \\
& \cdot e\sin(\beta+\delta)\cos\phi_0 \dot{\phi} + m\Omega^2 v - m\Omega^2 e\sin\phi_0 \phi \\
& + m\Omega^2 e\cos\phi_0 + 2m\Omega e\cos(\beta+\delta)\left[\dot{v}'\cos\phi_0 + \dot{w}'\sin\phi_0\right]
\end{aligned}
$$

$$
\begin{aligned}
p_z = {} & -m\ddot{w} - me\cos\phi_0 \ddot{\phi} - 2m\Omega\sin(\beta+\delta)\dot{v} + \\
& + 2m\Omega e\sin(\beta+\delta)\sin\phi_0 \dot{\phi} + m\Omega^2 \cancel{\sin^2(\beta+\delta)} w + \\
& + me\Omega^2 \cancel{\sin^2(\beta+\delta)}\cos\phi_0 \phi - m\Omega^2 \sin(\beta+\delta)\cos(\beta+\delta)\xi \\
& - m\Omega^2 e_0 \sin(\beta+\delta)\cos\beta - m\Omega^2 e\cancel{\sin^2(\beta+\delta)}\sin\phi_0 + \\
& + me\Omega^2 \cancel{\sin(\beta+\delta)}\cos(\beta+\delta)\left[v'\cos\phi_0 + w'\sin\phi_0\right]
\end{aligned}
$$

$$
\begin{aligned}
q_\xi = {} & me\sin\phi_0\,\ddot{v} - me\cos\phi_0\,\ddot{w} - mK_m^2\,\ddot{\phi} - 2m\Omega e\,\cdot \\
& \cdot\sin(\beta+\delta)\sin\phi_0\,\dot{w} - 2m\Omega e\sin(\beta+\delta)\cos\phi_0\,\dot{v} - \\
& - m\Omega^2\left(K_{m_2}^2 - K_{m_1}^2\right)\cos^2(\beta+\delta)\cos 2\phi_0\,\phi - \Omega^2 me\,\cdot \\
& \cdot\sin\phi_0\,v + m\Omega^2 e\cancel{\sin^2(\beta+\delta)}\cos\phi_0\,w + m\Omega^2 e\,\xi\,\cdot \\
& \cdot\sin(\beta+\delta)\cos(\beta+\delta)\sin\phi_0\,\phi + m\Omega^2 ee_0\cancel{\sin(\beta+\delta)}\cos\beta\,\cdot \\
& \sin\phi_0\,\phi - m\Omega^2\left(K_{m_2}^2 - K_{m_1}^2\right)\cos^2(\beta+\delta)\sin\phi_0\cos\phi_0 \\
& - m\Omega^2 e\,\xi\sin(\beta+\delta)\cos(\beta+\delta)\cos\phi_0 - m\Omega^2 ee_0\,\cdot \\
& \sin(\beta+\delta)\cos\beta\cos\phi_0 - m\Omega^2 e\cos(\beta+\delta)\left[\xi\cos(\beta+\delta)\right. \\
& \left. + e_0\cos\beta\right]\left[w'\cos\phi_0 - v'\sin\phi_0\right] + 2m\Omega^2\sin(\beta+\delta)\,\cdot \\
& \cdot\cancel{\cos(\beta+\delta)}\sin\phi_0\cos\phi_0\left(K_{m_2}^2 - K_{m_1}^2\right)w' + m\Omega^2\,\cdot \\
& \cdot\cancel{\sin(\beta+\delta)}\cos(\beta+\delta)\left[K_{m_2}^2\left(\cos^2\phi_0 - \sin^2\phi_0\right)\right. + \\
& \left. + K_{m_1}^2\left(\sin^2\phi_0 - \cos^2\phi_0\right)\right]v' - 2m\Omega\left(K_{m_2}^2 - K_{m_1}^2\right)\cdot \\
& \cdot\cos(\beta+\delta)\cos\phi_0\sin\phi_0\,\dot{v}' - 2m\Omega\left(K_{m_2}^2\sin^2\phi_0\right. + \\
& \left. + K_{m_1}^2\cos^2\phi_0\right)\cos(\beta+\delta)\,\dot{w}'
\end{aligned}
$$

$$
\begin{aligned}
q_y = {} & -2m\Omega e\cos(\beta+\delta)\sin\phi_0\,\dot{v} + 2m\Omega\cos(\beta+\delta)\,\cdot \\
& \cdot\left(K_{m_2}^2\sin^2\phi_0 + K_{m_1}^2\cos^2\phi_0\right)\dot{\phi} - m\Omega^2 e\left(\xi\cos^2(\beta+\delta)\right. \\
& \left. + e_0\cos(\beta+\delta)\cos\beta\right)\cos\phi_0\,\phi + m\Omega^2 e\cancel{\sin(\beta+\delta)}\,\cdot \\
& \cdot\cos(\beta+\delta)\sin\phi_0\,w + 2m\Omega^2\left(K_{m_2}^2 - K_{m_1}^2\right)\cancel{\sin(\beta+\delta)}\,\cdot \\
& \cdot\cos(\beta+\delta)\sin\phi_0\cos\phi_0\,\phi - m\Omega^2 e\left(\xi\cos^2(\beta+\delta)\right. + \\
& \left. + e_0\cos(\beta+\delta)\cos\beta\right)\sin\phi_0 + m\Omega^2\left(K_{m_2}^2\sin^2\phi_0\right. + \\
& \left. + K_{m_1}^2\cos^2\phi_0\right)\cancel{\sin(\beta+\delta)}\cos(\beta+\delta) + m\Omega^2\left(K_{m_2}^2\right.
\end{aligned}
$$

$$
\begin{aligned}
&- K_{m_1}^2 \big) \cancel{\cos^2(\beta+\delta)} \sin\phi_0 \cos\phi_0 \, v' + m\Omega^2 \big(K_{m_2}^2 \sin^2\phi_0 \\
&+ K_{m_1}^2 \cos^2\phi_0 \big) \cancel{\cos^2(\beta+\delta)} \, w' - m \cancel{\left(K_{m_2}^2 - K_{m_1}^2 \right)} \sin\phi_0 \cdot \\
&\cdot \cos\phi_0 \, \ddot{v}' - m \cancel{\left(K_{m_2}^2 \sin^2\phi_0 + K_{m_1}^2 \cos^2\phi_0 \right)} \ddot{w}'
\end{aligned}
$$

$$
\begin{aligned}
q_z = {} & - 2 m\Omega e \cos(\beta+\delta) \cos\phi_0 \, \mathring{v} + 2 m\Omega \left(K_{m_2}^2 - K_{m_1}^2 \right) \cdot \\
& \cdot \cos(\beta+\delta) \sin\phi_0 \cos\phi_0 \, \mathring{\phi} + m\Omega^2 e \left(\xi \cos^2(\beta+\delta) \right. \\
& \left. + e_0 \cos(\beta+\delta) \cos\beta \right) \sin\phi_0 \, \phi + m\Omega^2 \cancel{e \sin(\beta+\delta)} \cdot \\
& \cdot \cos(\beta+\delta) \cos\phi_0 \, w + m\Omega^2 \sin(\beta+\delta) \cancel{\left(K_{m_2}^2 - K_{m_1}^2 \right)} \cdot \\
& \cdot \cos(\beta+\delta) \cos 2\phi_0 \, \phi - m\Omega^2 e \left(\xi \cos^2(\beta+\delta) + \right. \\
& \left. + e_0 \cos(\beta+\delta) \cos\beta \right) \cos\phi_0 + m\Omega^2 \cancel{\left(K_{m_2}^2 - K_{m_1}^2 \right)} \cdot \\
& \cdot \sin(\beta+\delta) \cos(\beta+\delta) \sin\phi_0 \cos\phi_0 + m\Omega^2 \big(K_{m_2}^2 - \\
& - K_{m_1}^2 \big) \cancel{\cos^2(\beta+\delta)} \sin\phi_0 \cos\phi_0 \, w' + m\Omega^2 \big(K_{m_2}^2 \cdot \\
& \cdot \cos^2\phi_0 + K_{m_1}^2 \sin^2\phi_0 \big) \cancel{\cos^2(\beta+\delta)} \, v' - m \big(K_{m_2}^2 - \\
& - K_{m_1}^2 \big) \cancel{\sin\phi_0 \cos\phi_0} \, \ddot{w}' - m \cancel{\left(K_{m_2}^2 \cos^2\phi_0 - K_{m_1}^2 \sin^2\phi_0 \right)} \ddot{v}'
\end{aligned}
$$

Appendix B - Aerodynamic Loadings

Second order terms are shown deleted.

Let

$$
\begin{aligned}
b_1 &= -\Omega\cos(\beta+\delta)\sin\phi_o\,\xi - \Omega e_o\cancel{\cos\beta}\sin\phi_o + U_w(\sin\Omega t\cdot \\
&\quad \sin\phi_o - \cos\Omega t\,\cancel{\sin(\beta+\delta)}\cos\phi_o) + V_w(-\cos\Omega t\sin\phi_o - \\
&\quad -\sin\Omega t\,\cancel{\sin(\beta+\delta)}\cos\phi_o) + (W_w - v_i)\cos(\beta+\delta)\cos\phi_o \\
b_2 &= \Omega\cos(\beta+\delta)\cos\phi_o\,\xi + \Omega e_o\cancel{\cos\beta}\cos\phi_o + U_w(-\sin\Omega t\cdot \\
&\quad \cos\phi_o - \cos\Omega t\,\cancel{\sin(\beta+\delta)}\sin\phi_o) + V_w(\cos\Omega t\cos\phi_o \\
&\quad -\sin\Omega t\,\cancel{\sin(\beta+\delta)}\sin\phi_o) + (W_w - v_i)\cos(\beta+\delta)\sin\phi_o \\
\gamma_1 &= U_w\cos\Omega t\cos(\beta+\delta)\sin\phi_o + V_w\sin\Omega t\cos(\beta+\delta)\sin\phi_o \\
&\quad + (W_w - v_i)\,\cancel{\sin(\beta+\delta)}\sin\phi_o \\
\gamma_2 &= U_w\cos\Omega t\cos(\beta+\delta)\cos\phi_o + V_w\sin\Omega t\cos(\beta+\delta)\cos\phi_o \\
&\quad + (W_w - v_i)\,\cancel{\sin(\beta+\delta)}\cos\phi_o \\
\bar{F}_p &= -\frac{c}{4}\Big\{U_w\Omega(\cos\Omega t\sin\phi_o + \sin\Omega t\,\cancel{\sin(\beta+\delta)}\cos\phi_o) \\
&\qquad + V_w\Omega(\sin\Omega t\sin\phi_o - \cos\Omega t\,\cancel{\sin(\beta+\delta)}\cos\phi_o)\Big\} \\
&\quad - b_1 b_2 + \frac{c}{2}\Omega\,\cancel{\sin(\beta+\delta)}\,b_2
\end{aligned}
$$

$$
\bar{F}_t = b_1^2 - \cancel{\frac{c}{2}\Omega\sin(\beta+\delta)\,b_1} - \frac{c_{d_o}}{\alpha}b_2^2
$$

then

$$p_x = A_1 v' + A_2 w'$$

where

$$A_1 = -\cos\phi_0 \, \bar{\bar{F}}_t + \sin\phi_0 \, \bar{\bar{F}}_p$$
$$A_2 = -\sin\phi_0 \, \bar{\bar{F}}_t - \cos\phi_0 \, \bar{\bar{F}}_p$$

$$p_y = B_1 \ddot{v} + B_2 \ddot{w} + B_3 \ddot{\phi} + B_4 \dot{v} + B_5 \dot{w} + B_6 \dot{\phi} + B_7 v + B_8 w + B_9 \phi + B_{10} \dot{v}' + B_{11} \dot{w}' + B_{12} v' + B_{13} w' + B_{14}$$

where

$$B_1 = -\underline{\sin\phi_0} \, \tfrac{1}{2}\rho a c \left(\tfrac{c}{4} \sin\phi_0 \right)$$
$$B_2 = -\underline{\sin\phi_0} \, \tfrac{1}{2}\rho a c \left(-\tfrac{c}{4} \cos\phi_0 \right)$$
$$B_3 = -\underline{\sin\phi_0} \, \tfrac{1}{2}\rho a c \left(\tfrac{c}{4} \right)^2$$
$$B_4 = \underline{\cos\phi_0} \, \tfrac{1}{2}\rho a c \left[-2\sin\phi_0 \, b_1 + \tfrac{c}{2} \Omega \cancel{\sin(\beta+\delta)} \cdot \sin\phi_0 - 2\cos\phi_0 \tfrac{C_{d0}}{\alpha} b_2 \right] - \underline{\sin\phi_0} \, \tfrac{1}{2}\rho a c \left[\tfrac{c}{4} \Omega \cancel{\sin(\beta+\delta)} \cos\phi_0 - \left(1 + \cancel{\tfrac{C_{d0}}{\alpha}}\right) \cdot \left(-b_2 \sin\phi_0 + b_1 \cos\phi_0 \right) \right]$$
$$B_5 = \underline{\cos\phi_0} \, \tfrac{1}{2}\rho a c \left[2\cos\phi_0 \, b_1 - \tfrac{c}{2} \Omega \cancel{\sin(\beta+\delta)} \cdot \cos\phi_0 - 2\sin\phi_0 \tfrac{C_{d0}}{\alpha} b_2 \right] - \underline{\sin\phi_0} \, \tfrac{1}{2}\rho a c \left[\tfrac{c}{4} \Omega \cancel{\sin(\beta+\delta)} \sin\phi_0 - \left(1 + \cancel{\tfrac{C_{d0}}{\alpha}}\right) \left(b_2 \cos\phi_0 + b_1 \sin\phi_0 \right) \right]$$
$$B_6 = \underline{\cos\phi_0} \, \tfrac{1}{2}\rho a c \left(-\tfrac{c}{2} b_1 \right) - \underline{\sin\phi_0} \, \tfrac{1}{2}\rho a c \left(\tfrac{3c}{4} b_2 \right)$$

$$
\begin{aligned}
B_7 = {} & \underline{\cos\phi_0}\ \tfrac{1}{2}\rho a c\Big[\, 2\Omega\sin(\beta+\delta)\cos\phi_0\, b_1 - \tfrac{c}{2}\,\Omega^2\cancel{\sin^2(\beta+\delta)}\cos\phi_0 \\
& \qquad - 2 b_2\,\Omega\,\cancel{\tfrac{C_{d0}}{\alpha}\sin(\beta+\delta)}\sin\phi_0\Big] \\
& - \underline{\sin\phi_0}\ \tfrac{1}{2}\rho a c\Big[-\big(1+\cancel{\tfrac{C_{d0}}{\alpha}}\big)\Omega\sin(\beta+\delta)\,(b_2\cos\phi_0 + b_1\sin\phi_0) \\
& \qquad + \tfrac{c}{2}\,\Omega^2\cancel{\sin^2(\beta+\delta)}\sin\phi_0\Big] \\
B_8 = {} & \underline{\cos\phi_0}\ \tfrac{1}{2}\rho a c\Big[\, 2\Omega\sin(\beta+\delta)\sin\phi_0\, b_1 - \tfrac{c}{2}\,\Omega^2\cancel{\sin^2(\beta+\delta)}\,\cdot \\
& \qquad \cdot\sin\phi_0 + \tfrac{C_{d0}}{\alpha}\, 2 b_2\,\Omega\,\cancel{\sin(\beta+\delta)}\cos\phi_0\Big] \\
& - \underline{\sin\phi_0}\ \tfrac{1}{2}\rho a c\Big[-\big(1+\cancel{\tfrac{C_{d0}}{\alpha}}\big)\Omega\sin(\beta+\delta)\,(b_2\sin\phi_0 - b_1\cos\phi_0) \\
& \qquad - \tfrac{c}{2}\,\Omega^2\cancel{\sin^2(\beta+\delta)}\cos\phi_0\Big] \\
B_9 = {} & \underline{\cos\phi_0}\ \tfrac{1}{2}\rho a c\Big[-2 b_1 b_2 + \tfrac{c}{2}\, b_2\,\Omega\sin(\beta+\delta) - 2\,\tfrac{C_{d0}}{\alpha}\, b_1 b_2\Big] \\
& - \underline{\sin\phi_0}\ \tfrac{1}{2}\rho a c\Big[-\tfrac{c}{4}\Big\{ V_w\,\Omega\,(\cos\Omega t\cos\phi_0 - \sin\Omega t\sin(\beta+\delta)\,\cdot \\
& \qquad \cdot\sin\phi_0) + V_w\,\Omega\,(\sin\Omega t\cos\phi_0 + \\
& \qquad + \cos\Omega t\sin(\beta+\delta)\sin\phi_0)\Big\} - \big(1+\tfrac{C_{d0}}{\alpha}\big)\,\cdot \\
& \qquad \cdot\,(b_1^2 - b_2^2) + \tfrac{c}{2}\,\Omega\sin(\beta+\delta)\, b_1\Big] \\
& - \underline{\sin\phi_0}\ \bar{\bar{F}}_t - \underline{\cos\phi_0}\ \bar{\bar{F}}_p \\
B_{10} = {} & -\underline{\sin\phi_0}\ \tfrac{1}{2}\rho a c\,\big(-\tfrac{c}{4}\gamma_1\big) \\
B_{11} = {} & -\underline{\sin\phi_0}\ \tfrac{1}{2}\rho a c\Big[\tfrac{c}{4}\gamma_2 + \cancel{\big(\tfrac{c}{4}\big)^2\Omega}\Big] \\
B_{12} = {} & \underline{\cos\phi_0}\ \tfrac{1}{2}\rho a c\Big[\, 2 b_1\gamma_1 - \tfrac{c}{2}\,\Omega\,\cancel{\sin(\beta+\delta)}\,\gamma_1 + \tfrac{C_{d0}}{\alpha}\, 2 b_2\gamma_2\Big] \\
& - \underline{\sin\phi_0}\ \tfrac{1}{2}\rho a c\Big[-\tfrac{c}{4}\,\Omega\Big\{ -V_w\sin\Omega t\cos(\beta+\delta)\sin\phi_0 + \\
& \qquad + V_w\cos\Omega t\cos(\beta+\delta)\sin\phi_0\Big\} \\
& \qquad - \big(1+\cancel{\tfrac{C_{d0}}{\alpha}}\big)(b_2\gamma_1 - b_1\gamma_2) - \tfrac{c}{2}\,\Omega\,\cdot \\
& \qquad \cdot\cancel{\sin(\beta+\delta)}\,\gamma_2\Big]
\end{aligned}
$$

$$
\begin{aligned}
B_{13} = {} & \underline{\cos\phi_0}\ \tfrac{1}{2}\rho a c\Big[-2b_1\gamma_2 + \tfrac{c}{2}\Omega\cancel{\sin(\beta+\delta)}\gamma_2 - \tfrac{c}{2}\Omega b_1 \\
& \quad + 2b_2\gamma_1\tfrac{C_{do}}{\alpha}\Big] \\
& -\underline{\sin\phi_0}\ \tfrac{1}{2}\rho a c\Big[-\tfrac{c}{4}\Omega\Big\{U_w\sin\Omega t - V_w\cos\Omega t\Big\}\cos(\beta+\delta)\cdot \\
& \quad \cdot\cos\phi_0 + \Big(1+\cancel{\tfrac{C_{do}}{\alpha}}\Big)\big(b_2\gamma_2 + b_1\gamma_1\big) - \\
& \quad - \tfrac{c}{2}\Omega\cancel{\sin(\beta+\delta)}\gamma_1 + \tfrac{c}{2}\Omega b_2\Big]
\end{aligned}
$$

$$
\begin{aligned}
B_{14} = {} & \underline{\cos\phi_0}\ \tfrac{1}{2}\rho a c\Big[b_1^2 - \tfrac{c}{2}\Omega\cancel{\sin(\beta+\delta)}b_1 - \tfrac{C_{do}}{\alpha}b_2^2\Big] \\
& -\underline{\sin\phi_0}\ \tfrac{1}{2}\rho a c\Big[-\tfrac{c}{4}\Omega\Big\{U_w\big(\cos\Omega t\sin\phi_0 + \sin\Omega t\cdot \\
& \quad \cdot\sin(\beta+\delta)\cos\phi_0\big) + V_w\big(\sin\Omega t\sin\phi_0 - \\
& \quad - \cos\Omega t\sin(\beta+\delta)\cos\phi_0\big)\Big\} - \Big(1+\cancel{\tfrac{C_{do}}{\alpha}}\Big)\cdot \\
& \quad \cdot b_2 b_1 + \tfrac{c}{2}\Omega\sin(\beta+\delta)b_2\Big]
\end{aligned}
$$

$$
\begin{aligned}
p_z = {} & \Gamma_1\ddot{v} + \Gamma_2\ddot{w} + \Gamma_3\ddot{\phi} + \Gamma_4\mathring{v} + \Gamma_5\mathring{w} + \Gamma_6\mathring{\phi} + \\
& + \Gamma_7 v + \Gamma_8 w + \Gamma_9\phi + \Gamma_{10}\mathring{v}' + \Gamma_{11}\mathring{w}' + \Gamma_{12}v' + \\
& + \Gamma_{13}w' + \Gamma_{14}
\end{aligned}
$$

where the Γ_i coefficients can be obtained by replacing

$$\underline{\cos\phi_0} \rightsquigarrow \sin\phi_0$$

$$\underline{-\sin\phi_0} \rightsquigarrow \cos\phi_0$$

in the B_i coefficients.

$$
\begin{aligned}
q_\xi = {} & \Delta_1\ddot{v} + \Delta_2\ddot{w} + \Delta_3\ddot{\phi} + \Delta_4\mathring{v} + \Delta_5\mathring{w} + \Delta_6\mathring{\phi} \\
& + \Delta_7 v + \Delta_8 w + \Delta_9\phi + \Delta_{10}\mathring{v}' + \Delta_{11}\mathring{w}' + \Delta_{12}v' \\
& + \Delta_{13}w' + \Delta_{14}
\end{aligned}
$$

where

$$\Delta_1 = -\frac{1}{2}\rho a c\left(\frac{c}{4}\right)^2 \sin\phi_0$$

$$\Delta_2 = \frac{1}{2}\rho a c\left(\frac{c}{4}\right)^2 \cos\phi_0$$

$$\Delta_3 = -\frac{1}{2}\cancel{\rho a c\left(\frac{c}{4}\right)^2}\,\frac{3c}{8}$$

$$\Delta_4 = 0$$

$$\Delta_5 = 0$$

$$\Delta_6 = -\frac{1}{2}\rho a c\left(\frac{c}{4}\right)^2 2 b_2$$

$$\Delta_7 = -\frac{1}{2}\rho a c\left(\frac{c}{4}\right)^2 \Omega^2 \cancel{\sin^2(\beta+\delta)} \sin\phi_0$$

$$\Delta_8 = -\frac{1}{2}\rho a c\left(\frac{c}{4}\right)^2\left(-\Omega^2 \cancel{\sin^2(\beta+\delta)} \cos\phi_0\right)$$

$$\Delta_9 = -\frac{1}{2}\rho a c\left(\frac{c}{4}\right)^2\Big[\Omega \cancel{\sin(\beta+\delta)}\, b_1 - U_w \Omega\big(\cos\Omega t \cos\phi_0 - \sin\Omega t \cancel{\sin(\beta+\delta)} \sin\phi_0\big) - V_w \Omega\big(\sin\Omega t \cdot \cos\phi_0 + \cos\Omega t \cancel{\sin(\beta+\delta)} \sin\phi_0\Big]$$

$$\Delta_{10} = -\frac{1}{2}\rho a c\left(\frac{c}{4}\right)^2(-\gamma_1)$$

$$\Delta_{11} = -\frac{1}{2}\rho a c\left(\frac{c}{4}\right)^2 \gamma_2$$

$$\Delta_{12} = -\frac{1}{2}\rho a c\left(\frac{c}{4}\right)^2\Big[-\Omega \sin(\beta+\delta)\gamma_2 - \Omega\big(-U_w \sin\Omega t \cdot \cos(\beta+\delta)\sin\phi_0 + V_w \cos\Omega t \cos(\beta+\delta) \cdot \sin\phi_0\big)\Big]$$

$$\Delta_{13} = -\frac{1}{2}\rho a c\left(\frac{c}{4}\right)^2\Big[-\Omega \cancel{\sin(\beta+\delta)}\gamma_1 + \Omega b_2 - \Omega\big(V_w \sin\Omega t \cdot \cos(\beta+\delta)\cos\phi_0 - V_w \cos\Omega t \cos(\beta+\delta) \cdot \cos\phi_0\big)\Big]$$

$$\Delta_{14} = -\frac{1}{2}\rho a c\left(\frac{c}{4}\right)^2\Big[\Omega \cancel{\sin(\beta+\delta)}\, b_2 - U_w \Omega\big(\cos\Omega t \sin\phi_0 + \sin\Omega t \cancel{\sin(\beta+\delta)} \cos\phi_0\big) - V_w \Omega\big(\sin\Omega t \cdot \sin\phi_0 - \cos\Omega t \cancel{\sin(\beta+\delta)} \cos\phi_0\big)\Big]$$

Appendix C

L_i Matrices

$$\underset{\sim}{L}_1 = \int_0^{l_i} \underset{\sim}{H}_1''^T \underset{\sim}{H}_1'' dx = \frac{1}{l_i^3}\begin{bmatrix} 12 & 6l_i & -12 & 6l_i \\ & 4l_i^2 & -6l_i & 2l_i^2 \\ & & 12 & -6l_i \\ \text{SYM} & & & 4l_i^2 \end{bmatrix}$$

$$\underset{\sim}{L}_2 = \int_0^{l_i} \underset{\sim}{H}_1''^T \underset{\sim}{H}_0' dx = \frac{1}{l_i}\begin{bmatrix} 0 & 0 \\ 1 & -1 \\ 0 & 0 \\ -1 & 1 \end{bmatrix}$$

$$\underset{\sim}{L}_3 = \int_0^{l_i} \underset{\sim}{H}_0'^T \underset{\sim}{H}_0' dx = \frac{1}{l_i}\begin{bmatrix} 1 & -1 \\ -1 & 1 \end{bmatrix}$$

$$\underset{\sim}{L}_4 = \int_0^{l_i} \underset{\sim}{H}_1'^T \underset{\sim}{H}_1' dx = \frac{1}{30 l_i}\begin{bmatrix} 36 & 3l_i & -36 & 3l_i \\ & 4l_i^2 & -3l_i & -l_i^2 \\ & & 36 & -3l_i \\ \text{SYM} & & & 4l_i^2 \end{bmatrix}$$

$$\underset{\sim}{L}_5 = \int_0^{l_i} \underset{\sim}{H}_1''^T \underset{\sim}{H}_0 dx = \frac{1}{l_i}\begin{bmatrix} -1 & 1 \\ -l & 0 \\ 1 & -1 \\ 0 & l_i \end{bmatrix}$$

$$\underset{\sim}{L}_6 = \int_0^{l} \underset{\sim}{H}_1^T \underset{\sim}{H}_1 \, dx = \frac{l}{420} \begin{bmatrix} 156 & 22l & 54 & -13l \\ & 4l^2 & 13l & -3l^2 \\ & & 156 & -22l \\ \text{SYM} & & & 4l^2 \end{bmatrix}$$

$$\underset{\sim}{L}_7 = \int_0^{l} \underset{\sim}{H}_1^T \underset{\sim}{H}_1' \, dx = \frac{1}{60} \begin{bmatrix} -30 & 6l & 30 & -6l \\ -6l & 0 & 6l & -l^2 \\ -30 & -6l & 30 & 6l \\ 6l & l^2 & -6l & 0 \end{bmatrix}$$

$$L_8 = \int_0^{l} \underset{\sim}{H}_0^T \underset{\sim}{H}_0 \, dx = \frac{l}{6} \begin{bmatrix} 2 & 1 \\ 1 & 2 \end{bmatrix}$$

$$\underset{\sim}{L}_9 = \int_0^{l} \underset{\sim}{H}_0^T \underset{\sim}{H}_1 \, dx = \frac{l}{60} \begin{bmatrix} 21 & 3l & 9 & -2l \\ 9 & 2l & 21 & -3l \end{bmatrix}$$

$$\underset{\sim}{L}_{10} = \int_0^{l} \underset{\sim}{H}_0^T \underset{\sim}{H}_1' \, dx = \frac{1}{12} \begin{bmatrix} -6 & l & 6 & -l \\ -6 & -l & 6 & l \end{bmatrix}$$

$$\int_0^{l} H_1''^T \, dx = \begin{bmatrix} 0 \\ -1 \\ 0 \\ 1 \end{bmatrix}$$

$$\int_0^{l_i} \underset{\sim}{H}_1'^T \, dx = \begin{bmatrix} -1 \\ 0 \\ 1 \\ 0 \end{bmatrix}$$

$$\int_0^{l_i} \underset{\sim}{H}_1^T \, dx = l_i \begin{bmatrix} 2/4 \\ l_i/12 \\ 2/4 \\ -l_i/12 \end{bmatrix}$$

$$\int_0^{l_i} \underset{\sim}{H}_0'^T \, dx = \begin{bmatrix} -1 \\ 1 \end{bmatrix}$$

$$\int_0^{l_i} \underset{\sim}{H}_0^T \, dx = \frac{l_i}{2} \begin{bmatrix} 1 \\ 1 \end{bmatrix}$$

Appendix D

Uniform Cantilever Beam

Input (beam properties)

$m = 1\text{x}10^{-3}$ inslugs/in.	$\alpha_1 = 3.52$
$EI_1 = 6\text{x}10^9$ lb in^2	$\alpha_2 = 22.0$
$EI_2 = 12\text{x}10^9$ lb in^2	$\alpha_3 = 61.7$
$GJ = 4\text{x}10^8$ lb in^2	$b_1 = 1.571$
$K_{m_1} = 5.0$ in	$b_2 = 4.6$
$K_{m_2} = 6.5$ in	$e = 0.0$
$R = 718$ in	$e_A = 0.0$
$mK_m^2 = 6.725\text{x}10^{-2}\ \frac{\text{inslugs-in}^2}{\text{in}}$	$e_0 = 0.0$

$$\left.\begin{matrix}\alpha_1\\ \alpha_2\\ \alpha_3\end{matrix}\right\}\alpha_n \qquad \left.\begin{matrix}b_1\\ b_2\end{matrix}\right\}b_n$$

Results Obtained

	$\Omega = 0$		$\Omega = 4.191$ rad/s
Mode	Theoretical ω (Hz)	Numerical ω (Hz)	Numerical ω (Hz)
1stFlap	2.66	2.66	2.76
1stLag	3.76	3.76	3.78
2ndFlap	16.64	16.64	16.75
2ndLag	23.53	23.53	23.62
1stTorsion	26.85	26.85	26.93
3rdFlap	46.70	46.70	46.76

Appendix E

NASA/DOE MOD-0

e_o = 32 in

β = 7°

δ = 0°

x (in)	m (inslugs/in)	EI_1 (lbs in^{2}x10^8)	EI_2 (lbs in^{2}x10^8)	GJ (lbs in^{2}x10^8)
0.0	0.0246	173	173	132
71.8	0.00829	144	232	150
143.6	0.00751	96	179	72
215.4	0.00699	62	143	40
287.2	0.00725	42	120	25
359.0	0.00699	29	97	16
430.8	0.00570	17	72	8.5
502.6	0.00466	8	44	4.5
574.4	0.00311	2.3	19	2.0
646.2	0.00181	0.4	9.5	0.9
718.0	0.00168	0.2	0.6	0.4

e (in)	e_A (in)	EB_1 (lb in^{4}x10^{13})	EB_2 (lb in^{3}x10^{12})	ϕ_o (degrees)
-8.2	-4.9	4.3	-0.85	24.5
-8.2	-4.9	6.3	-1.50	24.5
-8.2	-4.9	7.7	-1.65	16.0
-7.5	-4.5	5.0	-1.35	10.5
-4.8	-4.1	3.95	-0.95	6.5
-4.3	-3.7	2.25	-0.70	3.5
-3.8	-3.3	1.35	-0.50	2.0
-3.3	-2.8	0.8	-0.35	0.5
-2.8	-2.2	0.4	-0.25	-0.5
-2.3	-1.8	0.25	-0.15	-1.2
-1.8	-1.4	0.15	-0.10	-1.6

K_A (in)	K_{m_1} (in)	K_{m_2} (in)
15.53	8.35	8.35
14.36	9.27	11.77
13.19	8.84	12.11
12.02	7.64	11.61
10.85	6.05	10.23
9.69	5.05	9.25
8.52	4.16	8.57
7.35	3.17	7.60
6.18	2.44	7.01
5.01	1.46	7.12
3.84	1.16	6.35

Appendix F

Uniform Flat Plate

Input (plate properties)

$m = 0.777 \times 10^{-4}$	inslugs/in		ϕ_o =	0
$EI_1 = 0.262 \times 10^{4}$	lbs in^2		e =	0
$EI_2 = 0.236 \times 10^{7}$	lbs in^2		e_A =	0
$GJ = 0.4 \times 10^{4}$	lbs in^2		K_A =	0.866 in
$EB_1 = 0.142 \times 10^{7}$			K_{m_1} =	0.029 in
$EB_2 = 0$			K_{m_2} =	0.866 in
$R = 6$ in			e_o =	0

Results Obtained

Mode	Untwisted ω (Hz)	0° - 30° ω (Hz)	0° - 60° ω (Hz)	0° - 90° ω (Hz)
First Flap	90.26	90.55	91.39	92.75
First Torsion	345.4	664.7	1187.1	
Second Flap	565.7	508.7	407.7	
Second Torsion	1044.7			
Third Flap	1584.3	1519.8		
Third Torsion	1769.7			
First Lag			1389.0	326.6
Second Lag				1245.6
Third Lag				1738.3

Appendix G

Reference (6) Test Case

Input (blade properties)

Ω = 4.191 rad/s

R = 718 in/s

m = 7.767×10^{-3} inslugs/in

EI_1 = 529.52×10^{6} lb in^2

EI_2 = 971.19×10^{6} lb in^2 (soft-in-plane case)

EI_2 = 6.053×10^{9} lb in^2 (stiff-in-plane case)

GJ = 205.69×10^{6} lb in^2

K_{m_1} = 0.0

K_{m_2} = 17.95 in

e_A = e_o = e = 0

K_A = 21.98 in

ϕ_o = β = δ = 0.0

α = 2π

C_{d_o} = 0.01

σ = 0.1

c = 56.39 in

ρ = 50.8857×10^{-9} inslugs/in^3

v_i = -1.854 in/s (soft-in-plane case)

v_i = -0.401 in/s (stiff-in-plane case)

Comparison of Results Obtained

Soft-In-Plane Case

	$\gamma/\Omega \pm i\,\omega/\Omega$	
Mode	This Report	Reference (4)
1^{st} Lag	$-0.00670 \pm i\ 0.6924$	$-0.0011 \pm i\ 0.7014$
1^{st} Flap	$-0.3203 \pm i\ 1.0938$	$-0.3245 \pm i\ 1.0751$
1^{st} Torsion	$-0.3613 \pm i\ 4.966$	$-0.3622 \pm i\ 4.9875$

Stiff-In-Plane Case

	$\gamma/\Omega \pm i\,\omega/\Omega$	
Mode	This Report	Reference (4)
1^{st} Lag	$-0.00365 \pm i\ 1.5089$	$-0.0011 \pm i\ 1.5002$
1^{st} Flap	$-0.3233 \pm i\ 1.0842$	$-0.3246 \pm i\ 1.0741$
1^{st} Torsion	$-0.3613 \pm i\ 4.9661$	$-0.3625 \pm i\ 4.9888$

Appendix H

Reference (8) Test Case

Input (blade properties)

$R = 718$ in

$\Omega = 4.191$ rad/s

$m = 7.767\text{x}10^{-3}$ inslugs/in

$EI_1 = 525.2123\text{x}10^{6}$ lb in^2

$EI_2 = 6.0515\text{x}10^{9}$ lb in^2

$GJ = 33.5373\text{x}10^{6}$ lb in^2

$K_{m_1} = 0$

$K_{m_2} = 17.95$ in

$e = e_A = e_o = 0$

$K_A = 26.925$ in

$c = 56.3916$ in

$\beta = 2.865°$

$\delta = 0°$

$\alpha = 6.0$

$C_{D_0} = 0.0095$

$\rho = 53.2859\text{x}10^{-9}$ inslugs/in^3

$\sigma = 0.1$

Comparison of Results Obtained

For $C_T/\sigma = 0.1$

	ω/Ω	
Vibration Modes	This Report	Reference (6)
1^{st} Flap	1.145	1.121
1^{st} Lag	1.501	1.518
1^{st} Torsion	2.632	2.4702

	$\mu/\Omega \pm i\ \omega/\Omega$	
Flutter Analysis Modes	This Report	Reference (6)
1^{st} Flap	-0.325 ± i 1.099	-0.31448 ± i 1.10
1^{st} Lag	-0.023 ± i 1.525	-0.03034 ± i 1.58
1^{st} Torsion	-0.333 ± i 2.546	-0.35209 ± i 2.38

Appendix I - Inertia Accelerations

Let

$$\mu_1 = -\cos^2(\beta+\delta)\cos\hat{\alpha}\cos\hat{\beta} + \sin(\beta+\delta)\cos(\beta+\delta)\sin\hat{\beta}$$
$$\mu_2 = \cos^2(\beta+\delta)\cos\hat{\alpha}\sin\hat{\beta} + \sin(\beta+\delta)\cos(\beta+\delta)\cos\hat{\beta}$$
$$\mu_3 = \sin(\beta+\delta)\cos(\beta+\delta)\cos\hat{\alpha}\cos\hat{\beta} - \sin^2(\beta+\delta)\sin\hat{\beta}$$
$$\mu_4 = \sin(\beta+\delta)\cos(\beta+\delta)\cos\hat{\alpha}\sin\hat{\beta} + \sin^2(\beta+\delta)\cos\hat{\beta}$$

Then

$$\begin{aligned}
a_x = {} & \Omega^2\mu_1 u + \Omega^2\cos^2(\beta+\delta)\sin\hat{\alpha}\, v + \Omega^2\mu_2 w \\
& + \Omega^2\left[-\mu_1(w'\sin\phi_0 + v'\cos\phi_0) + \cos^2(\hat{\beta}+\delta)\sin\hat{\alpha}\cdot(\cos\phi_0 \right. \\
& \left. - \phi\sin\phi_0) + \mu_2(\sin\phi_0 + \phi\cos\phi_0)\right]\eta + \\
& + \Omega^2\left[\mu_1(-w'\cos\phi_0 + v'\sin\phi_0) + \cos^2(\beta+\delta)\sin\hat{\alpha}\cdot \right. \\
& \left. (-\sin\phi_0 - \phi\cos\phi_0) + \mu_2(\cos\phi_0 - \phi\sin\phi_0)\right]\zeta \\
& - \Omega^2 x_0\cos^2(\beta+\delta) + \Omega^2\mu_1\xi - \Omega^2 e_0\cos(\beta+\delta)\cos\beta \\
& + \Omega^2 z_0\sin(\beta+\delta)\cos(\beta+\delta) + 2\Omega\left(-\cos(\beta+\delta)\sin\hat{\alpha}\,\cdot\right. \\
& \left.\cdot\cos\hat{\beta}\,\dot{u} - \cos(\beta+\delta)\cos\hat{\alpha}\,\dot{v} + \cos(\beta+\delta)\sin\hat{\beta}\sin\hat{\alpha}\,\dot{w}\right) \\
& + 2\Omega\left[-\cos(\beta+\delta)\sin\hat{\alpha}\cos\hat{\beta}(-\dot{w}'\sin\phi_0 - \dot{v}'\cos\phi_0) + \right. \\
& + \cos(\beta+\delta)\cos\hat{\alpha}\,\dot{\phi}\sin\phi_0 + \cos(\beta+\delta)\sin\hat{\beta}\sin\hat{\alpha}\,\dot{\phi}\,\cdot \\
& \left.\cos\phi_0\right]\eta + 2\Omega\left[-\cos(\beta+\delta)\sin\hat{\alpha}\cos\hat{\beta}(-\dot{w}'\cos\phi_0 + \right. \\
& + \dot{v}'\sin\phi_0) + \cos(\beta+\delta)\cos\hat{\alpha}\,\dot{\phi}\cos\phi_0 - \cos(\beta+\delta)\,\cdot \\
& \left.\cdot\sin\hat{\beta}\sin\hat{\alpha}\,\dot{\phi}\sin\phi_0\right]\zeta + \cos\hat{\alpha}\cos\hat{\beta}\,\ddot{u} - \sin\alpha\,\ddot{v}
\end{aligned}$$

$$
\begin{aligned}
&- \sin\hat{\beta}\cos\hat{\alpha}\,\ddot{w} + \Big[\cos\hat{\alpha}\cos\hat{\beta}\left(-\ddot{w}'\sin\phi_0 - \ddot{v}'\cos\phi_0\right) \\
&+ \sin\hat{\alpha}\,\ddot{\phi}\sin\phi_0 - \sin\hat{\beta}\cos\hat{\alpha}\,\ddot{\phi}\cos\phi_0\Big]\eta + \Big[\cos\hat{\alpha}\cos\hat{\beta}\,\cdot \\
&\cdot\left(-\ddot{w}'\cos\phi_0 + \ddot{v}'\sin\phi_0\right) + \sin\hat{\alpha}\,\ddot{\phi}\cos\phi_0 + \sin\hat{\beta}\cos\hat{\alpha}\,\cdot \\
&\cdot\,\ddot{\phi}\sin\phi_0\Big]\zeta
\end{aligned}
$$

$$
\begin{aligned}
a_y = {} & -\Omega^2\sin\hat{\alpha}\cos\hat{\beta}\,u - \Omega^2\cos\hat{\alpha}\,v + \Omega^2\sin\hat{\beta}\sin\hat{\alpha}\,w \\
& + \Omega^2\Big[-\sin\hat{\alpha}\cos\hat{\beta}\left(-w'\sin\phi_0 - v'\cos\phi_0\right) - \cos\hat{\alpha}\left(\cos\phi_0 - \right. \\
& \left. - \phi\sin\phi_0\right) + \sin\hat{\beta}\sin\hat{\alpha}\left(\sin\phi_0 + \phi\cos\phi_0\right)\Big]\eta \\
& + \Omega^2\Big[-\sin\hat{\alpha}\cos\hat{\beta}\left(-w'\cos\phi_0 + v'\sin\phi_0\right) + \cos\hat{\alpha}\,\cdot \\
& \left(\sin\phi_0 + \phi\cos\phi_0\right) + \sin\hat{\beta}\sin\hat{\alpha}\left(\cos\phi_0 - \phi\sin\phi_0\right)\Big]\zeta \\
& - \Omega^2 y_0 - \Omega^2\sin\hat{\alpha}\cos\hat{\beta}\,\xi + 2\Omega\Big[\big(\cos(\beta+\delta)\cos\hat{\alpha}\,\cdot \\
& \cdot\cos\hat{\beta} - \sin(\beta+\delta)\sin\hat{\beta}\big)\mathring{u} - \cos(\beta+\delta)\sin\hat{\alpha}\,\mathring{v} - \\
& - \big(\cos(\beta+\delta)\sin\hat{\beta}\cos\hat{\alpha} + \sin(\beta+\delta)\cos\hat{\beta}\big)\mathring{w}\Big] + \\
& + 2\Omega\Big[\big(\cos(\beta+\delta)\cos\hat{\alpha}\cos\hat{\beta} - \sin(\beta+\delta)\sin\hat{\beta}\big)\,\cdot \\
& \cdot\left(-\mathring{w}'\sin\phi_0 - \mathring{v}'\cos\phi_0\right) + \cos(\beta+\delta)\sin\hat{\alpha}\,\mathring{\phi}\sin\phi_0 - \\
& - \big(\cos(\beta+\delta)\sin\hat{\beta}\cos\hat{\alpha} + \sin(\beta+\delta)\cos\hat{\beta}\big)\mathring{\phi}\cos\phi_0\Big]\eta \\
& + 2\Omega\Big[\big(\cos(\beta+\delta)\cos\hat{\alpha}\cos\hat{\beta} - \sin(\beta+\delta)\sin\hat{\beta}\big)\,\cdot \\
& \cdot\left(\mathring{w}'\cos\phi_0 + \mathring{v}'\sin\phi_0\right) + \cos(\beta+\delta)\sin\hat{\alpha}\,\mathring{\phi}\cos\phi_0 + \\
& + \big(\cos(\beta+\delta)\sin\hat{\beta}\cos\hat{\alpha} + \sin(\beta+\delta)\cos\hat{\beta}\big)\mathring{\phi}\sin\phi_0\Big]\zeta \\
& + \sin\hat{\alpha}\cos\hat{\beta}\,\ddot{u} + \cos\hat{\alpha}\,\ddot{v} - \sin\hat{\beta}\sin\hat{\alpha}\,\ddot{w} \\
& + \Big[\sin\hat{\alpha}\cos\hat{\beta}\left(-\ddot{w}'\sin\phi_0 - \ddot{v}'\cos\phi_0\right) - \cos\hat{\alpha}\,\ddot{\phi}\sin\phi_0 - \\
& - \sin\hat{\beta}\sin\hat{\alpha}\,\ddot{\phi}\cos\phi_0\Big]\eta + \Big[\sin\hat{\alpha}\cos\hat{\beta}\left(-\ddot{w}'\cos\phi_0 + \right. \\
& \left. + \ddot{v}'\sin\phi_0\right) - \cos\hat{\alpha}\,\ddot{\phi}\cos\phi_0 + \sin\hat{\beta}\sin\hat{\alpha}\,\ddot{\phi}\sin\phi_0\Big]\zeta
\end{aligned}
$$

$$
\begin{aligned}
\alpha_z = {} & \Omega^2 \mu_3 u - \Omega^2 \sin\hat{\alpha} \sin(\beta+\delta)\cos(\beta+\delta) v - \Omega^2 \mu_4 w \\
& + \Omega^2 \Big[-\mu_3 \left(w' \sin\phi_0 + v' \cos\phi_0 \right) - \sin\hat{\alpha} \sin(\beta+\delta) \cos(\beta+\delta) \cdot \\
& \cdot \left(\cos\phi_0 - \phi \sin\phi_0 \right) - \mu_4 \left(\sin\phi_0 + \phi\cos\phi_0 \right) \Big] \eta \\
& + \Omega^2 \Big[\mu_3 \left(-w' \cos\phi_0 + v' \sin\phi_0 \right) + \sin\hat{\alpha} \sin(\beta+\delta) \cos(\beta+\delta) \\
& \cdot \left(\sin\phi_0 + \phi \cos\phi_0 \right) - \mu_4 \left(\cos\phi_0 - \phi \sin\phi_0 \right) \Big] \zeta \\
& + \Omega^2 \sin(\beta+\delta) \cos(\beta+\delta)\, x_0 + \Omega^2 \mu_3 \xi - \Omega^2 \sin^2(\beta+\delta) \cdot \\
& \cdot z_0 + \Omega^2 e_0 \sin(\beta+\delta) \cos\beta + 2\Omega \Big[\sin(\beta+\delta) \cdot \\
& \cdot \sin\hat{\alpha} \cos\hat{\beta}\, \mathring{u} + \sin(\beta+\delta) \cos\hat{\alpha}\, \mathring{v} - \sin(\beta+\delta) \sin\hat{\beta} \cdot \\
& \cos\hat{\alpha}\, \mathring{w} \Big) + 2\Omega \Big[-\sin(\beta+\delta) \sin\hat{\alpha} \cos\hat{\beta} \left(\mathring{w}' \sin\phi_0 + \right. \\
& \left. + \mathring{v}' \cos\phi_0 \right) - \sin(\beta+\delta) \cos\hat{\alpha}\, \mathring{\phi} \sin\phi_0 - \sin(\beta+\delta) \cdot \\
& \cdot \sin\hat{\beta} \sin\hat{\alpha}\, \mathring{\phi} \cos\phi_0 \Big] \eta + 2\Omega \Big[\sin(\beta+\delta) \sin\hat{\alpha} \cos\hat{\beta} \cdot \\
& \cdot \left(-\mathring{w}' \cos\phi_0 + \mathring{v}' \sin\phi_0 \right) - \sin(\beta+\delta) \cos\hat{\alpha}\, \mathring{\phi} \cos\phi_0 + \\
& + \sin(\beta+\delta) \sin\hat{\beta} \sin\hat{\alpha}\, \mathring{\phi} \sin\phi_0 \Big] \zeta + \sin\hat{\beta}\, \overset{\circ\circ}{u} + \\
& + \cos\hat{\beta}\, \overset{\circ\circ}{w} + \Big[\sin\hat{\beta} \left(-\overset{\circ\circ}{w}' \sin\phi_0 - \overset{\circ\circ}{v}' \cos\phi_0 \right) + \\
& + \overset{\circ\circ}{\phi} \cos\phi_0 \cos\hat{\beta} \Big] \eta + \Big[\sin\hat{\beta} \left(-\overset{\circ\circ}{w}' \cos\phi_0 + \overset{\circ\circ}{v}' \sin\phi_0 \right) - \\
& - \overset{\circ\circ}{\phi} \sin\phi_0 \cos\hat{\beta} \Big] \zeta
\end{aligned}
$$

Appendix J - Inertia Loadings

Let

$$
\begin{aligned}
\mu_5 = {} & m\Omega^2 K_{m_2}^2\left[\cos^2(\beta+\delta)\sin\hat{\alpha}\cos\phi_0 + \mu_2 \sin\phi_0\right] - \\
& - me\Omega^2 x_0 \cos^2(\beta+\delta) + me\Omega^2 \sin(\beta+\delta)\cos(\beta+\delta)\, z_0 \\
& - me\Omega^2 e_0 \cos(\beta+\delta)\cos\hat{\beta} + me\Omega^2 \mu_1 \xi \\
\mu_6 = {} & m\Omega^2 K_{m_2}^2\left[-\cos\hat{\alpha}\cos\phi_0 + \sin\hat{\beta}\sin\hat{\alpha}\sin\phi_0\right] - me\Omega^2 y_0 \\
& - me\Omega^2 \sin\hat{\alpha}\cos\hat{\beta}\,\xi \\
\mu_7 = {} & m\Omega^2 K_{m_2}^2\left[-\sin\hat{\alpha}\sin(\beta+\delta)\cos(\beta+\delta)\cos\phi_0 - \mu_4 \sin\phi_0\right] \\
& + me\Omega^2\left[\sin(\beta+\delta)\cos(\beta+\delta)\, x_0 - \sin^2(\beta+\delta)\, z_0 \right. \\
& \left. + e_0 \sin(\beta+\delta)\cos\beta + \mu_3 \xi\right] \\
\mu_8 = {} & m K_{m_1}^2 \Omega^2\left[-\cos^2(\beta+\delta)\sin\hat{\alpha}\sin\phi_0 + \mu_2 \cos\phi_0\right] \\
\mu_9 = {} & m K_{m_1}^2 \Omega^2\left[\cos\hat{\alpha}\sin\phi_0 + \sin\hat{\beta}\sin\hat{\alpha}\cos\phi_0\right] \\
\mu_{10} = {} & m K_{m_1}^2 \Omega^2\left[\sin\hat{\alpha}\sin(\beta+\delta)\cos(\beta+\delta)\sin\phi_0 - \mu_4 \cos\phi_0\right] \\
\mu_{11} = {} & -\cos\hat{\alpha}\cos\hat{\beta}\left[\Omega^2\cos^2(\beta+\delta)\sin\hat{\alpha}\cos\phi_0\, m K_{m_2}^2 + \right. \\
& + m\Omega^2 \mu_2 \sin\phi_0 K_{m_2}^2 + m\Omega^2 e\left(-x_0\cos^2(\beta+\delta) + z_0 \cdot \right. \\
& \left.\left. \cdot \sin(\beta+\delta)\cos(\beta+\delta) - e_0\cos(\beta+\delta)\cos\beta + \mu_1 \xi\right)\right] \\
& - \sin\hat{\alpha}\cos\hat{\beta}\left[m\Omega^2 K_{m_2}^2\left(-\cos\hat{\alpha}\cos\phi_0 + \sin\hat{\alpha}\sin\hat{\beta}\sin\phi_0\right)\right. \\
& \left. - me\Omega^2 y_0 - me\Omega^2 \sin\hat{\alpha}\cos\hat{\beta}\,\xi\right] \\
& - \sin\hat{\beta}\left[-m\Omega^2 \sin\hat{\alpha}\sin(\beta+\delta)\cos(\beta+\delta)\cos\phi_0 K_{m_2}^2\right. \\
& - m\Omega^2 \mu_4 \sin\phi_0 K_{m_2}^2 + me\Omega^2\left(\sin(\beta+\delta)\cos(\beta+\delta)\, x_0\right.
\end{aligned}
$$

$$- \sin^2(\beta+\delta)\, z_0 \;+\; e_0 \sin(\beta+\delta)\cos\beta \;+\; \mu_{13}\,\xi \,)\Big]$$

$$\begin{aligned}
\mu_{12} \;=\; & -\cos\hat\alpha\cos\hat\beta\Big[\, m\Omega^2 K_{m_1}^2 \big(-\cos^2(\beta+\delta)\sin\hat\alpha\sin\phi_0 \;+ \\
& + \mu_{2}\cos\phi_0 \big)\Big] \;-\; \sin\hat\alpha\cos\hat\beta\Big[\, m\Omega^2 K_{m_1}^2 \big(\cos\hat\alpha\sin\phi_0 \\
& + \sin\hat\beta\sin\hat\alpha\cos\phi_0 \big)\Big] \;-\; \sin\hat\beta\Big[\, m\Omega^2 K_{m_1}^2 \big(\sin\hat\alpha\sin(\beta+\delta)\cdot \\
& \cos(\beta+\delta)\sin\phi_0 \;-\; \mu_{4}\cos\phi_0 \big)\Big]
\end{aligned}$$

then

$$\begin{aligned}
p_{12} \;=\; & E_1\ddot u + E_2\ddot v + E_3\ddot w + E_4\ddot\phi + E_5\ddot v' \\
& + E_6\ddot w' + E_7 u + E_8 v + E_9 w + E_{10}\phi \\
& + E_{11} v' + E_{12} w'
\end{aligned}$$

where

$$\begin{aligned}
E_1 \;=\; & -\underline{\cos\hat\alpha\cos\hat\beta}\,(m\cos\hat\alpha\cos\hat\beta) - \underline{\sin\hat\alpha\cos\hat\beta}\,(m\sin\hat\alpha\,\cdot \\
& \cdot\cos\hat\beta) - \underline{\sin\hat\beta}\,(m\sin\hat\beta) \\
E_2 \;=\; & -\underline{\cos\hat\alpha\cos\hat\beta}\,(-m\sin\hat\alpha) - \underline{\sin\hat\alpha\cos\hat\beta}\,(m\cos\hat\alpha) \\
E_3 \;=\; & -\underline{\cos\hat\alpha\cos\hat\beta}\,(-m\sin\hat\beta\cos\hat\alpha) - \underline{\sin\hat\alpha\cos\hat\beta}\,(-m\sin\hat\beta \\
& \sin\hat\alpha) - \underline{\sin\hat\beta}\,(m\cos\hat\beta) \\
E_4 \;=\; & -\underline{\cos\hat\alpha\cos\hat\beta}\, me\,(\sin\hat\alpha\sin\phi_0 - \sin\hat\beta\cos\hat\alpha\cos\phi_0) \\
& -\underline{\sin\hat\alpha\cos\hat\beta}\, me\,(-\cos\hat\alpha\sin\phi_0 - \sin\hat\beta\sin\hat\alpha\cos\phi_0) \\
& -\underline{\sin\hat\beta}\, me\cos\phi_0\cos\hat\beta \\
E_5 \;=\; & -\underline{\cos\hat\alpha\cos\hat\beta}\, me\,(-\cos\hat\alpha\cos\hat\beta\cos\phi_0) - \underline{\sin\hat\alpha\,\cdot} \\
& \underline{\cos\hat\beta}\, me\,(-\sin\hat\alpha\cos\hat\beta\cos\phi_0) - \underline{\sin\hat\beta}\, me\,(-\sin\hat\beta\,\cdot \\
& \cdot\cos\phi_0)
\end{aligned}$$

$$E_6 = -\underline{\cos\hat{\alpha}\cos\hat{\beta}}\, me\left(-\cos\hat{\alpha}\cos\hat{\beta}\sin\phi_0\right) - \underline{\sin\hat{\alpha}\cos\hat{\beta}} \cdot me\left(-\sin\hat{\alpha}\cos\hat{\beta}\sin\phi_0\right) - \underline{\sin\hat{\beta}}\, me\left(-\sin\hat{\beta}\cdot\sin\phi_0\right)$$

$$E_7 = -\underline{\cos\hat{\alpha}\cos\hat{\beta}}\left(m\Omega^2\mu_1\right) - \underline{\sin\hat{\alpha}\cos\hat{\beta}}\left(-m\Omega^2\sin\hat{\alpha}\cdot\cos\hat{\beta}\right) - \underline{\sin\hat{\beta}}\left(\Omega^2 m\mu_3\right)$$

$$E_8 = -\underline{\cos\hat{\alpha}\cos\hat{\beta}}\left(m\Omega^2\cos^2(\beta+\delta)\sin\hat{\alpha}\right) - \underline{\sin\hat{\alpha}\cos\hat{\beta}}\cdot\left(-\Omega^2 m\cos\hat{\alpha}\right) - \underline{\sin\hat{\beta}}\left(-\Omega^2 m\sin\hat{\alpha}\sin(\beta+\delta)\cdot\cos(\beta+\varepsilon)\right)$$

$$E_9 = -\underline{\cos\hat{\alpha}\cos\hat{\beta}}\left(m\Omega^2\mu_2\right) - \underline{\sin\hat{\alpha}\cos\hat{\beta}}\left(\Omega^2 m\sin\hat{\beta}\cdot\sin\hat{\alpha}\right) - \underline{\sin\hat{\beta}}\left(-m\Omega^2\mu_4\right)$$

$$E_{10} = -\underline{\cos\hat{\alpha}\cos\hat{\beta}}\left[me\Omega^2\left(-\sin\phi_0\cos^2(\beta+\delta)\sin\hat{\alpha} + \mu_2\cos\phi_0\right)\right] - \underline{\sin\hat{\alpha}\cos\hat{\beta}}\left[me\Omega^2\left(\cos\hat{\alpha}\sin\phi_0 + + \sin\hat{\beta}\sin\hat{\alpha}\cos\phi_0\right)\right] - \underline{\sin\hat{\beta}}\left[me\Omega^2\left(\sin\hat{\alpha}\cdot\sin(\beta+\delta)\cos(\beta+\delta)\sin\phi_0 - \mu_4\cos\phi_0\right)\right]$$

$$E_{11} = -\underline{\cos\hat{\alpha}\cos\hat{\beta}}\left(-me\Omega^2\mu_1\cos\phi_0\right) - \underline{\sin\hat{\alpha}\cos\hat{\beta}}\cdot\left(me\Omega^2\sin\hat{\alpha}\cos\hat{\beta}\cos\phi_0\right) - \underline{\sin\hat{\beta}}\left(-me\Omega^2\cdot\mu_3\cos\phi_0\right)$$

$$E_{12} = -\underline{\cos\hat{\alpha}\cos\hat{\beta}}\left(-me\Omega^2\mu_1\sin\phi_0\right) - \underline{\sin\hat{\alpha}\cos\hat{\beta}}\cdot\left(me\Omega^2\sin\hat{\alpha}\cos\hat{\beta}\sin\phi_0\right) - \underline{\sin\hat{\beta}}\left(-me\Omega^2\cdot\mu_3\sin\phi_0\right)$$

where

$\mu_1, \mu_2, \mu_3, \mu_4$ are given in appendix I.

$$
\begin{aligned}
p_y = {} & Z_1 \ddot{u} + Z_2 \ddot{v} + Z_3 \ddot{w} + Z_4 \ddot{\phi} + Z_5 \ddot{v}' \\
& + Z_6 \ddot{w}' + Z_7 u + Z_8 v + Z_9 w + Z_{10} \phi \\
& + Z_{11} v' + Z_{12} w'
\end{aligned}
$$

the Z_i coefficients are obtained if the following substitutions are made in the underlined terms of the E_i coefficients.

$$
\begin{aligned}
-\underline{\cos\hat{\alpha} \cos\hat{\beta}} & \longrightarrow \sin\hat{\alpha} \\
-\underline{\sin\hat{\alpha} \cos\hat{\beta}} & \longrightarrow -\cos\hat{\alpha} \\
-\underline{\sin\hat{\beta}} & \longrightarrow 0
\end{aligned}
$$

$$
\begin{aligned}
p_z = {} & H_1 \ddot{u} + H_2 \ddot{v} + H_3 \ddot{w} + H_4 \ddot{\phi} + H_5 \ddot{v}' \\
& + H_6 \ddot{w}' + H_7 u + H_8 v + H_9 w + H_{10} \phi \\
& + H_{11} v' + H_{12} w'
\end{aligned}
$$

the H_i coefficients are obtained if the following substitutions are made in the underlined terms of the E_i coefficients.

$$
\begin{aligned}
-\underline{\cos\hat{\alpha} \cos\hat{\beta}} & \longrightarrow \sin\hat{\beta} \cos\hat{\alpha} \\
-\underline{\sin\hat{\alpha} \cos\hat{\beta}} & \longrightarrow \sin\hat{\beta} \sin\hat{\alpha} \\
-\underline{\sin\hat{\beta}} & \longrightarrow -\cos\hat{\beta}
\end{aligned}
$$

$$
\begin{aligned}
q_{\xi} = {} & \Theta_1 \ddot{u} + \Theta_2 \ddot{v} + \Theta_3 \ddot{w} + \Theta_4 \ddot{\phi} + \Theta_5 \ddot{v}' \\
& + \Theta_6 \ddot{w}' + \Theta_7 u + \Theta_8 v + \Theta_9 w + \Theta_{10} \phi \\
& + \Theta_{11} v' + \Theta_{12} w'
\end{aligned}
$$

where

$$
\begin{aligned}
\Theta_1 = {} & me\, \underline{\cos\phi_o} \Big[\underline{\cos\hat{\alpha} \sin\hat{\beta}} \left(\cos\hat{\alpha} \cos\hat{\beta} \right) + \underline{\sin\hat{\alpha} \sin\hat{\beta}} \cdot \\
& \cdot \left(\sin\hat{\alpha} \cos\hat{\beta} \right) - \underline{\cos\hat{\beta}} \sin\hat{\beta} \Big] \\
\Theta_2 = {} & me \sin\phi_o + me\, \underline{\cos\phi_o} \Big[\underline{\cos\hat{\alpha} \sin\hat{\beta}} \left(-\sin\hat{\alpha} \right) + \\
& + \underline{\sin\hat{\alpha} \sin\hat{\beta}} \left(\cos\hat{\alpha} \right) \Big] \\
\Theta_3 = {} & me\, \underline{\cos\phi_o} \Big[\underline{\cos\hat{\alpha} \sin\hat{\beta}} \left(-\sin\hat{\beta} \cos\hat{\alpha} \right) + \underline{\sin\hat{\alpha} \sin\hat{\beta}} \cdot \\
& \cdot \left(-\sin\hat{\beta} \sin\hat{\alpha} \right) - \underline{\cos\hat{\beta}} \left(\cos\hat{\beta} \right) \Big] \\
\Theta_4 = {} & -m \left(K_{m_2}^2 \sin^2\phi_o + K_{m_1}^2 \cos^2\phi_o \right) \\
& + \underline{\cos\phi_o} \Big[\underline{\cos\hat{\alpha} \sin\hat{\beta}}\, m K_{m_2}^2 \left(\sin\hat{\alpha} \sin\phi_o - \sin\hat{\beta} \cdot \right. \\
& \left. \cdot \cos\hat{\alpha} \cos\phi_o \right) + \underline{\sin\hat{\alpha} \sin\hat{\beta}}\, m K_{m_2}^2 \left(-\cos\hat{\alpha} \sin\phi_o \right. \\
& \left. - \sin\hat{\beta} \sin\hat{\alpha} \cos\phi_o \right) - \underline{\cos\hat{\beta}}\, m K_{m_2}^2 \left(\cos\phi_o \cos\hat{\beta} \right) \Big] \\
& - \underline{\sin\phi_o} \Big[\underline{\cos\hat{\alpha} \sin\hat{\beta}}\, m K_{m_1}^2 \left(\sin\hat{\alpha} \cos\phi_o + \sin\hat{\beta} \cdot \right. \\
& \left. \cdot \cos\hat{\alpha} \sin\phi_o \right) + \underline{\sin\hat{\alpha} \sin\hat{\beta}}\, m K_{m_1}^2 \left(-\cos\hat{\alpha} \cos\phi_o \right. \\
& \left. + \sin\hat{\beta} \sin\hat{\alpha} \sin\phi_o \right) - \underline{\cos\hat{\beta}}\, m K_{m_1}^2 \left(-\sin\phi_o \cos\hat{\beta} \right) \Big] \\
\Theta_5 = {} & \underline{\cos\phi_o} \Big[\underline{\cos\hat{\alpha} \sin\hat{\beta}}\, m K_{m_2}^2 \left(-\cos\hat{\alpha} \cos\hat{\beta} \cos\phi_o \right) + \\
& + \underline{\sin\hat{\alpha} \sin\hat{\beta}}\, m K_{m_2}^2 \left(-\sin\hat{\alpha} \cos\hat{\beta} \cos\phi_o \right) \Big] \\
& - \underline{\sin\phi_o} \Big[\underline{\cos\hat{\alpha} \sin\hat{\beta}}\, m K_{m_1}^2 \left(\cos\hat{\alpha} \cos\hat{\beta} \sin\phi_o \right)
\end{aligned}
$$

$$+ \underline{\sin\hat{\alpha}\sin\hat{\beta}}\, m K_{m_1}^2 \left(\sin\hat{\alpha}\cos\hat{\beta}\sin\phi_0\right)\Big] +$$
$$+ \underline{\cos\phi_0}\left[-\underline{\cos\hat{\beta}}\left(-m K_{m_2}^2 \sin\hat{\beta}\cos\phi_0\right)\right] - \underline{\sin\phi_0}\Big[-\underline{\cos\hat{\beta}} \cdot$$
$$\cdot \left(m K_{m_1}^2 \sin\hat{\beta}\sin\phi_0\right)\Big]$$

$$\Theta_6 = \left(-\sin\phi_0\sin\hat{\alpha} + \underline{\cos\phi_0}\,\underline{\cos\hat{\alpha}\sin\hat{\beta}}\right) m K_{m_2}^2 \cdot$$
$$\cdot \left(-\sin\phi_0\cos\hat{\alpha}\cos\hat{\beta}\right) + \Big(\sin\phi_0\cos\hat{\alpha} + \underline{\cos\phi_0} \cdot$$
$$\cdot \underline{\sin\hat{\alpha}\sin\hat{\beta}}\Big) m K_{m_2}^2 \left(-\sin\phi_0\sin\hat{\alpha}\cos\hat{\beta}\right) +$$
$$+ \left(-\cos\phi_0\sin\hat{\alpha} - \underline{\sin\phi_0}\,\underline{\cos\hat{\alpha}\sin\hat{\beta}}\right) m K_{m_1}^2 \Big(-\cos\phi_0 \cdot$$
$$\cdot \cos\hat{\alpha}\cos\hat{\beta}\Big) + \left(\cos\phi_0\cos\hat{\alpha} - \underline{\sin\phi_0}\,\underline{\sin\hat{\alpha}\sin\hat{\beta}}\right) \cdot$$
$$\cdot m K_{m_1}^2 \left(-\cos\phi_0\sin\hat{\alpha}\cos\hat{\beta}\right) + \underline{\cos\phi_0}\left(-\underline{\cos\hat{\beta}}\right) \cdot$$
$$\cdot m K_{m_2}^2 \sin\hat{\beta}\left(-\sin\phi_0\right) - \underline{\sin\phi_0}\left(-\underline{\cos\hat{\beta}}\right) \cdot$$
$$\cdot m K_{m_1}^2 \sin\hat{\beta}\left(-\cos\phi_0\right)$$

$$\Theta_7 = \sin\phi_0\left[-\sin\hat{\alpha}\, m e \Omega^2 \mu_1 - \cos\hat{\alpha}\, m e \Omega^2 \sin\hat{\alpha}\cos\hat{\beta}\right]$$
$$+ \cos\phi_0\Big[\cos\hat{\alpha}\sin\hat{\beta}\, m e \Omega^2 \mu_1 - \sin\hat{\alpha}\sin\hat{\beta}\, m e \Omega^2 \sin\hat{\alpha} \cdot$$
$$\sin\hat{\beta} - \cos\hat{\beta}\, m e \Omega^2 \mu_3\Big]$$

$$\Theta_8 = \sin\phi_0\, m e \Omega^2\Big[-\sin\hat{\alpha}\left(\cos^2(\hat{\beta}+\delta)\sin\hat{\alpha}\right) + \cos\hat{\alpha} \cdot$$
$$\left(-\cos\hat{\alpha}\right)\Big] + \underline{\cos\phi_0}\, m e \Omega^2\Big[\underline{\cos\hat{\alpha}\sin\hat{\beta}}\Big(\cos^2(\hat{\beta}+\delta) \cdot$$
$$\cdot \sin\hat{\alpha}\Big) + \underline{\sin\hat{\alpha}\sin\hat{\beta}}\left(-\cos\hat{\alpha}\right) - \underline{\cos\hat{\beta}}\Big(-\sin\hat{\alpha} \cdot$$
$$\cdot \sin(\hat{\beta}+\delta)\cos(\hat{\beta}+\delta)\Big)\Big]$$

$$\Theta_9 = \sin\phi_0\, m e \Omega^2\left[-\sin\hat{\alpha}\,\mu_2 + \cos\hat{\alpha}\left(-\sin\hat{\alpha}\sin\hat{\beta}\right)\right]$$
$$+ \underline{\cos\phi_0}\, m e \Omega^2\Big[\underline{\cos\hat{\alpha}\sin\hat{\beta}}\,\mu_2 - \underline{\sin\hat{\alpha}\sin\hat{\beta}}\Big(\sin\hat{\alpha} \cdot$$
$$\cdot \sin\hat{\beta}\Big) + \underline{\cos\hat{\beta}}\,\mu_4\Big]$$

$$\Theta_{10} = \sin\phi_0\, m K_{m_2}^2 \Omega^2\Big[-\sin\hat{\alpha}\left(-\sin\phi_0\cos^2(\hat{\beta}+\delta)\sin\hat{\alpha} +\right.$$

$$
\begin{aligned}
&+\cos\phi_0\,\mu_2\Big) + \cos\hat{\alpha}\left(\sin\phi_0 + \sin\hat{\beta}\sin\hat{\alpha}\cos\phi_0\right)\Big] + \\
&+ \cos\phi_0\, m K_{m_1}^2 \Omega^2\Big[-\sin\hat{\alpha}\big(\cos^2(\beta+\delta)\sin\hat{\alpha}(-\cos\phi_0) - \\
&\quad - \sin\phi_0\,\mu_2\big) + \cos\hat{\alpha}\left(\cos\hat{\alpha}\cos\phi_0 - \sin\hat{\beta}\sin\hat{\alpha}\sin\phi_0\right)\Big] \\
&+ \cos\phi_0\left[-\sin\hat{\alpha}\,\mu_5 + \cos\hat{\alpha}\,\mu_6\right] - \sin\phi_0\Big[-\sin\hat{\alpha}\,\mu_8 + \\
&+ \cos\hat{\alpha}\,\mu_9\Big] + \cos\phi_0\, m K_{m_2}^2 \Omega^2\Big[\cos\hat{\alpha}\sin\hat{\beta}\big(-\sin\phi_0 \cdot \\
&\cdot \cos^2(\beta+\delta)\sin\hat{\alpha} + \mu_2\cos\phi_0\big) + \sin\hat{\alpha}\sin\hat{\beta}\big(\sin\phi_0 + \\
&+ \sin\hat{\beta}\sin\hat{\alpha}\cos\phi_0\big)\Big] - \sin\phi_0\, m K_{m_1}^2 \Omega^2\Big[\cos\hat{\alpha}\sin\hat{\beta} \cdot \\
&\big(\cos^2(\beta+\delta)\sin\hat{\alpha}(-\cos\phi_0) - \mu_2\sin\phi_0\big) + \sin\hat{\alpha}\sin\hat{\beta} \cdot \\
&\cdot\left(\cos\hat{\alpha}\cos\phi_0 - \sin\hat{\beta}\sin\hat{\alpha}\sin\phi_0\right)\Big] - \sin\phi_0\Big[\sin\hat{\beta} \cdot \\
&\cdot \cos\hat{\alpha}\,\mu_5 + \sin\hat{\beta}\sin\hat{\alpha}\,\mu_6 - \cos\hat{\beta}\,\mu_7\Big] - \cos\phi_0 \cdot \\
&\cdot\left[\sin\hat{\beta}\cos\hat{\alpha}\,\mu_8 + \sin\hat{\beta}\sin\hat{\alpha}\,\mu_9 - \cos\hat{\beta}\,\mu_{10}\right]
\end{aligned}
$$

$$
\begin{aligned}
\Theta_{11} = {} & \sin\phi_0\,\mu_{11} + \cos\phi_0\,\mu_{12} + \sin\phi_0\Big[-\sin\hat{\alpha}\, m K_{m_2}^2 \Omega^2 \cdot \\
&\cdot(-\mu_1\cos\phi_0) + \cos\hat{\alpha}\, m K_{m_2}^2 \Omega^2\left(\sin\hat{\alpha}\cos\hat{\beta}\cos\phi_0\right)\Big] \\
&+ \cos\phi_0\Big[-\sin\hat{\alpha}\, m K_{m_1}^2 \Omega^2(\mu_1\sin\phi_0) + \cos\hat{\alpha}\, m K_{m_1}^2 \cdot \\
&\cdot \Omega^2\left(-\sin\hat{\alpha}\cos\hat{\beta}\sin\phi_0\right)\Big] + \cos\phi_0\Big[\cos\hat{\alpha}\cos\hat{\beta}\, m K_{m_2}^2 \cdot \\
&\cdot\Omega^2(-\mu_1\cos\phi_0) + \sin\hat{\alpha}\sin\hat{\beta}\, m K_{m_2}^2 \Omega^2\left(\sin\hat{\alpha}\cos\hat{\beta}\cos\phi_0\right) \\
&- \cos\hat{\beta}\, m K_{m_2}^2 \Omega^2(-\mu_3\cos\phi_0)\Big] - \sin\phi_0\Big[\cos\hat{\alpha}\sin\hat{\beta} \cdot \\
&\cdot m K_{m_1}^2 \Omega^2(\mu_1\sin\phi_0) + \sin\hat{\alpha}\sin\hat{\beta}\, m K_{m_1}^2 \Omega^2\big(-\sin\hat{\alpha} \cdot \\
&\cdot\cos\hat{\beta}\sin\phi_0\big) - \cos\hat{\beta}\, m \Omega^2 K_{m_1}^2(\mu_3\sin\phi_0)\Big]
\end{aligned}
$$

$$
\begin{aligned}
\Theta_{12} = {} & -\cos\phi_0\,\mu_{11} + \sin\phi_0\,\mu_{12} + \sin\phi_0\, m K_{m_2}^2 \Omega^2\Big[-\sin\hat{\alpha} \cdot \\
&\cdot(-\mu_1\sin\phi_0) + \cos\hat{\alpha}\sin\hat{\alpha}\cos\hat{\beta}\sin\phi_0\Big] +
\end{aligned}
$$

$$+ \cos\phi_o\, m K_{m_1}^2 \Omega^2\left[-\sin\hat{\alpha}(-\mu_1\cos\phi_o) + \cos\hat{\alpha}\sin\hat{\alpha}\cdot\right.$$
$$\left.\cdot\cos\hat{\beta}\cos\phi_o\right] + \underline{\cos\phi_o}\, m\Omega^2 K_{m_2}^2\left[\underline{\cos\hat{\alpha}\sin\hat{\beta}}(-\mu_1\cos\phi_o)\right.$$
$$\left.+ \underline{\sin\hat{\beta}\sin\hat{\alpha}}(\sin\hat{\alpha}\cos\hat{\beta}\cos\phi_o) - \underline{\cos\hat{\beta}}(-\mu_3\sin\phi_o)\right]$$
$$- \underline{\sin\phi_o}\, m\Omega^2 K_{m_1}^2\left[\underline{\cos\hat{\alpha}\sin\hat{\beta}}(-\mu_1\cos\phi_o) + \underline{\sin\hat{\alpha}\sin\hat{\beta}}\cdot\right.$$
$$\left.\cdot\sin\hat{\alpha}\cos\hat{\beta}\cos\phi_o - \underline{\cos\hat{\beta}}(-\mu_3\cos\phi_o)\right]$$

$$q_y = I_1\ddot{u} + I_2\ddot{v} + I_3\ddot{w} + I_4\ddot{\phi} + I_5\ddot{v}' + I_6\ddot{w}' + I_7 u + I_8 v + I_9 w + I_{10}\phi + I_{11}v' + I_{12}w'$$

the I_i coefficients are obtained from the Θ_i coefficients if all the products that DO NOT include underlined terms are set to zero and then the following substitutions are made in the products which include underlined terms

$$\underline{\cos\hat{\alpha}\sin\hat{\beta}} \longrightarrow -\cos\hat{\alpha}\cos\hat{\beta}$$
$$\underline{\sin\hat{\alpha}\sin\hat{\beta}} \longrightarrow -\sin\hat{\alpha}\cos\hat{\beta}$$
$$-\underline{\cos\hat{\beta}} \longrightarrow -\sin\hat{\beta}$$
$$\underline{\cos\phi_o} \longrightarrow -\sin\phi_o$$
$$\underline{\sin\phi_o} \longrightarrow \cos\phi_o$$

$$q_z = K_1\ddot{u} + K_2\ddot{v} + K_3\ddot{w} + K_4\ddot{\phi} + K_5\ddot{v}' + K_6\ddot{w}' + K_7 u + K_8 v + K_9 w + K_{10}\phi + K_{11}v' + K_{12}w'$$

the K_i coefficients are obtained from the θ_i coefficients if all the products that DO NOT include underlined terms are set to zero and then the following substitutions are made in the underlined terms

$$\underline{\cos\hat{\alpha}\cos\hat{\beta}} \longrightarrow -\cos\hat{\alpha}\cos\hat{\beta}$$

$$\underline{\sin\hat{\alpha}\sin\hat{\beta}} \longrightarrow -\sin\hat{\alpha}\cos\hat{\beta}$$

$$-\underline{\cos\hat{\beta}} \longrightarrow -\sin\hat{\beta}$$

$$\underline{\cos\phi_o} \longrightarrow -\cos\phi_o$$

$$\underline{\sin\phi_o} \longrightarrow -\sin\phi_o$$

Appendix K

Uniform Cantilever Beam

Input (beam properties)

$EI_1 = EI_2 = 0.3043 \times 10^6$ lbs in^2

$e = e_o = e_A = EB_1 = EB_2 = 0$

$\rho_b A = 0.7324 \times 10^{-4}$ lbs/in

$GJ = 0.2318 \times 10^6$ lbs in^2

$\phi_o = \beta_1 = \delta = \hat{\beta} = \hat{\alpha} = 0$

$m = 0.7324 \times 10^{-4}$ inslugs/in

$EA = 0.2968 \times 10^7$ lbs

$K_{m_1} = K_{m_2} = 0.32$ in

$R = L = 140$ in

Inner radius of the cross section = r_1 = .5 in

Outer radius of the cross section = r_2 = .6 in

Theoretical data or frequencies are based on the following formulae for circular tube cantilever beams

First bending $$\frac{\omega}{2\pi} = \frac{1.758}{\pi L^2}\sqrt{\frac{EI_1}{\rho_b A}} \quad (Hz)$$

Second bending $$\frac{\omega}{2\pi} \doteq \frac{11.015}{\pi L^2}\sqrt{\frac{EI_1}{\rho_b A}} \quad (Hz)$$

Third bending $$\frac{\omega}{2\pi} = \frac{30.85}{\pi L^2}\sqrt{\frac{EI_1}{\rho_b A}} \quad (Hz)$$

First torsion $$\frac{\omega}{2\pi} = \frac{1}{4L}\sqrt{\frac{2GJ}{\pi \rho_b (r_2^4 - r_1^4)}} \quad (Hz)$$

Results Obtained

Mode	Theoretical ω (Hz)	Numerical ω (Hz)
First bending	1.840	1.840
Second bending	11.531	11.535
Third bending	32.294	32.327
First torsion	164.0	164.0

Appendix L

$\underset{\sim}{T}_M$, $\underset{\sim}{T}_B$ Matrices

If instead of

$$\underset{\sim}{q}^T = \left\{ u_1\ u_2\ v_1\ v_1'\ v_2\ v_2'\ w_1\ w_1'\ w_2\ w_2'\ \phi_1\ \phi_2 \right\}$$

we use

$$\underset{\sim}{q}^T = \left\{ u_1\ v_1\ v_1'\ w_1\ w_1'\ \phi_1\ u_2\ v_2\ v_2'\ w_2\ w_2'\ \phi_2 \right\}$$

and

$$\underset{\sim}{q}_L^T = \left\{ u_{L_1}\ v_{L_1}\ v_{L_1}'\ w_{L_1}\ w_{L_1}'\ \phi_{L_1}\ u_{L_2}\ v_{L_2}\ v_{L_2}'\ w_{L_2}\ w_{L_2}'\ \phi_{L_2} \right\}$$

then

$$\underset{\sim}{q}_L^T = \underset{\sim}{T}_B\ \underset{\sim}{q}$$

where

$$\underset{\sim}{T}_B = \begin{bmatrix} \underset{\sim}{T}_M & \underset{\sim}{0} \\ \underset{\sim}{0} & \underset{\sim}{T}_M \end{bmatrix}$$

and

$$\underset{\sim}{T}_M = \begin{bmatrix} \cos\hat\alpha\cos\hat\beta & \sin\hat\alpha\cos\hat\beta & 0 & \sin\hat\beta & 0 & 0 \\ -\sin\hat\alpha & \cos\hat\alpha & 0 & 0 & 0 & 0 \\ 0 & 0 & \cos\hat\beta & 0 & \sin\hat\alpha\sin\hat\beta & -\cos\hat\alpha\sin\hat\beta \\ -\cos\hat\alpha\sin\hat\beta & -\sin\hat\alpha\sin\hat\beta & 0 & \cos\hat\beta & 0 & 0 \\ 0 & 0 & 0 & 0 & \cos\hat\alpha & \sin\hat\alpha \\ 0 & 0 & \sin\hat\beta & 0 & -\sin\hat\alpha\cos\hat\beta & \cos\hat\alpha\cos\hat\beta \end{bmatrix}$$

Appendix M - Useful Integrals

$$\iint_A d\eta\, d\zeta = A \qquad \iint_A \eta\, d\eta\, d\zeta = A e_A$$

$$\iint_A \zeta\, d\eta\, d\zeta = 0 \qquad \iint_A \eta\zeta\, d\eta\, d\zeta = 0$$

$$\iint_A \eta(\eta - e_A)\, d\eta\, d\zeta = I_2 \qquad \iint_A \zeta^2\, d\eta\, d\zeta = I_1$$

$$\iint_A (\eta^2 + \zeta^2)\, d\eta\, d\zeta = A K_A^2 = J$$

$$E \iint_A (\eta^3 + \eta\zeta^2 - K_A^2 \eta)\, d\eta\, d\zeta = E B_2$$

$$E \iint_A \left[\eta^4 + \zeta^4 + 2\eta^2\zeta^2 - K_A^2(\eta^2 + \zeta^2)\right] d\eta\, d\zeta = E B_1$$

$$\iint_A (\eta^2 + \zeta^2)^2\, d\eta\, d\zeta = B_1 + A K_A^4$$

$$\iint_A \eta(\eta^2 + \zeta^2)\, d\eta\, d\zeta = B_2 + A K_A^2 e_A$$

$$\iint_A \rho_b\, d\eta\, d\zeta = m \qquad \iint_A \rho_b \eta\, d\eta\, d\zeta = m e$$

$$\iint_A \rho_b \zeta\, d\eta\, d\zeta = 0 \qquad \iint_A \rho_b \eta\zeta\, d\eta\, d\zeta = 0$$

$$\iint_A \rho_b \eta^2\, d\eta\, d\zeta = m K_{m_2}^2 \qquad \iint_A \rho_b \zeta^2\, d\eta\, d\zeta = m K_{m_1}^2$$

$$\iint_A \rho_b (\eta^2 + \zeta^2)\, d\eta\, d\zeta = m K_m^2$$

150

ORIGINAL PAGE IS
OF POOR QUALITY

References

(1) Houbolt, J.C. and Brooks, C.W., "Differential Equations for Combined Flapwise Bending, Chordwise Bending and Torsion of Twisted Nonuniform Rotor Blades," NACA Rept. 1346, 1958.

(2) Hodges, H.D. and Ormiston, R.A., "Stability of Elastic Bending and Torsion of Uniform Cantilever Rotor Blades in Hover with Variable Structural Coupling," NASA Technical Note D-8192, April 1976.

(3) Kottapalli, S.B.R., Friedmann, P.P. and Rosen, A., "Aeroelastic Stability and Response of Horizontal Axis Wind Turbine Blades," AIAA Journal, Vol. 17, No. 12, December 1979.

(4) Friedmann, P.P., "Application of the Finite Element Method to Rotary-Wing Aeroelasticity," Journal of the American Helicopter Society, January 1980.

(5) Staub, F.K. and Friedmann, P.P., "A Galerkin Type Finite Element Method for Rotary-Wing Aeroelasticity in Hover and Forward Flight," Paper No. 15, Sixth European Rotorcraft and Powered Lift Aircraft Forum, Bristol, England, September 16-19, 1980.

(6) Stephens, W.B., Hodges, D.H., Avila, J.H. and Kung, R.M., "Stability of Nonuniform Rotor Blades in Hover Using a Mixed Formulation." Paper No. 13, Sixth European Rotorcraft and Powered Lift Aircraft Forum, Bristol, England, September 16-19, 1980.

(7) Kaza, K.R.V., "Nonlinear Aeroelastic Equations of Motion of Twisted, Nonuniform, Flexible, Horizontal Axis, Wind Turbine Blades." The University of Toledo, DOE/NASA/3139-1, July 1980.

(8) Sivaneri, N.T., Chopra, I., "Dynamic Stability of a Rotor Blade Using Finite Element Analysis," AIAA Journal, Vol. 20, No. 5, May 1982.

(9) Tong, P. and Rossettos, N.N., "Finite-Element Method, Basic Technique and Implementation," M.I.T. Press, Cambridge, Massachusetts and London, England.

(10) Bathe, K-J. and Wilson, E.L., "Numerical Methods in Finite Element Analysis," Prentice-Hall, Inc., Englewood Cliffs, New Jersey.